Non-canonical TGF-beta signaling drives neuronal guidance in *C. elegans*

Oguzhan Baltaci

MSc, Istanbul Technical University

BSc, Halic University

A thesis submitted for the degree of Doctor of Philosophy at

Monash University in 2019

Monash Biomedicine Discovery Institute

Department of Anatomy and Developmental Biology

Copyright notice

Abstract

Animal development requires strict regulation of cellular processes such as proliferation, differentiation and cell migration. The transforming growth factor beta (TGF-β) family pathway is one of the major regulators of these processes and dysregulation of this pathway is associated with wide range of developmental disorders, however its role in brain development is poorly understood. Here, I present the discovery of a non-canonical mechanism where TGF-β signaling regulates the development of hermaphrodite-specific motor neurons (HSN) of the roundworm *Caenorhabditis elegans*. In this mechanism, I propose that the TGF-β type I receptor SMA-6 controls HSN development independently of the type II receptor DAF-4, non-cell autonomously from hypodermis. Multiple TGF-β family ligands – UNC-129, TIG-2 and TIG-3 – act through SMA-6 to control HSN development, by regulating specific intracellular signaling molecules called Smads – SMA-2, SMA-3 and SMA-4. Through an RNA interference (RNAi) screen, I discovered that knockdown of *neurexin-like receptor 1* (*nlr-1*) suppresses the HSN defects caused by loss of TGF-β signaling. Taken together, my findings show that TGF-β signaling controls development of the HSN neurons in a non-canonical manner. Thereby, these results provide novel insight into how cell signaling events regulate neuronal migration and axon guidance during development. Considering the association of the TGF-β pathway with neurodevelopmental diseases such as epilepsy and schizophrenia, my findings may have wide-ranging disease implications.

Declaration

This thesis is an original work of my research and contains no material which has been accepted for the award of any other degree or diploma at any university or equivalent institution and that, to the best of my knowledge and belief, this thesis contains no material previously published or written by another person, except where due reference is made in the text of the thesis.

Signature:

Print Name: Oguzhan Baltaci

Date: 31/12/2019

Publications during enrolment

Snieckute, G., **Baltaci, O**., Li, H., Li, L., Hu, Z., Pocock, R., *mir-234 controls neuropeptide release at the Caenorhabditis elegans neuromuscular junction.* Molecular and Cellular Neuroscience, 2019. **98**: p. 70-81.

Torpe, N., Gopal, S., **Baltaci, O**., Rella, L., Handley, A., Korswagen H., Pocock, R., *A Protein Disulfide Isomerase Controls Neuronal Migration through Regulation of Wnt Secretion.* Cell Reports, 2019. **26**(12): p. 3183-3190 e5.

Acknowledgements

My greatest appreciation goes to my main supervisor Roger Pocock, who has endlessly supported me throughout my PhD, from the application process to the last day of my thesis submission. Your passion and work ethic have truly been inspirational, and I am grateful to be part of your science journey.

I would like to thank to the members of Pocock lab, especially my co-supervisor Sandeep Gopal for his support in many aspects of the project and his friendship, as well as Goda Snieckute and Teresa Rojo, who taught me the essentials of worm research and be amazing friends. Also, I want to thank to the former members, Mikael Pedersen and Matilda Haas who has previously worked in this project. I want to thank Ava Handley and Rasoul Godini who helped me with RNA sequencing experiments and Tessa Sherry for the critical discussions during the thesis writing process. Also, I would like to express my gratitude to the members of Neumann lab, for their friendship and feedback on my work.

I also would like to express my sincere gratitude to Hakan Tarakci, who has been an amazing friend and made my transition into Australia much easier.

I would like to thank Monash Biomedicine Discovery Institute who made my PhD study possible by providing funding. My PhD gave me the opportunity to work with an amazing pioneer organism, *C. elegans*, therefore I am grateful to all the researchers around the world who made this possible.

Finally, I would like to thank my family for their endless and unconditional support and my wife, Seda Simsek, for her love and encouragement. Thank you for coming to all the way down to Australia and spending countless stressful days and nights with me.

Table of contents

List of Figures and Tables

Abbreviations

ANOVA	Analysis of variance
BMP	Bone morphogenetic protein
bp	Base pairs
cDNA	Complementary DNA
DEG	Differentially expressed genes
DNA	Deoxyribonucleic acid
DNC	Dorsal nerve cord
GFP	Green Fluorescent Protein
h	Hour
min	Minute
ml	Milliliter
mM	Millimolar
n.s.	Not significant
NGM	Nematode Growth Medium
p	p-value
PCR	Polymerase Chain Reaction
qRT-PCR	quantitative real-time polymerase chain reaction
RNA	Ribonucleic acid
RNAi	RNA interference
SDS-PAGE	Sodium dodecyl sulfate-polyacrylamide gel electrophoresis
sec	Second
SEM	Standard Error of Mean
TGF-β	Transforming growth factor beta
VNC	Ventral nerve cord

1. Introduction

1.1 TGF-β Family Pathway

The transforming growth factor beta (TGF-β) family pathway is a major regulator of development. It controls multiple cellular processes including cell proliferation, differentiation and migration. As such, dysregulation of TGF-β signaling results in neurological disorders, cardiovascular abnormalities, autoimmune disease and cancer [1]. Since its discovery in late 1970s [2-4], TGF-β family signaling has been associated with wide range of biological processes and owing to its large number of members, functions of this pathway are highly context-dependent [5]. These members include ligands, receptors and intracellular signaling molecules as well as extracellular and intracellular regulators that act in a signaling cascade [5].

The TGF-β signaling cascade (Fig. 1.1) starts with binding of an extracellular ligand to the TGF-β type II receptor, which is a serine/threonine kinase. This interaction causes the recruitment of another kinase, the TGF-β type I receptor, which is phosphorylated, and thereby activated by the TGF-β type II receptor. Subsequently, the TGF-β type I receptor phosphorylates intracellular transducers called receptor-regulated Smads (R-Smads), which then associate with co-Smads and translocate into the nucleus to regulate target gene expression [1, 5, 6]. This process can differ in bone morphogenetic proteins (BMP)-like sub-group, where the ligands can bind to the type I and type II receptors independently. However, the ligand-binding has been shown to be more stable when both type I and type II receptors are present [7, 8].

1.2 TGF-β Family Members

The TGF-β family is comprised primarily of two functional classes: the TGF-β-like group, which plays a key role in the formation of the three germ layers in vertebrates, and the bone morphogenetic proteins (BMP)-like group, which is associated with body patterning and axis formation [9]. The TGF-β-like group is comprised of subcategories activated by TGF-β, Nodal, Activin or some of the Growth Differentiation Factors (GDF) while BMP-like group includes BMPs, most GDFs and Anti-Müllerian Hormone (AMH).

Collectively, there are over thirty ligands in the TGF-β family pathway, which require strict regulation at multiple levels [5].

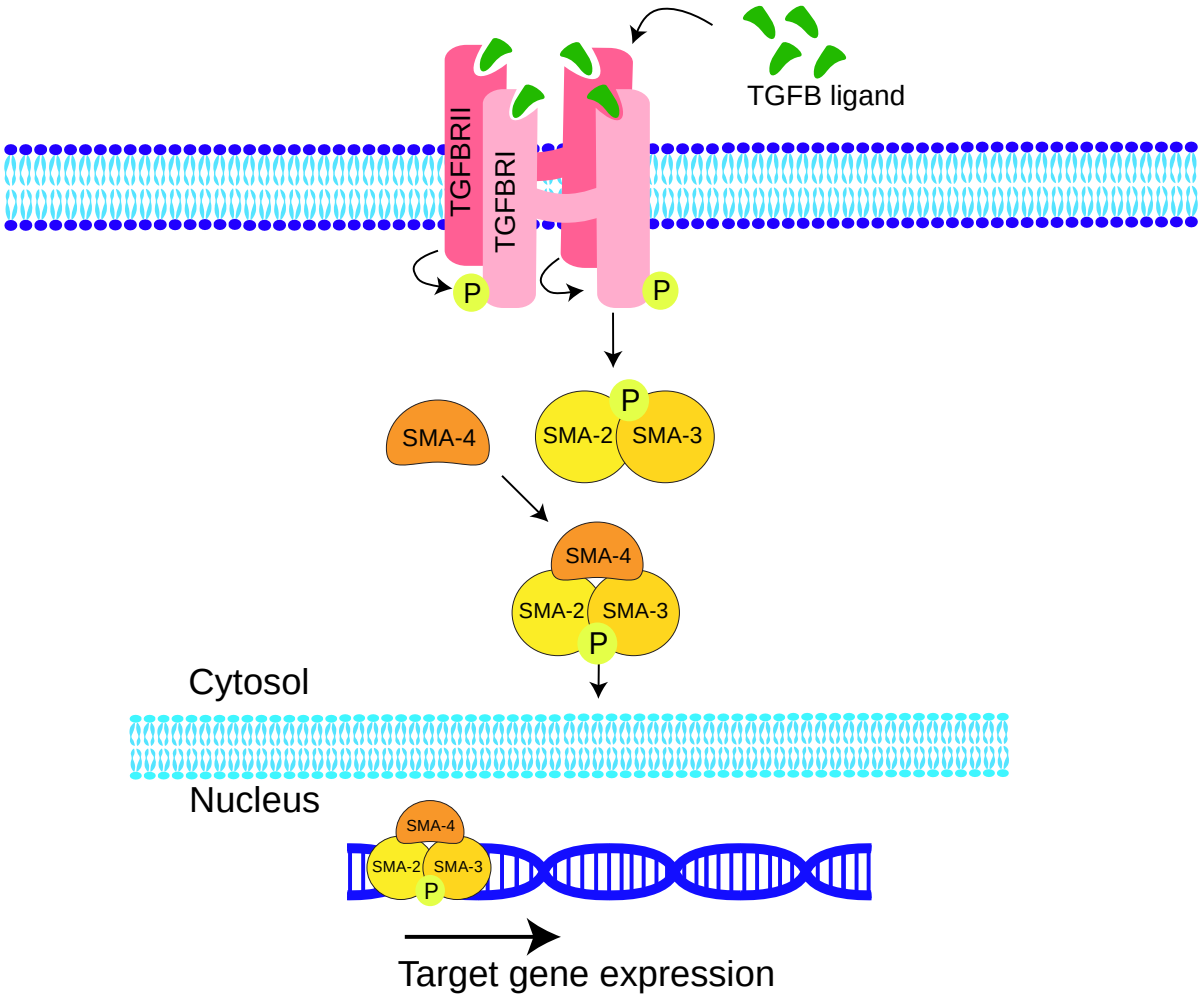

Fig. 1.1. TGF-β signaling cascade.

Ligand binding to the type II receptor causes the recruitment of the type I receptor. Activated type I receptor phosphorylates R-Smads which then bind to co-Smads. The activated Smad complex migrates to the nucleus and act as a transcription factor.

1.2.1 Ligands

The TGF-β family ligands are comprised of more than thirty ligands in mammals which are derivatives of TGF-β, Nodal, Activin, BMP, GDF and AMH. These ligands are initially produced in long precursor forms that contain an N-terminal localization signal, a pro-domain required for folding and a C-terminal active domain required for function [10]. In order for TGF-β family ligands to function, they need to be in their mature forms

which require processing by proteolytic enzymes. In this process, the N-terminal signal peptide is removed, then a non-covalent bond is formed between the prodomain and mature domain called a cysteine knot. The cysteine knot consists of six cysteines that form disulfide bonds that are catalyzed by protein disulfide isomerases (PDI). Then, the pro form of the ligand is cleaved from a conserved consensus peptide between the prodomain and active domain. However, studies showed that some BMPs such as BMP4, BMP5 and BMP7 can be secreted while still bound to their prodomains [11-13]. At this point, the ligand is bound by a specific protein called latent TGF-β binding protein (LTBP) which holds the ligand in its inactive form. The LTBP-bound ligand is secreted to the extracellular matrix (ECM) and interacts with specific ECM molecules such as integrin. This results in the release and binding of the mature form to its target receptor. This process is crucial for determination of the signaling activity [10].

The action of these ligands determines the signaling intensity and duration; therefore, the regulation of ligand action is crucial for developmental processes requiring TGF-β mediation. Ligand action depends on many factors such as the level of ligand expression and the release and presentation of ligands to the receptors. For example, a *Drosophila melanogaster* BMP homolog Decapentaplegic (DPP), acts in a gradient for patterning of anterior-posterior axis during wing development [14, 15] which shows the importance of expression level. In addition, the proteogylcan Cripto acts as an accessory receptor to mediates Nodal binding to activin receptors [10]. Finally, mutations in *fibrillin 1* has been shown to interfere with anchoring of TGFβ-binding proteins which leads to faulty TGF-β release, and therefore altered signaling [16, 17]. Taken together these examples show that a variety of factors play roles in ligand function, and thereby signaling intensity and duration.

1.2.2 Receptors

To date, seven TGF-β type I and five TGF-β type II receptors have been described in humans. Receptor complex formation between the TGF-β type I and II receptors is essential for TGF-β signaling initiation. Previous studies reported that both proteins can form homodimers on the cell membrane and establish heterotetrameric structures upon ligand binding [18, 19], however they are mostly found as monomers and

application of TGF-β ligand leads to the formation of a type II dimer and then recruitment of type I [20]. Both types of receptor share similar structural features including an N-terminus enriched in cysteines, a single-pass transmembrane domain and a cytoplasmic C-terminal region that contains kinase domains [21]. The N-terminus contains a cysteine box with $CCX_{4-5}CN$ consensus, which is important for ligand-binding, while the C-terminus contains serine and tyrosine residues important for kinase activity. In spite of structural similarities, regulation of kinase activity differs between the two receptor types. The TGF-β type II receptor is capable of autophosphorylation at serine residues 213 and 409, which are required for the kinase activity, whereas phosphorylation at Ser416 has an inhibitory effect on the protein [22]. The TGF-β type I receptor in contrast, is not able to activate itself and must be phosphorylated at the TTSGSGSG motif, called the GS domain, for activation [23]. However, the replacement the threonine residue with an aspartic acid near the GS domain resulted with constitutively active type I receptor *in vitro* [24]. Furthermore, a mutation that replaced the 253rd glutamine with an aspartic acid residue in the type I receptor of *Drosophila* caused the same constitutively-active state [14]. The TGF-β type I receptor has an inactive conformation due to interactions between its GS domain and the N-terminus. Phosphorylation by the TGF-β type II receptor changes its conformation to an active state [25]. The two TGF-β receptors are found as homodimers and create tetrameric complexes upon ligand binding. Gly-261 and Gly-322 residues in the TGF-β type I receptor are required for correct function of the ligand-induced receptor complex because substitution of these residues with aspartate and glutamate, respectively causes inactivation of the TGF-β type I receptor [26]. Furthermore, these positions map to the interface of homodimer structure according to a reported crystal structure, hence could be also important for dimerization [25].

In addition to phosphorylation, the activity of TGF-β receptors is regulated by other post-translational modifications such as ubiquitylation, sumoylation and neddylation [6, 27, 28]. For example, it has been shown that the TGF-β type I and II receptors can be degraded by polyubiquitylation [27]. Furthermore, some subtypes of the TGF-β type I receptor are sumoylated [29], which controls their activity and localization, while TGF-β type II can be regulated by neddylation which coordinates activity, localization and stability [30].

1.2.3 Smads

After activation of the TGF-β family receptor complex, signaling is propagated through intracellular signaling molecules called Smads [5]. These molecules primarily act in complexes as transcriptional regulators and activate or repress the expression of their target genes. There are three subtypes of Smad proteins: R-Smads (Smad1, 2, 3, 5 and 8), the common Smad (Smad4) and inhibitory Smads which are Smad6 and Smad7. While Smad4 is common for both the TGF-β and BMP signaling pathways, Smad2 and 3 are specific for TGF-β, Nodal and activin ligands whereas Smad1, 5 and 8 are predominantly involved in BMP- and GDF-activated signaling [31]. R-Smads share an SXS phosphorylation motif that is located at the end of the C-terminus. Phosphorylation of this motif is required for their activation and nuclear localization [32]. There are also two other conserved polypeptide segments called MAD homology 1 and 2 (MH1 and MH2). MH1 consists of nuclear localization signals and a β-hairpin structure required for DNA binding, whereas MH2 forms an L3 loop structure that is crucial for the interaction with TGF-β type I receptors as well as DNA-binding partners [33]. Smads share a common DNA binding domain which recognizes the same DNA motif CAGAC. However, Smad1 also binds to GC-rich sequences due to the difference of the location of DNA binding domain. Smad4, the common Smad, lacks the SXS motif, but contains the MH2 domain. R-Smads associate with Smad4 through this domain, then this complex translocates into the nucleus transcriptionally regulate target genes [5].

The presence of Smad proteins in cells can be in two different states. These are the basal state in which Smads shuttle between the nucleus and the cytoplasm and the receptor-induced active state in which the Smads form an oligomeric complex upon phosphorylation by the type I receptor. After their activation, the Smad oligomer translocates into the nucleus to regulate transcription of target genes [34, 35]. Due to their limited affinity and low specificity for DNA, Smads require binding partners to stabilize their DNA binding and increase the specificity for binding sites [36-38]. For example, Foxh1 was the first binding partner shown to be required for the recruitment of Smad complex to the promoter of Mix.2 gene in *Xenopus* embryos [37]. A later study showed that loss of Foxh1 causes a phenotype that also occurs upon reduction in

Nodal signaling [39], further highlighting the requirement of binding partners for Smad activity.

Smads function to activate or repress specific target molecules through wide range of processes. These processes include direct transcriptional regulation, epigenetic regulation and regulation of the transcriptional outputs from other mechanisms [5]. Chromatin remodeling refers to the dynamic changes in chromatin structure and these changes determine the accessibility of DNA to the transcriptional machinery. Ross et al showed that SMARCA4, an ATPase involved in chromatin remodelling, is recruited by TGF-β-activated Smad complex and is required for the activation of Smad targets. Furthermore, Smads recruit histone acetyltransferases to chromatin allowing the acetylation of histones that results with transcriptional activation [40]. Interestingly, this transcriptional activation only occurs from a chromatin template but not from naked DNA. In addition to transcriptional activation, Smads can regulate chromatin remodeling, resulting in transcriptional inhibition. It has been shown that TGF-β-activated Smad3 recruits histone deacetylases, leading to repression of Runx2 in osteoblast differentiation [41]. Taken together, these findings show the correlation between chromatin remodeling and TGF-β family signaling. In other cases, there may be a combination of direct and indirect regulation of transcription determined by TGF-β signaling. Kang et al. reported that Smad3 activates the transcription of ATF3. Interestingly, ATF3 recruits Smad3 upon its activation and the complex formed between Smad3 and ATF3 represses the transcription of *Id1* gene which leads to inhibition of epithelial cell growth [42]. This process indicates that Smads can also act in a self-enabling mechanism.

Aside from transcriptional regulation, Smads have been shown to function in different mechanisms such as the production of non-coding RNAs [43]. Smads activated by TGF-β or BMP signaling can be recruited to the same complex with Drosha which is an enzyme required for microRNA (miRNA) processing [44]. In this study, particular miRNAs were analyzed, and they were found to possess a common region for the recognition of Smads. After Smad binding on the primary transcript of the miRNA (pri-miRNA), these molecules are recruited to the Drosha complex which processes the pri-miRNA into the precursor miRNA and eventually increasing miRNA production.

The TGF-β family pathway is a highly context-dependent process in which the same subclasses of pathways can affect the cell development and behavior in different ways. Various factors can play a role in determining this context-dependent function. One of these factors is the presence of large number of molecules regulating the accessibility of the receptors for ligand-binding and Smad activation. For instance, LON-2/glypican has been shown to restrict ligand binding to its receptors, thus negatively regulating TGF-β family signaling in *C. elegans* [45]. Smad7, an inhibitory Smad, competes with R-Smads in receptor binding, therefore restricting their activities [46]. Another factor is the varying binding partners of Smads such as transcription factors and chromatin remodeling molecules. These binding partners are instrumental in determining target genes that will be regulated by signaling as well as controlling positive or negative regulation [46]. Taken together, these factors control the transduction of signaling to the downstream molecules, regulating vital mechanisms during development.

1.3 Cooperation of TGF-β with other pathways

As mentioned earlier, TGF-β signaling regulates an enormous diversity of biological processes during development. This function can be direct or in cooperation with other conserved signaling mechanisms such as Hippo, Wnt and RTK pathways [35]. In human embryonic stem cells, it has been shown that TAZ - an effector molecule of Hippo pathway -interacts with Smad2/3-4 complex to regulate self-renewal upon TGF-β stimulation [47]. Another example is the interaction between Smad2/3 and the tumor suppressor protein p53. It has been shown that the phosphorylation of p53 upon induction by RTK signaling leads to binding of p53 to Smad complex which is crucial for mesoderm specification [48]. Finally, cooperation between Wnt and TGF-β signaling has been reported in a wide range of developmental processes. For example, BMP-2 and BMP-4 act with WNT-8 in the specification of ventral fate while inhibiting dorsal mesoderm development [49]. Taken together, these studies demonstrate the importance of cooperation between multiple conserved signaling mechanisms and TGF-β signaling.

1.4 TGF-β pathway in neurological disorders

TGF-β signaling is a fundamental pathway that controls multiple developmental processes in metazoa. Mutations in components of this pathway have been associated with cardiovascular disease, musculoskeletal defects and cancer, as well as neurological disorders.

Epilepsy is a complex neurological disorder characterized by recurrent seizures that occur due to abnormal neuronal activity. Amygdala-kindling systems, which induce the development of seizures using electrical stimulation to the amygdala region of the brain, are commonly used to create epilepsy models and TGF-β upregulation has been shown in neurons of amygdala-kindled rats [50]. In another study, TGF-β signaling in astrocytes is associated with epileptogenesis and using a drug that has an antagonistic effect on TGF-β pathway has been shown to prevent the development of seizures in rats [51].

Activin, which is a TGF-β ligand has been implicated in neurodegenerative diseases such as Huntington's and Parkinson's disease. Administration of activin into a rodent model of Huntington's disease has been shown to promote the survival of striatal interneurons and projection neurons [52]. Furthermore, application of activin also protected dopaminergic midbrain neurons against cell death in a mouse model of Parkinson's disease [53]. Activin is also implicated in cognitive performance, as demonstrated by a behavioral study in mice where disruption of an activin receptor results in a low-anxiety phenotype [54].

It can be concluded that TGF-β activity is highly context-dependent and can vary according to the cell type, association with other signaling pathways and types of diseases. This makes the pathway quite challenging to study, however, further studies should be carried out to illuminate its roles in neurological disorders to enable the generation of potential therapeutics.

TGF-β signaling is highly conserved across most organisms including primates, rodents, fish and nematodes. Previous research of the TGF-β signaling pathway in the transparent roundworm *Caenorhabditis elegans* has helped us to identify and understand key mechanisms and molecules involved in this pathway [55-57].

1.5 *Caenorhabditis elegans* as a model organism

In 1963, Sydney Brenner proposed *Caenorhabditis elegans* (*C. elegans*) as a model organism to decipher the riddles of neurobiology and since then it has been used to uncover many scientific breakthroughs such as RNA interference, whole genome sequencing, microRNAs and apoptosis. *C. elegans* is used in a wide range of areas in modern biology including cellular development, neurobiology, aging, fat storage and behavioral studies [58].

C. elegans is a small transparent nematode that is 1 mm in length and can be found worldwide. They feed on bacteria and can be found in rotting vegetal matter such as fruits and flowers [59, 60]. *C. elegans* exist as self-fertilizing hermaphrodites possessing two symmetrical uteri and spermathecae. They are surrounded by a flexible cuticle layer which is pressured by the body cavity (pseudocoelome) to provide rigidity to the animals [58]. They have an invariant number of cells, 959 in the hermaphrodite [58] [61], and a rapid 3-day life cycle which make *C. elegans* a very powerful model organism.

1.5.1 Development

C. elegans are primarily found as hermaphrodites, with only 0.1% males in the population. Hermaphrodites produce both oocytes and sperm, which permit self-fertilization of up to 300 progeny. However, this number can increase up to 1000 through sexual mating with males [58].

The life cycle of *C. elegans* starts with embryogenesis that takes approximately 9 hours after fertilization (Fig. 1.2). At the end of the embryonic stage, eggs hatch to worms with fully differentiated tissues and organs. These worms then develop through 4 larval stages (L1, L2, L3, L4) and start producing progeny once they reach adulthood [58]. Under adverse environmental conditions, such as starvation, development is arrested and larvae switch to an alternative L3 stage called dauer, in which orifices are sealed, fat is stored, and stress resistance pathways are activated. Until environmental conditions become favorable, they can remain in this stage and survive for up to 4 months [62].

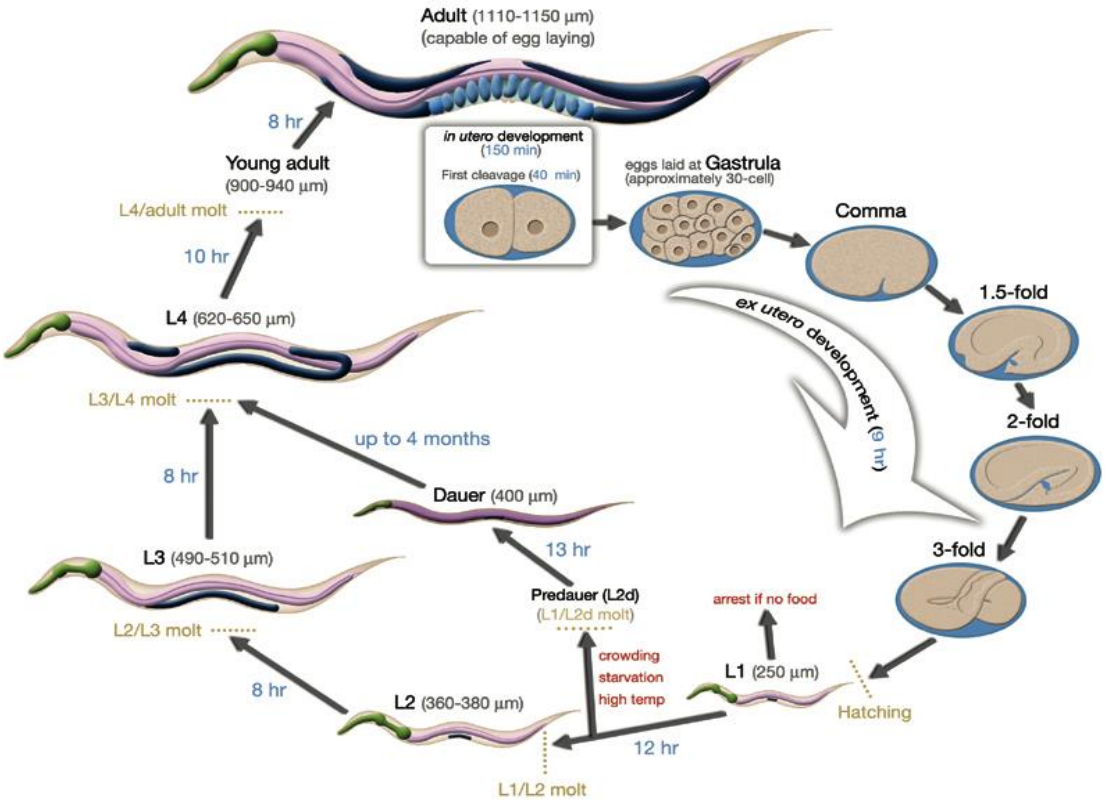

Fig. 1.2. Life cycle of hermaphrodite *C. elegans*.

Numbers in blue shows the time spent in each stage. Numbers in parenthesis indicates the length of the animal in micrometers. Eggs are laid after 150 minutes after fertilization (adapted from Wormatlas).

1.5.2 Genetics

C. elegans has six chromosomes comprising five autosomal diploid chromosomes and one X chromosome that makes the sexual difference. Hermaphrodites have a pair of X chromosomes while males carry only one due to the mis-segregation during germline meiosis [58]. Although males are useful to generate strains with different genetic composition, genetic analysis is mostly based on hermaphrodites that are capable of self-fertilizing. This ability facilitates stock maintenance. In addition, self-fertilization follows the Mendelian pattern of inheritance, which greatly simplifies the identification of mutant worms of interest in the population. This is due to the prediction that a heterozygous mother for a recessive mutation will produce progeny in which 25% of animals will carry that mutation in a homozygous state [58].

C. elegans was the first multicellular organism to have its genome sequenced which created the basis of comparative genomics. The genome includes 20,444 protein-coding genes, which are relatively small due to short intronic sequences compared to vertebrate genes [63]. According to a meta-analysis by Shaye and Greenwald, 7,663 of these genes (38%) are conserved in humans [64]. A majority of these orthologs include transcription factors, kinases, nuclear hormone receptors that are involved in crucial developmental pathways such as TGF-β, Notch, Wnt and insulin signaling [64]. This conservation together with the genetic amenability of *C. elegans* makes it an important model for studying human biology and disease.

1.5.3 Nervous System

C. elegans has a small nervous system that is composed of 302 neurons in adult hermaphrodites (Fig. 1.3) and 385 in males mainly due to additional neurons in the specialized tail region [65, 66]. The nervous system can be divided into two independent groups which are somatic system that comprise the majority of neurons and a small pharyngeal system that includes 20 neurons in the head [66]. Neurons are organized in ganglia in the head, tail and a spinal cord-like structures which are dorsal and ventral nerve cords [67]. Neurons can be categorized into 118 classes based on their morphologies and connectivities. Unlike the nervous system of mammals, synapse formation is made *en passant* in *C. elegans,* which means the processes of neurons run in parallel and make connections along their length. The number of chemical synapses between the neurons varies considerably ranging from one single synapse to nineteen. Collectively, they make more than 6000 chemical synapses and gap junctions. As in vertebrates, there are neuronal support cells (glia) in *C. elegans* that are mainly associated with sensory neurons in the head. Also, most common neurotransmitters such as serotonin, dopamine, acetylcholine and GABA are expressed in the *C. elegans* nervous system [68].

As in vertebrates, neurons are functionally classified into three types which are sensory, motor and interneurons. Sensory neurons regulate many processes such as mechanosensation, thermosensation and nociception [68]. Interneurons process information by receiving and relaying signals from other neurons [66]. Motor neurons synapse onto the muscles at neuromuscular junctions (NMJ) and are responsible for

muscle stimulation [66]. In contrary to vertebrate nervous system where the muscles are innervated by neuronal processes, *C. elegans* possesses muscle arms that reach out and synapse onto the processes of motor neurons which are confined to the ventral and dorsal nerve cords [67]. Furthermore, some of these motor neurons possess processes that are postsynaptic at NMJs.

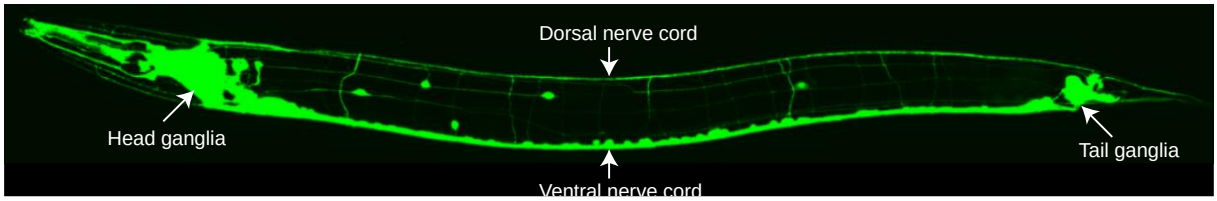

Fig. 1.3. The nervous system of *C. elegans*.
Image of an adult hermaphrodite expressing a transgenic GFP reporter that marks all 302 neurons. The nervous system comprises distinct neuron centers that coordinate sensing, integration and responses to environmental cues. Anterior to the left, lateral view. Image is provided by Roger Pocock.

Due to the genetically tractable nervous system that is composed of an invariant number of neurons, *C. elegans* has been widely used as an important model in neurobiology to investigate many different pathways such as neuronal degeneration, axon guidance, synapse formation, mechanosensation and chemosensation [68]. For example, researchers have used *C. elegans* to examine amyloid-beta accumulation and toxicity which is the definitive indicator of Alzheimer's disease [69]. In another example, target genes of alpha-synuclein, a protein related to development of Parkinson's Disease (PD), were screened via RNAi knockdown and ablation of twenty genes were shown to cause misfolding of alpha-synuclein which is an indicator of PD [70]. These studies suggest that *C. elegans* can be used to enlighten the progression of diseases and create potential therapeutics.

1.5.4 Neuronal Migration and Axon Guidance

Neurons are specialized cells that are capable of sensing and responding to the environmental changes. They are composed of a cell body and processes called axons and dendrites. For neurons to function properly, they undergo complex processes during development. These include neuron specification, migration, axonal outgrowth,

axonal termination and synapse formation [71]. The migration of neurons is a vital mechanism that is crucial for wiring the brain architecture. This process requires a variety of complex molecular pathways that direct neurons to their specific functional coordinate. Depending on where they originate, neurons can be guided by specialized molecules in the extracellular matrix or glial cells which are non-neuronal cells that support and protect neurons. Upon migration, they form contacts with their targets via axons and dendrites [66, 68, 71]

In *C. elegans*, the majority of neuronal migrations occur during embryogenesis [71]. Some neurons migrate long distances such as the HSNs that migrate anteriorly from the tail to the mid body [67]. After migration, neurons extend axons along axon tracts to make connections with their target neurons. Many of these neuronal processes grow in close contact with hypodermal cells that secrete guidance cues for the correct development of these processes. The majority of axonal outgrowth occurs circumferentially in dorso-ventral axis or longitudinally in the anterior-posterior axis. The major difference between the neurons that extend processes along these axes is that the axons extend longitudinally in anterior-posterior axis are in close contact with other neurons and require pioneering axons. For example, AVG is the pioneering neuron that directs the axonal outgrowth of the neurons in the ventral nerve cord [71]and laser ablation of AVG has been shown to perturb the organization of the ventral nerve cord [71]. In contrast, the axons extending circumferentially in the dorso-vental axis need to find their paths independently of pioneering axons [71].

Most of the cellular pathways regulating neuronal migration and axon guidance are conserved across species including mammals and nematodes. *C. elegans* has played an important part in the discovery of some of these pathways and being the only organism to have its neuronal wiring diagram mapped makes it a great tool in elucidating the cues of neuronal migration and axon guidance. These processes are regulated by many intercellular and intracellular molecules such as secreted proteins, receptors, adhesion molecules and transcription factors controlling the expression of these molecules. Proteoglycans, Netrin, Ephrin, Robo/slit and Wnt signaling are the most well-known pathways that are involved in this process [71].

Netrins are a protein family discovered in *C. elegans*. UNC-6, the netrin ligand, associates with Netrin receptors, UNC-5 or UNC-40. Worms lacking these proteins

exhibit axon guidance defects of several neurons such as PVQs, ALMs and HSNs [72]. UNC-40 is expressed in HSNs and is distributed asymmetrically which is important for the initial site of axon formation. As a result of *unc-6* or *unc-40* mutations, axons extend laterally rather than entering the ventral nerve cord [73].

Slit/Robo signaling is another pathway that regulates neuronal migration and axon guidance. It was discovered in *Drosophila* and is conserved in humans and *C. elegans*. The Slit ligand and Robo receptor act to repel axons from the midline [74]. Mutations in *sax-3* which encodes the Robo homologue in *C. elegans*, causes the formation of axons that inappropriately cross the ventral midline since axons cannot be repelled properly [75]. Slit/Robo signaling antagonizes the netrin signaling which is a pathway that attracts axons to the midline [76, 77]. However, it acts in parallel pathways with Ephrin signaling in which the *C. elegans* ephrin receptor, VAB-1, inhibits the axon extension [78].

Ephrin signaling is another conserved pathway and has been extensively studied in *C. elegans*. It comprises of a single receptor, VAB-1 and four cell surface-bound proteins which are VAB-2, EFN-2, EFN-3 and EFN-4 [79]. Collectively, the components of Ephrin signaling have been shown to be required for axon guidance events of many neurons such as HSNs and PVQs [71]. It has also been shown that ephrins can act independently of the VAB-1 receptor where they control the axon guidance of SDQ neurons [79] Another class of membrane-bound proteins is reticulon (RTN) family which is required for the trafficking events between the endoplasmic reticulum (ER) and Golgi [80, 81]. *C. elegans* possesses only one reticulon, RET-1, which has been shown to be required for axon navigation of HSNs and D-type motor neurons [82]. Interestingly, the level of VAB-2/ephrin has been shown to be elevated in *ret-1* mutants and in concurrence with this, mutating *vab-2* in ret-1 mutant animals was found to suppress the HSN defects of *ret-1* mutants [82].

Wnt signaling has been shown to regulate neuronal migration and axon guidance events in both vertebrates and [71]. The *C. elegans* Wnt ligand EGL-20 is responsible for repelling HSNs from the tail and the Wnt receptor, MIG-1, directs the movement of HSN cell bodies from tail to the mid-body [83]. Wnt signaling is a highly conserved developmental pathway and it has been shown to be involved in a variety of processes including the development of the mouse brain and *Drosophila* wings [84].

Many other molecules are involved in neuronal migration and axon guidance. Therefore, the concentration and distribution of these cues should be strictly controlled. Biochemical and cell culture experiments have demonstrated that proteoglycans which are glycosylated proteins found in plasma membrane associate with guidance molecules [85]. Furthermore, *in vivo* experiments in *C. elegans* have shown that a proteoglycan LON-2 is required for correct HSN development [86]. Overall, these findings highlight that guidance of neurons is a complex process; hence deeper insight into the roles of these pathways in development and diseases is required.

1.5.5 Hermaphrodite-specific Neurons (HSNs)

The HSNs are sexually dimorphic motor neurons that produce serotonin to control the egg-laying process. They innervate the vulval muscles to stimulate egg laying and laser ablation of these neurons leads to egg-laying defective phenotype [87]. These defects can be rescued by exogenous serotonin [87].

During embryogenesis, the two bilaterally symmetrical HSNs (HSN left and right) are born in the tail 400 minutes post-fertilization and migrate to the mid body to a point that is slightly posterior to the presumptive vulva (Fig. 1.4). In males, the HSNs undergo apoptosis during embryogenesis since they are not required. During the L2-L3 stages, the HSNs start extending their axons anteriorly along the left and right fascicles of the ventral nerve cord and by the young adult stage they complete their axonal outgrowth by entering the nerve ring where they make synapses with target neurons [87].

Synaptic circuitry of HSNs is predominantly presynaptic. Among different muscle cells, they exclusively synapse onto vulval muscle. In terms of neurons, they synapse onto ventral cord neurons (VCn) near the NMJs between VCn and vulval muscles and receive synapse from BDU, AVF and PLM neurons [67].

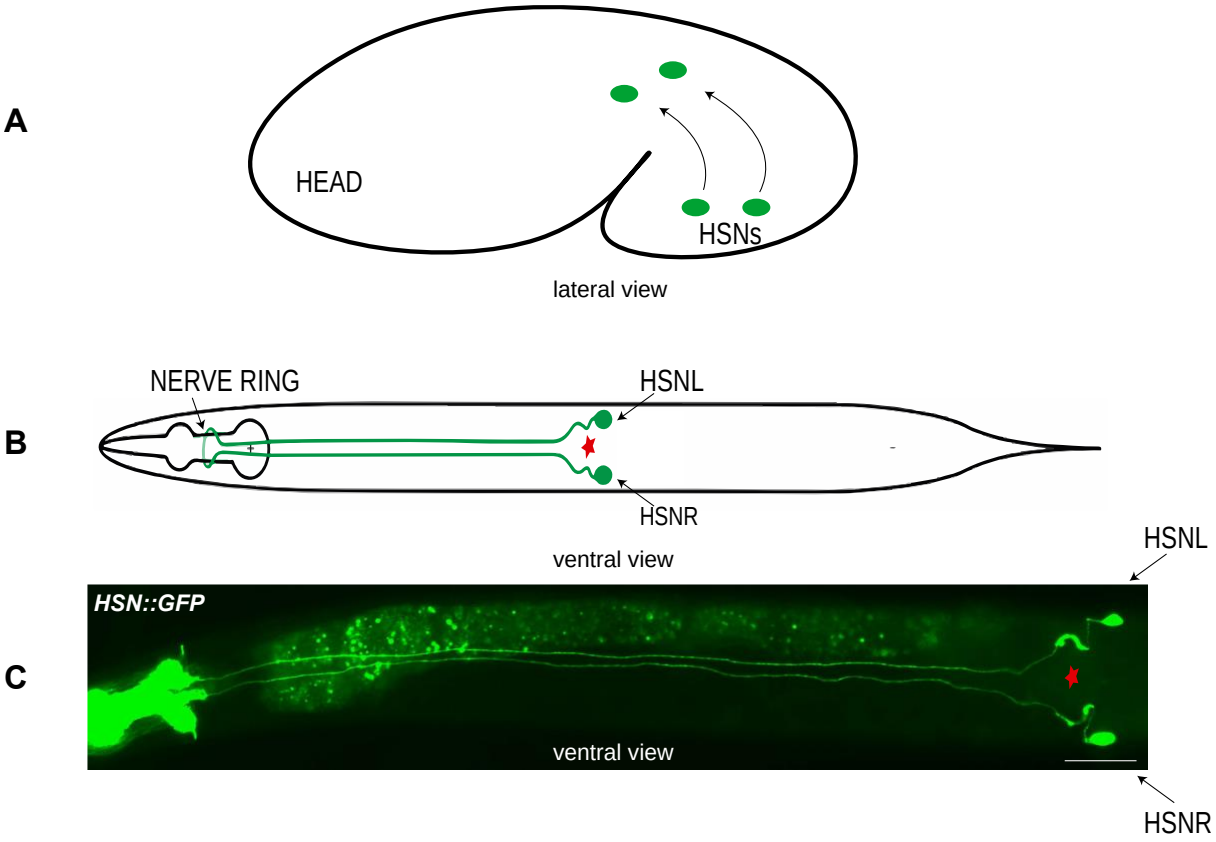

Fig. 1.4. HSN development and anatomy.

(A) HSN migration during embryogenesis. Green circles represent the HSN cell bodies. Anterior to the left. (B) Schematic representation of HSN axonal development during the larval stages. Red star represents the vulva. Anterior to the left, ventral view. (C) A one-day adult worm expressing a transgene driving GFP in the HSNs. Star sign marks the vulva. Anterior to the left, lateral view, scale bar = 50 µm.

The development of the HSNs is complex and is controlled by many different molecular pathways such as netrin, ephrin and Wnt signaling as well as extracellular molecules such as heparan sulfate proteoglycans and glypicans.

As stated earlier, Wnt signaling is crucial for the migration of HSNs [83]. This process is directed by the EGL-20/Wnt morphogen gradient for the correct anteroposterior location of HSNs as overexpression of the EGL-20 has been shown to cause overmigration where HSNs migrate anterior to vulva, whereas the downregulation results with undermigrated HSNs [88]. Furthermore, interference with Wnt signaling has also been shown to perturb axon guidance of HSNs [89]. Wnt gradient secretion is controlled by highly conserved mechanisms. For example, MIG-14 - an ortholog of human Wnt ligand secretion mediator (WLS) - has been shown to be required for EGL-20 secretion and the loss of MIG-14 results with EGl-20-related HSN migration defects

[90]. Furthermore, PDI-1 - a protein disulfide isomerase - has been shown to control the secretion of Wnt3a in human cells via hypothetically controlling the disulfide bond formation [91]. In concurrence with this finding, loss of PDI-1 in *C. elegans* has been shown to cause HSN migration defects [91].

Heparan sulfate proteoglycans (HSPG) regulate wide range of developmental processes including cell migration and morphology [92]. They function as cofactors and regulators of conserved signaling pathways such as Wnt and TGF-β signaling [93]. In *C. elegans,* there are four HSPG core proteins which are SDN-1/syndecan, GPN-1/glypican, UNC-52/perlecan and LON-2/glypican. Except for GPN-1, all the HSPGs have been shown to be involved in HSN development [93]. The null mutant of *sdn-1* leads to severe migration and guidance defects which are suppressed by mutating *trp-1* and *trp-2* genes that encode calcium transport channels [94]. Perturbing LON-2/glypican signaling has been reported to cause HSN migration and guidance defects [86]. In this study, a conserved miRNA, *mir-79* has been shown to regulate the LON-2/glypican signaling via controlling the expression of a chondroitin synthase and UDP-sugar transporter enzymes. A mutation in *mir-79* leads to decreased heparan sulfate production which perturbs LON-2 function in HSN development [86].

vab-8 which encodes a kinesin-like protein has been shown to direct HSN migration and axon guidance [89, 95]. This is associated with the increased activity of EGL-20/Wnt signaling which is mediated by CAN neurons [88]. As HSNs undergo long-range migration and axon guidance events during development, their development is quite complex. Although many conserved signaling mechanisms such as Wnt, Ephrin and Netrin have been studied extensively in the context of HSN development, the potential role of TGF-β signaling is unclear.

1.6 TGF-β Pathway in *C. elegans*

Model organisms are critical for elucidating how particular biological phenomena function across other species, especially in humans. Studies in *C. elegans* have played key roles in providing insights to TGF-β signaling, which is a highly conserved and crucial pathway for the development of organisms. As mentioned earlier, the TGF-β superfamily comprises of a large number of proteins, predominantly categorized as

TGF-β-like and BMP-like families. However, in *C. elegans* this distinction is not as clear as in vertebrates. There are mainly two subcategories; Sma/Mab and dauer pathways. Collectively, these pathways include 17 members which are composed of ligands, receptors and Smads as well as DNA-binding partners for transcriptional regulation [96].

1.6.1 Ligands

The TGF-β family ligands in *C. elegans* is composed of five molecules which are DBL-1, DAF-7, UNC-129, TIG-2 and TIG-3. Based on the structural information, DAF-7 and TIG-3 are TGF-β-like ligands, while DBL-1, TIG-2 and UNC-129 are BMP-like ligands. *daf-7* encodes the first discovered ligand of TGF-β family in *C. elegans* [97], which is primarily expressed in the nervous system. DAF-7 is produced under favorable environmental conditions to promote larval development by blocking dauer formation [97, 98]. Furthermore, it has been shown to regulate longevity and fat storage [99, 100]. DPP/BMP-like ligand (DBL-1) is the ligand component of Sma/Mab pathway required for an array of processes such as body size regulation and cell fate specification [56, 101]. *dbl-1* is primarily expressed in nervous system from which it regulates aversive olfactory learning [102], however its expression site for its function in body size regulation is not important [103]. The uncharacterized members of the *C. elegans* TGF-β family are transforming growth factors 2 and 3 (TIG-2 and TIG-3). To date, these ligands have not been associated with either the Sma/Mab nor dauer pathway, therefore they might be acting through an unknown non-canonical mechanism. *tig-2* expression has been reported to be in the nervous system and pharyngeal muscle [104, 105], whereas the only available expression information on *tig-3* is the single cell sequencing data which shows a very low expression levels across different tissue types such as intestine, germline, hypodermis and nervous system [106].

The last ligand member of the *C. elegans* TGF-β family is UNC-129, which shares conserved domains of TGF-β family ligands, however no function through TGF-β family signaling has been reported. *unc-129* is primarily expressed in the nervous system and body wall muscle [107] and its aberrant or ectopic expression leads to axon guidance defects [107, 108]. As a result of damaged muscle innervations, *unc-129* mutants

display an uncoordinated movement – hence the name “unc” for this gene [107]. Interestingly, this uncoordinated movement has not been reported for any other mutant strains of TGF-β family components. In addition, *unc-129* mutant animals do not display an altered body size or a dauer-related phenotype, therefore these findings suggest that UNC-129 acts independently of TGF-β family receptors in a non-canonical manner. The expression of *unc-129* in ventral body wall muscles is inhibited by the forkhead transcription factor UNC-130 [109], which limits *unc-129* expression to the dorsal body wall muscles and the resulting UNC-129 gradient acts as guidance cues for axon pathfinding [107, 109]. Interestingly, mutations in the components of netrin signaling have been shown to cause axon guidance defects, similar to *unc-129* mutant animals [107]. Furthermore, UNC-129 binds to one of the netrin receptors, UNC-5, and has been shown to enhance netrin signaling [108]. These findings indicate that UNC-129 modulates netrin signaling and its function in TGF-β family signaling is yet to be discovered.

1.6.2 Receptors

As previously mentioned in detail, TGF-β family ligands signal through two types of receptors, type I and type II. *daf-4* encodes the only TGF-β family type II receptor in *C. elegans*, whereas DAF-1 and SMA-6 are the type I receptors that act with DAF-4 in dauer and Sma/Mab pathways, respectively [96]. These receptors are single-pass serine/threonine kinases and contain the conserved generic domains. *daf-4* encodes a TGF-β-like receptor that resembles human activin type II receptor B (ActIIRB). Furthermore, this protein is highly conserved as it has been shown to bind to human BMP ligands *in vitro* [110]. *daf-4* is expressed in a wide range of tissue types such as hypodermis, intestine and body wall muscle [111, 112]. Being the only type II receptor, DAF-4 functions both in Sma/Mab and dauer pathways, therefore its loss leads to many developmental phenotypes such as small body size and dauer-constitutive state [96]. The first *C. elegans* TGF-β family type I receptor discovered was DAF-1 [113] which acts in the dauer pathway with DAF-4. *daf-1* is primarily expressed in the nervous system [112] and is involved in many processes such as dauer formation, egg-laying and fat storage [113, 114]. According to the canonical TGF-β signaling, DAF-1 is

activated by DAF-4 in order to function, however DAF-1 has been shown to be weakly active in the absence of DAF-4 [112].

The second TGF-β family type I receptor in *C. elegans* is SMA-6 that acts in the Sma/Mab pathway with DAF-4 [96]. *sma-6* is expressed in the pharynx, hypodermis and intestine as well as in the male tail. *sma-6* expression starts in early embryogenesis and is maintained throughout life. During the L1 and L2 larval stages, *sma-6* expression escalates remarkably in the pharynx and distal posterior region of the animal. Subsequently, expression starts in the posterior part of the intestine and propagates anteriorly [57, 102, 115]. In the hypodermis, *sma-6* expression starts in the mid-embryonic stage and continues through adulthood and it has been reported that this hypodermal expression is essential and sufficient for body size regulation [115].

SMA-6 has a molecular weight of 72.2 kD, composed of 636 amino acids, and it shares 65.4% sequence homology with human bone morphogenetic protein receptor 1A (BMPR1A). It has the three SG repeats of the GS domain, but lacks the tyrosine residues which suggests SMA-6 might not have tyrosine kinase activity in addition to its serine/threonine kinase activity [96]. In the extracellular domain, there is a putative ligand-binding domain that is enriched in cysteine residues. This motif is also conserved with the human TGF-β type I receptor with the consensus sequence $CCX_{4-5}CN$ [96]. However, studies of this region are limited since the major focus of ligand-binding is on TGF-β type II receptors. Although human TGF-β type I and II receptors have been shown to operate as tetrameric structures, there is no clear evidence whether the tetramer formation is essential for proper function.

In order for receptors to function properly, their intracellular trafficking between the plasma membrane and cytosol is crucial as impaired transportation of receptors has been reported to interfere the strength and timing of signaling pathways [96, 116, 117]. What makes the TGF-β pathway unique is that signaling occurs through two different receptors unlike the other signaling mechanisms such as Wnt, Hedgehog and Notch pathways. Therefore, this indicates additional regulatory layers may be involved. After signaling takes place, receptors are internalized to the cytosol. Here, they are either transported to the lysosome for degradation, and hence termination of signaling or directed back to the plasma membrane for more cycles of signaling. The recycling

occurs via early endosomes or retromers, proteins that are required for transporting the cargo to Golgi and eventually to the plasma membrane [96].

The existence of two receptors in the TGF-β pathway poses the question as to whether these receptors are recycled separately. Interestingly, Gleason et al. found that SMA-6 and DAF-4 are recycled via distinct pathways [117]. They showed that absence of the receptor-mediated endocytosis protein 1 (RME-1) caused distinct effects on SMA-6 and DAF-4 transportation in which DAF-4 has been shown to be accumulated in vesicles, whereas the levels of SMA-6 declined significantly due to inappropriate degradation. Furthermore, they found that SMA-6 interacts with VPS-35, a component of the retromer complex and removal of VPS-35 caused the same SMA-6 degradation detected in *rme-1* mutants. In contrast, DAF-4 transport was not affected in the absence of VPS-35, however it was disrupted in the absence of a small GTPase ARF-6 [117], which mediates a retromer-independent receptor trafficking process [118]. These findings indicate that receptor trafficking of TGF-β type I and type II receptors are controlled by distinct pathways which could be critical to dissect their functions.

1.6.3 Smads

The Smad family in *C. elegans* is composed of SMA-2, SMA-3, DAF-8, DAF-14 (R-Smads), SMA-4 and DAF-3 (co-Smads). DAF-8, DAF-14 and DAF-3 function in dauer pathway, while SMA-2, SMA-3 and SMA-4 – the founding members of Smads - are involved in the Sma/Mab pathway [55, 96]. Therefore, each pathway possesses an individual co-Smad which makes *C. elegans* unique. SMA-2 and SMA-3 form a heterotrimeric complex with SMA-4 after phosphorylation by SMA-6 and then translocate to the nucleus to regulate target gene expression (Fig. 1.5) This was the first finding that showed multiple Smads function in the same pathway [55]. As in humans, Smads harbour two conserved domains, MH1 and MH2, and an unconserved linker region. SMA-2 has the SSXS motif at the carboxyl terminus which is important for phosphorylation. However, SMA-3 contains one serine residue in that region which is potentially phosphorylated by SMA-6.

R-Smads of the dauer pathway – DAF-8 and DAF-14 – structurally resemble TGF-β-like Smads, although they display differences in their structure and function compared

to the Smads of Sma/Mab pathway. For instance, DAF-14 does not possess the conserved MH1 domain, which contains DNA binding and nuclear localization sequences [96]. Furthermore, the co-Smad DAF-3 has been shown to antagonize DAF-8 and DAF-14, in contrary to the co-Smad SMA-4 in Sma/Mab pathway [111].

In addition to these Smads, *C. elegans* possess TAG-68, which is a potential inhibitory Smad (I-Smad) based on its structure. *tag-68* expression has been detected in head muscle and neurons as well as in ventral nerve cord and intestine [119], however its precise function is yet to be identified.

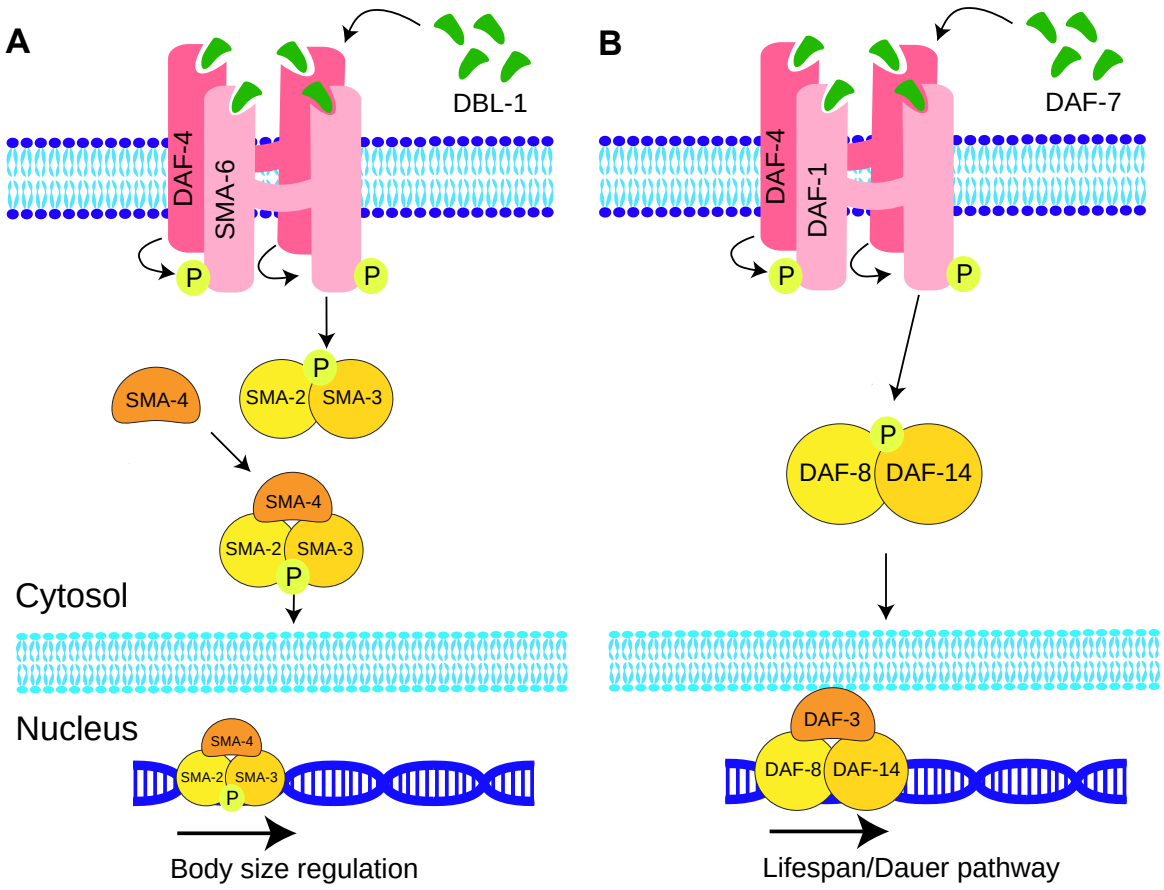

Fig. 1.5. TGF-β family signaling in *C. elegans*.

(A) The Sma/Mab pathway that regulates body size. Mutation of any components in this pathway results in small body size and abnormal male tail. (B) Dauer pathway controls the dauer formation that occurs under unfavorable environmental conditions. Mutation in the genes regulating the pathway results in dauer formation even under the favorable conditions.

1.6.4 Intracellular and extracellular regulators

As mentioned earlier, Smads possess low affinity to DNA, therefore they require binding partners to initiate transcriptional activation or repression. SMA-9, a Schnurri homolog acts with Smads in the Sma/Mab pathway to promote body growth, however it antagonizes Smads in cell fate specification [101, 120]. *daf-5* encodes a member of Sno/Ski family proteins, which binds to DAF-3 for a potential transcriptional repression of DAF-8 and DAF-14 in dauer formation [121, 122].

The activity of TGF-β family members are also controlled by extracellular regulators. *sma-10* encodes a transmembrane protein that is a member of leucine-rich repeats and immunoglobulin-like domains (LRIG) family. SMA-10/LRIG is a positive regulator of body size and has been shown to be interact with SMA-6 and DAF-4 receptors *in vitro* [123]. Furthermore, the absence of SMA-10 results in SMA-6 accumulation in cells, and therefore disruption of Sma/Mab signaling [124]. ADT-2, a secreted metalloprotease belongs to ADAMTS family, is another positive regulator of body size which is required for cuticle development [125]. In contrast, LON-2 – a heparin sulfate proteoglycan core protein- negatively regulates Sma/Mab signaling by binding to DBL-1 and preventing its binding to the receptors. Corroborating these findings, *lon-2* mutation leads to increased worm body size [45].

1.6.5 Sma/Mab Pathway

The Sma/Mab pathway controls many processes such as body size, innate immunity, reproductive aging and cell fate specification [96]. Initial findings regarding Sma/Mab pathway was on *daf-4* which encodes the *C. elegans* ortholog of TGF-β family type II receptor. *daf-4* mutant animals displayed small body size (Sma) and males possessed abnormally shaped tails (Mab), therefore became the founding member of the Sma/Mab pathway [96].

The DPP/BMP-like ligand (DBL-1) is the secreted ligand that initiates the Sma/Mab signaling. This ligand acts through to the type II receptor DAF-4 which in turn activates the type I receptor SMA-6. The R-Smads activated by SMA-6 are SMA-2 and SMA-3 while SMA-4 is the co-Smad. Upon activation, these Smads form a complex,

translocate into nucleus and act as transcriptional regulators [96]. For their binding to DNA, SMA-9/Schnurri acts as a co-factor for transcriptional regulation in a context-dependent manner as it promotes the DBL-1 signaling in body size regulation [120], while antagonizing in mesoderm differentiation [101].

Sma/Mab pathway activity is crucial for correct body size development as mutations in the components of this pathway result with decreased body size [55, 56]. Interestingly, these mutants possess the same number of cell nuclei compared to wild-type animals [126], implying that the displayed small phenotype is attributable to decreased cell size rather than lower cell number. Yoshida et al. showed that hypodermal rescue of *sma-6* in *sma-6* mutant animals restores the wild-type body size, whereas intestinal and pharyngeal muscle *sma-6* expression were found dispensable for body size regulation [115]. In another study, hypodermal *sma-3* expression was also found to be required for normal body size [127], which suggests that body size is regulated through hypodermis. In contrary to the strict requirement of *sma-3* and *sma-6* expression in hypodermis, rescue of the Sma/Mab ligand DBL-1 in various tissues such as hypodermis, pharyngeal muscle and VNC neurons restored the body size of *dbl-1* mutants [103]. Furthermore, overexpression of *dbl-1* has been shown to cause longer body size compared to wild-type worms [56], therefore these findings suggest that the level of DBL-1, but not site of expression, is critical for the regulation of body size via Sma/Mab signaling. The regulation of body size by DBL-1 signaling has been shown to be through direct and indirect transcriptional regulation of cuticle collagen genes such as *col-41*, *col-141* and *col-142* [128]. This process occurs in a stage-specific manner as these genes can be positively or negatively regulated by DBL-1 signaling through Smad activity depending on the developmental stage of the worm [128].

The role of TGF-β family signaling in immunity is conserved across many organisms including humans, *Drosophila* and *C. elegans* [129]. *C. elegans* possesses innate immunity which has been shown to be controlled by action of multiple mechanisms including Sma/Mab pathway [129]. This was identified by comparing the mRNA transcripts of wild-type worms with worms infected by the gram-negative bacteria *Serratia marcescens*. In the infected worms, the levels of lipases and lysozymes, known targets of TGF-β pathway, were elevated [130]. Furthermore, loss of DBL-1 was found to increase the susceptibility to bacterial infection [130]. A microarray study that

compares the *dbl-1* overexpression and loss of function also showed elevated pro-immunity genes encoding lysozymes in *dbl-1* overexpression condition [131]. Taken together, these findings present the importance of Sma/Mab pathway in the regulation of immune response.

Another function of the Sma/Mab pathway is the regulation of cell fate specification which was identified in an EMS screen on worms that display altered numbers of coelomocytes [101]. The critical gene identified in this screen was *sma-9* which encodes a Schnurri homolog and has previously been shown to regulate body size and male tail development as a downstream component of Sma/Mab Pathway [132]. It has been shown that mutation of *sma-9* results with transformation of dorsal M lineage-derived cells into ventral M lineage-derived cells, whereas mutations in the other components of Sma/Mab pathway did not cause a phenotype in this context [101]. In contrast, mutating Sma/Mab pathway components in *sma-9* mutant animals resulted with the suppression of M-lineage defects, while not causing any change on the altered body size [101]. This shows that Sma/Mab signaling regulates mesodermal patterning in a unique way. The role of Sma/Mab pathway in cell fate specification is not limited by hermaphrodites. Savage et al. identified that the loss of the components of this pathway interferes with the specification of male sensory rays which are required for recognizing vulva of hermaphrodites during mating [55].

Recent findings show that the role of Sma/Mab pathway is not limited by these processes. Qi et al. showed that SMA-3 interacts with the insulin signaling transcription factor DAF-16 to promote germline proliferation [133]. Clark et al. found that another process requires an interplay between Sma/Mab and insulin signaling, in which DAF-2 acts downstream of DBL-1 signaling to control lipid metabolism [134]. Taken together, these findings show that the activity of Sma/Mab pathway is vital for the development *C. elegans*.

1.6.6 Dauer Pathway

Under adverse environmental conditions such as starvation and high temperature, worms undergo an alternative larval stage called dauer. In this form, worms can survive up to 4 months and when the environmental conditions become more favorable, they

continue their development through to adulthood [62]. This alternative developmental stage is controlled by TGF-β family signaling, specifically the dauer pathway. In the dauer pathway, a TGF-β-like ligand DAF-7 acts through the sole type II receptor DAF-4 and type I receptor DAF-1. DAF-8 and DAF-14 are the R-Smads, whereas DAF-3 is the co-Smad [96]. Under favorable environmental conditions, dauer formation is blocked due to DAF-7 activity from ASI neurons and loss of DAF-7 results with dauer-constitutive phenotype [97, 98]. In contrast to the Sma/Mab pathway, the co-Smad DAF-3 acts antagonistically with the other components of dauer pathway as the loss of this co-Smad leads to dauer-defective phenotype [111]. DAF-5 has been identified as the suppressor of dauer-constitutive phenotype of *daf-7* mutant animals and loss of DAF-5 has been shown to phenocopy the dauer-defective phenotype of *daf-3* mutant animals [121]. In a later study, it was shown that *daf-5* encodes a novel protein that belongs to the Sno/Ski superfamily and the encoded protein binds to DAF-3 according to the yeast two-hybrid experiments [122]. Therefore, it was suggested that DAF-5 acts with DAF-3, downstream of the dauer pathway as the co-factor of transcriptional regulation. In addition to TGF-β family pathway, insulin and guanylyl cyclase pathways have been identified as regulators of dauer formation acting in parallel with TGF-β family pathway [96] as the double mutant generation among the components of these pathways leads to increased severity in dauer phenotype of single mutants [121].

Another process mediated by the activity of TGF-β-related dauer pathway and insulin pathway is aging. In *C. elegans*, *daf-2* encodes the sole insulin receptor. It has been shown that the *daf-2* mutants display an increased lifespan compared to the wild-type worms [135]. Furthermore, mutations in the components of the dauer pathway such as DAF-7 also result with increased longevity and this function of DAF-7 has been shown to be through regulating the location of DAF-16 - a transcription factor in insulin pathway - as well as regulating the expression of DAF-16-regulated genes [100]. This suggests that TGF-β-related dauer pathway regulates longevity through insulin pathway.

The TGF-β-related dauer pathway also regulates fat metabolism [99]. In *C. elegans*, fat is stored in the hypodermis and intestine. Fat storage is especially critical prior to dauer formation as fat becomes the source of energy in dauer larvae [99]. It has been shown that loss of DAF-7 leads to increased fat storage which is also suppressed by

mutations in *daf-3* [114]. The regulation of fat storage by DAF-7 signaling is achieved through RIM and RIC interneurons [114].

These findings show that TGF-β family pathway controls an array of biological processes, however their role in neurodevelopment is poorly understood and requires further investigation.

1.7 Thesis overview

Correct function of neurons requires signaling molecules that guide neurons to their specific location in the body. Disruption of these signals can result in neurological diseases. TGF-β family signaling is a highly conserved pathway that orchestrate a wide range of fundamental processes during development, however, its role in neuronal migration and axon guidance is not clear. This thesis focuses on the role of TGF-β family signaling in neuronal development using the hermaphrodite-specific neurons (HSN) of *C. elegans* as a model. We predict that the mechanisms identified in this project will have wide-ranging implications in TGF-β family pathway and its importance in neuronal development and diseases.

AIM 1: Investigating the Sma/Mab and dauer pathways in HSN development

The two TGF-β family pathways in *C. elegans* – Sma/Mab and dauer pathways – were investigated for their role in neuronal development. Mutant components of these pathways as well as their extracellular and intracellular regulators were crossed with *HSN::GFP* reporter strains and their HSN phenotypes examined. In addition, the focus of action for TGF-β family signaling was investigated by performing tissue-specific rescue experiments.

AIM 2: Characterizing the structural forms and functions of TGF-β family ligands in HSN development.

The role of TGF-β family ligands in HSN development were investigated. Mutant strains of these ligands were crossed with *HSN::GFP* reporter strains and their HSN phenotypes examined. Furthermore, the HSN phenotypes of double mutants of TGF-β family ligands among each other as well as with the TGF-β family type I receptor

SMA-6 were examined in order to investigate a potential convergent role among these molecules. Finally, interactions between SMA-6 and specific TGF-β family ligands were examined using mammalian HEK293T cells.

AIM 3: Identifying the transcriptional targets of TGF-β family pathway in HSN development

In order to identify the downstream targets of TGF-β family signaling in HSN development, RNA sequencing was performed using *sma-3* mutants as well as wild-type animals. Based on statistical significance and biological relevance, candidate genes differentially expressed in *sma-3* mutants compared to wild-type animals were selected and their role in TGF-β-mediated HSN development were investigated by conducting RNAi experiments.

2. Materials and Methods

2.1 Materials

2.1.1 Chemicals and reagents

- 1X Bolt™ Sample Reducing Agent (Life Technologies)
- 1X D-PBS (Life Technologies)
- 1X MOPS running buffer (Life Technologies)
- 4X Bolt LDS Sample Buffer (Thermo Fisher Scientific)
- 6X Loading Dye Solution (Fermentas)
- 30% Acrylamide/Bis Solution, 37.5:1 (Bio-Rad)
- Agar (Merck)
- Ammonium persulfate (APS) (Merck)
- Ampicillin sodium salt (Astral Scientific Pty. Ltd., Gymea, NSW, Australia)
- Bovine serum albumin (BSA) (Merck)
- Cholesterol (Merck)
- Chloroform - isoamyl alcohol mixture (Fluka Analytical, now Merck)
- cOmplete™, EDTA-free Protease Inhibitor Cocktail (Merck)
- CutSmart® Buffer (New England Biolabs)
- Deoxynucleotide triphosphates (dNTPs) (Fisher Biotech, Australia)
- DMEM (Life Technologies)
- Dynabeads Protein G (Thermo Fisher Scientific)
- Ethanol (Merck)
- Ethidium bromide solution (Merck)
- Ethylenediaminetetraacetic acid (EDTA) (Ajax Finechem Pty. Ltd.)
- EZ-ECL Chemiluminescence Detection Kit for HRP (Biological Industries)
- Fetal Bovine Serum, qualified, USDA-approved regions (Thermo Fisher Scientific)
- GenerulerTM DNA ladder mix (Progen Industries, Darra, QLD, Australia)
- Isopropanol (Merck)
- Isopropyl β-D-1-thiogalactopyranoside (IPTG) (Biochemicals, Gymea, NSW, Australia)
- Lipofectamine 2000 transfection reagent (Thermo Fischer Scientific)

- Magnesium sulfate heptahydrate (Merck)
- Methanol (Merck)
- Nonyl phenoxypolyethoxyethanol [NP-40 (Igepal)) (Merck]
- Opti-MEM® I - Glutamax™-I (Thermo Fisher Scientific)
- Peptone (Merck)
- Potassium chloride (BDH Chemicals, Port Fairy, VIC, Australia)
- Potassium dihydrogen phosphate (Merck)
- Sodium chloride (Merck)
- Sodium dodecyl sulfate (Merck)
- Sodium hydroxide (Ajax Finechem Pty. Ltd.)
- Sodium hypochlorite 12.5% w/v solution (Nuplex Industries (Australia) Pty. Ltd., Seven Hills, Australia)
- Tetramethylethylenediamine (TEMED) (Merck)
- Tris-hydroxymethyl-methylamine (Tris) (Ajax Finechem Pty. Ltd.)
- Triton X-100 (Merck)
- TRIzol™ Reagent (Invitrogen™)
- Tween 20 (AMRESCO LLC, Solon, OH, USA)
- UltraPure™ Agarose (Invitrogen™)

2.1.2 Enzymes

- FastAP Thermosensitive Alkaline Phosphatase (Thermo Fisher Scientific)
- FastDigest HindIII (Thermo Fisher Scientific)
- FastDigest KpnI (Thermo Fisher Scientific)
- FastDigest DpnI (Thermo Fisher Scientific)
- FastDigest NcoI (Thermo Fisher Scientific)
- FastDigest NheI (Thermo Fisher Scientific)
- KLD Enzyme Mix (New England Biolabs)
- Phusion® High-Fidelity DNA Polymerase (New England Biolabs)
- Proteinase K (Boehringer Ingelheim Pty. Ltd., North Ryde, NSW, Australia)
- Q5® High-Fidelity DNA Polymerase (New England Biolabs)
- RNAse-Free DNase (Qiagen)

- T4 DNA ligase (New England Biolabs)
- T4 Polynucleotide Kinase (New England Biolabs)

2.1.3 Antibodies

- Goat anti-Rabbit IgG (H+L) secondary antibody, HRP conjugate (65-620, Thermo Fisher Scientific)
- Goat anti-Mouse IgG (H+L) secondary antibody, HRP conjugate (32430, Thermo Fisher Scientific)
- Mouse anti-FLAG/DYKDDDDK tag antibody (2368, Cell Signaling)
- Mouse anti-Histidine tag antibody (AD1.1.10, Bio-Rad)
- Mouse anti-V5 tag antibody (SV5-Pk1, Bio-Rad)
- Rabbit anti-Myc tag antibody (ab9106, abcam)

2.1.4 Plasmids

Plasmids used in this thesis were listed in Table 2.x. OFB represents the plasmids generated by myself.

Table 2.1. Plasmids used in this thesis.

Plasmid name	Plasmid content	Source
RJP346	*pdpy-7::sma-6*	OFB
RJP409	*unc-129::V5*	OFB
RJP410	*tig-3::HIS*	OFB
RJP411	*ptph-1::sma-6*	OFB
RJP521	*⊿sma-6::MYC*	OFB
RJP152	*tig-2::FLAG*	Pocock lab
RJP349	*sma-6::MYC*	Pocock lab
pRG62	*pelt-3::sma-6::GFP*	Richard Padgett

Plasmid name	Plasmid content	Source
pcDNA™ 3.1/Zeo(+)	Empty backbone	Thermo Fisher Scientific
pcDNA-Wnt3A-V5	Empty backbone	Addgene
pCF90	*pmyo-2::mCherry::unc-54 3'UTR*	Erik Jorgensen (Addgene plasmid 19327)
pPD95.75	Empty backbone	Andrew Fire
pTB80	*pdpy-7::GFP*	Oliver Hobart
L4440	Empty backbone	Andrew Fire (Addgene plasmid 1654)
L4440	*sgk-1*	Vidal library
	slt-1	Vidal library
	vab-8	Ahringer library
	nlr-1	Ahringer library
	max-1	Ahringer library
	lad-2	Ahringer library
	kpc-1	Ahringer library
	sdn-1	Ahringer library
	vab-19	Ahringer library
RJP428	*mec-1* RNAi	OFB
RJP430	*mboa-6* RNAi	OFB
Plasmid name	Plasmid content	Source
pDD162	*peft-3::cas-9*	Addgene
RJP522	*peft-3::cas-9* + *daf-4* sgRNA 1	OFB
RJP523	*peft-3::cas-9* + *daf-4* sgRNA 2	OFB

2.1.5 Commercial kits

- ImProm-II™ Reverse Transcription System (Promega)
- In-Fusion® HD Cloning Kit (Takara Bio, USA)
- Q5® Site-Directed Mutagenesis Kit (NEB)
- QIAprep Spin Miniprep Kit (Qiagen)
- QIAquick Gel Extraction Kit (Qiagen)
- QIAquick PCR Purification Kit (Qiagen)
- RNeasy® Mini Kit (Qiagen)

2.1.6 Equipment

- ChemiDoc XRS+ Gel Documentation System (Bio-Rad)
- Compact Digital Rocker (Thermo Fisher Scientific)
- Eppendorf MasterCycler EP S Thermal Cycler (Eppendorf AG, Hamburg, Germany)
- EVE™ Automatic Cell Counter (Alpha Metrix Biotech)
- iBlot™ 2 Gel Transfer Device (Thermo Fisher Scientific)
- iBlot™ 2 Transfer Stacks, PVDF (Thermo Fisher Scientific)
- Mini Gel Tank (Thermo Fisher Scientific)
- Nanodrop1000 Spectrophotometer (Thermo Fisher Scientific)
- Olympus MVX10 fluorescence microscope with X-Cite® 120Q lamp (formerly Lumen Dynamics, now Excilitas Technologies, Waltham, MA, USA)
- Olympus BX51 microscope fitted with an Olympus F-View II camera (Olympus)
- Olympus SZ51 stereo microscope (Olympus Corporation, Shinjuku-ku, Tokyo, Japan)
- P-97 Flaming/Brown micropipette puller (Sutter Instrument Co., Novato, CA, USA)
- Tube Revolver/Rotator (Thermo Fisher Scientific)
- Zeiss Axio Imager M2 microscope fitted with Zeiss Axiocam 506 mono camera (Zeiss, Oberkochen, Germany)
- Zeiss Axio Vert A1 microscope fitted with Eppendorf FemtoJet 4X and Eppendorf InjectMan 4 (Eppendorf)

2.1.7 Software

- Adobe Photoshop (Adobe Inc., San Jose, CA, USA)
- Adobe Illustrator (Adobe Inc., San Jose, CA, USA)
- Excel 2017 (Microsoft Corporation, Redmond, WA, USA)
- Graphpad Prism® (GraphPad Software, San Diego, CA, USA)
- ImageLabTM software (Bio-Rad)
- Serial Cloner 2.6.1 (Serial Basics)
- Zen 2 pro (Zeiss)
- 2.1.7 Bacterial strains
- OP50 Escherichia coli (E. coli)
- HT115 (DE3) E. coli [F-, mcrA, mcrB, IN(rrnD-rrnE)1, rnc14::Tn10(DE3 lysogen: lavUV5 promoter -T7 polymerase]
- NEB® 5-alpha Competent E. coli (High Efficiency) (NEB)

2.1.8 *C. elegans* strains

In *C. elegans*, gene names are written in lowercase italics, while protein names are written in uppercase non-italics. P in front of a gene name represent promoter. Chromosome names are written in roman numerals except X being the sex chromosome. Strains that carry transgenes as extrachromosomal arrays include Ex in their genotype information, whereas integrated transgenes are written as Is. External strains were obtained from Caenorhabditis Genetics Center (CGC), Shohei Mitani [Tokyo Women's Medical University School of Medicine, Japan Japanese National Bioresource Project for the Experimental Animal Nematode C. elegans (NBP)], Yun Zhang (Harvard University, USA) and Gary Ruvkun (Harvard University, USA). OFB represents the strains generated by myself.

Table 2.2. Strains used in this study.

Code	Genotype	Source
N2	Wild-type, Bristol strain	CGC
AH205	*sdn-1(zh20)* X	CGC
CB1364	*daf-4(e1364)* III	CGC
CB1372	*daf-7(e1372)* III	CGC
CB1376	*daf-3(e1376)* X	CGC
CB1393	*daf-8(e1393)* I	CGC
CB1482	*sma-6(e1482)* II	CGC
CB502	*sma-2(e502)* III	CGC
CS389	*adt-2(wk156)* X	CGC
CS619	*sma-3(wk30)* III*; qcIs59*	CGC
CS67	*sma-9(qc3)* X	CGC
CX5000	*slt-1(eh15)* X	CGC
DH1201	*rme-1(b1045)* V	CGC
DR1369	*sma-4(e729)* III	CGC
DR63	*daf-4(m63)* III	CGC
DR77	*daf-14(m77)* IV	CGC
LT121	*dbl-1(wk70)* V	CGC
LT186	*sma-6(wk7)* II	CGC
NW427	*vab-8(ev411)* V	CGC
NW987	*unc-129(ev554)* IV	CGC
RB1739	*sma-10(ok2224)* IV	CGC

Code	Genotype	Source
RB2476	*tig-2(ok3416) V*	CGC
SK4013	*zdIs13 [ptph-1::GFP] IV*	CGC
VC2197	*sma-6(ok2894) II*	CGC
VC547	*daf-4(ok828) III*	CGC
ZC1334	*sma-6(wk7) II; yxEx615 [psma-6::sma-6; punc-122::gfp]*	Yun Zhang
ZC1398	*sma- 6(wk7) II; yxEx660 [pelt-2::sma-6; punc-122::gfp]*	Yun Zhang
ZC1573	*sma-6(wk7) II; yxEx765 [pges-1::sma-6; punc-122::gfp]*	Yun Zhang
GR1333	*mgIs71 [tph-1::gfp, rol-6(su1006)]*	Gary Ruvkun
arf-6	*arf-6(tm1447) IV*	Shoei Mitani (NBP)
snx-3	*snx-3(tm1595) I*	Shoei Mitani (NBP)
tig-3	*tig-3(tm2092) II*	Shoei Mitani (NBP)
RJP18	*rpEx6 [ptph-1::GFP + psra-6::RFP]*	Roger Pocock
RJP582	*sdn-1(zh20) X; zdIs13 IV*	Roger Pocock
RJP1153	*daf-7(e1372) III; zdIs13 IV*	Roger Pocock
RJP1330	*tig-2(ok3416) V; zdIs13 IV*	Roger Pocock
RJP1334	*tig-3(tm2092) II; zdIs13 IV*	Roger Pocock
RJP1398	*sma-4(e729) III; zdIs13 IV*	Roger Pocock
RJP1551	*sma-6(wk7) II; zdIs13 IV*	Roger Pocock
RJP1554	*sma-2(e502) III; zdIs13 IV*	Roger Pocock
RJP1555	*daf-14(m77) IV; mgIs71*	Roger Pocock
RJP1611	*daf-8(e1393) I; zdIs13 IV*	Roger Pocock
RJP1917	*tig-2(ok3416) V; tig-3(tm2092) II; zdIs13 IV*	Roger Pocock

Code	Genotype	Source
RJP2018	*sma-6(e1482) II; zdIs13 IV*	Roger Pocock
RJP3228	*daf-3(e1376) X; zdIs13 IV*	Roger Pocock
RJP3333	*sma-3(wk30) III; zdIs13 IV*	Roger Pocock
RJP4505	*sma-6(wk7) II; sdn-1(zh20) X; zdIs13 IV*	Roger Pocock
RJP1553	*sma-6(wk7) II; zdIs13IV; yxEx615[sma-6p::sma-6; unc-122p::gfp]*	Roger Pocock
RJP3337	*daf-4(m63) III; zdIs13 IV*	OFB
RJP3519	*daf-4(e1364) III; zdIs13 IV*	OFB
RJP3520	*daf-4(ok828) III; zdIs13 IV*	OFB
RJP3603	*sma-6(wk7) II; tig-2(ok3416) V; zdIs13 IV*	OFB
RJP3755	*sma-6(ok2894) II; zdIs13 IV*	OFB
RJP3786	*dbl-1(wk70) V; zdIs13 IV*	OFB
RJP3800	*sma-6(wk7) II; rme-1(b1045) V; zdIs13 IV*	OFB
RJP3821	*unc-129(ev554) IV; rpEx6*	OFB
RJP3837	*sma-6(wk7) II; tig-3(tm2092) II; zdIs13 IV*	OFB
RJP3843	*rme-1(b1045) V; zdIs13 IV*	OFB
RJP3871	*arf-6(tm1447) IV; mgIs71*	OFB
RJP3894	*snx-3(tm1595) I; zdIs13 IV*	OFB
RJP4047	*daf-4(rp122) III; zdIs13 IV*	OFB
RJP4048	*daf-4(rp123) III; zdIs13 IV*	OFB
RJP4070	*sma-6(wk7) II; unc-129(ev554) IV; rpEx6*	OFB
RJP4158	*sma-6(wk7) II; zdIs13; yxEx765 [ges-1p::sma-6; unc-122p::gfp]*	OFB

Code	Genotype	Source
RJP4161	*unc-129(ev554) IV; tig-2(ok3416) V; rpEx6*	OFB
RJP4162	*unc-129(ev554) IV; tig-3(tm2092) II; rpEx6*	OFB
RJP4163	*unc-129(ev554) IV; tig-2(ok3416) V; tig-3(tm2092) II; rpEx6*	OFB
RJP4217	*sma-6(wk7) II; zdIs13 IV; rpEx1792 [ptph-1::sma-6::GFP + pmyo-2::mcherry]*	OFB
RJP4218	*sma-6(wk7) II; zdIs13 IV; rpEx1792 [ptph-1::sma-6::GFP + pmyo-2::mcherry]*	OFB
RJP4331	*sma-3(wk30) III; slt-1(eh15) X; zdIs13 IV*	OFB
RJP4332	*sma-3(wk30) III; vab-8(ev411) V; zdIs13 IV*	OFB
RJP4333	*vab-8(ev411) V; zdIs13 IV*	OFB
RJP4376	*adt-2(wk156) X; zdIs13 IV*	OFB
RJP4379	*sma-9(qc3) X; zdIs13 IV*	OFB
RJP4380	*sma-10(ok2224) IV; rpEx6*	OFB
RJP4446	*sma-6(wk7) II; zdIs13 IV; rpEx1904 [pelt-3::sma-6::GFP + pmyo-2::mCherry]*	OFB
RJP4447	*sma-6(wk7) II; zdIs13 IV; rpEx1905 [pelt-3::sma-6::GFP + pmyo-2::mCherry]*	OFB
RJP4448	*sma-6(wk7) II; zdIs13 IV; rpEx1906 [pelt-3::sma-6::GFP + pmyo-2::mCherry]*	OFB

2.1.9 Cell line

Human embryonic kidney cells, HEK293T, were used to perform biochemical experiments.

2.1.10 External procedures

- Sanger sequencing and RNA sequencing were performed by Micromon Sequencing Facility (Melbourne, Australia).
- Oligonucleotides were generated by Merck (Castle Hill, Australia).

2.2 Methods

2.2.1 Nematode maintenance

Worms were cultured at 20°C following standard protocol by Brenner [60]. Unless otherwise stated, experiments on worms were performed at 20°C. The Bristol strain N2 was used as wild-type. Worms were fed on *E. coli* OP50 that were grown on NGM plates at 20°C. All strains were backcrossed to N2s at least three times prior to scoring.

2.2.2 Genotyping

Genotype of the strains were determined by performing PCR reaction using following conditions. Sequences of the primers can be found in Appendix, Table 8.1.

Table 2.3. PCR reactions for genotyping.

Gene	Allele	Deletion size (bp)	Primers	Extension time (min:sec)	Product size (bp)
sma-6	*ok2894*	304	OFB77 OFB79	1:00	Wild-type: 827 Mutant: 523
rme-1	*b1045*	1526	OFB66 OFB68	2:00	Wild-type: 2113 Mutant: 587
arf-6	*tm1447*	2263	OFB81 OFB82	0:40	Wild-type: 653 Mutant: No band
snx-3	*tm1595*	482	OFB84 OFB86	1:15	Wild-type: 1191 Mutant: 709
tig-2	*ok3416*	804	GSN19 GSN18	1:15	Wild-type: 1188 Mutant: 384
tig-3	*tm2092*	703	GSN10 GSN9	1:05	Wild-type: 1086 Mutant: 383
slt-1	*eh15*	1945	OFB156 OFB158	2:15	Wild-type: 2358 Mutant: 413

2.2.3 Microscopy

Worms were mounted on 5% agarose pads and anesthetized with 15 µl 20 mM NaN_3. Imaging was performed with Zeiss AXIO Imager M2 fitted with an Axiocam 506 mono camera using the Zen 2 pro software (Zeiss).

2.2.4 Microinjections

Transgenic animals were generated by injecting young adult worms using the protocol by Mello [136]. Constructs were injected with a concentration ranging from 1 to 40 ng/µl

(Table 2.4). 5 ng/µl *pmyo-2::mcherry* plasmid was injected as a co-injection marker. Total concentration of DNA was made 150 ng/µl with digested bacterial DNA.

Table 2.4. Microinjections.

Purpose	Strain Injected	Plasmid/DNA	Concentration (ng/µl)
Hypodermal *sma-6* expression	N2	*pelt-3::sma-6::GFP*	10
		pmyo-2::mCherry	5
		Bacterial DNA	135
sma-6 expression in HSNs	N2	*ptph-1::sma-6*	10
		pmyo-2::mCherry	5
		Bacterial DNA	135
CRISPR targeting *daf-4*	N2	*peft-3::cas-9* + *daf-4* sgRNA 1	50
		peft-3::cas-9 + *daf-4* sgRNA 2	50
		pmyo-2::mCherry	5
		Bacterial DNA	45

2.2.5 CRISPR-Cas9

Two single guide RNAs (sgRNA) targeting the first exon of *daf-4* were designed using the CRISPR design tool [137] that is available at http://crispr.mit.edu. The sgRNAs, OFB123 and OFB124, were cloned into the Cas9 vector separately using In-Fusion® HD Cloning Kit (Takara Bio, USA) and were confirmed by Sanger sequencing. After that, these vectors were injected into wild-type worms at a final concentration of 50 ng/µl per construct. The *daf-4* CRISPR-knockout candidates were selected based on the small and/or dauer phenotype. Selected worms were put into separate plates and incubated at 15°C incubators for dauer recovery. After their recovery, the mutations were identified by Sanger sequencing using the PCR products amplified from different

regions of *daf-4* gene of the candidate worms. Based on the sequencing results, two independent alleles have been identified, named *rp122* and *rp123*, which possess frameshift mutations resulting with premature stop codons. After characterization of these alleles, they were backcrossed to N2s three times to remove potential unspecific background mutations.

Table 2.5. sgRNAs targeting *daf-4*.

Name	Target at *daf-4* locus	Sequence
OFB123	Exon 1	GCCCATTTCCTATAAGGTGC
OFB124	Exon 1	CTACAAGAACCTTACAAGAG

2.2.6 Molecular cloning

Constructs were generated using In-Fusion® HD Cloning Kit according to the manufacturer's instructions (Takara Bio, USA). Sequences were confirmed by Sanger sequencing. Detailed information about the individual constructs can be found in the methods sections of the experimental Chapters 3, 4 and 5.

2.2.7 Site-directed mutagenesis

Mutagenesis of the constructs were performed using Q5 Site-Directed Mutagenesis Kit according to the manufacturer's instructions (New England BioLabs, USA). Detailed information about the individual constructs can be found in the methods sections of the experimental chapters 3, 4 and 5.

2.2.8 HSN phenotype analysis

Neuronal phenotypes were examined in Day 1 adults using fluorescent reporter strains based on the position of cell bodies and axonal outgrowth. All the analyses were performed in three biological replicates and at least hundred worms were examined for each strain. The position of HSN neurons were determined with respect to vulva and

the seam cell daughters V1.a to V6.p. Cell bodies of the HSN neurons are situated slightly posterior to the vulva and axons run parallel to each other along the ventral mid line. For neuronal migration, cell bodies situated anterior to vulva and V4 seam cell were defined as overmigrated, while cell bodies situated posterior to V4 seam cell were defined as undermigrated. For axon guidance, the axons that joined in ventral midline or leave the ventral midline reported as defective.

2.2.9 RNA interference (RNAi)

RNAi clones were isolated from Ahringer Library and Vidal Library and sequenced using Sanger Sequencing. All the clones were grown in HT115 strain of *E. coli*. For the missing clones, molecular cloning was performed using In-Fusion® HD Cloning Kit. RNAi was performed using the feeding method (adapted from [138]). Briefly, L4-stage worms were picked onto empty NGM plates and let to crawl for 5 min to remove the residual OP50. Then, they were put onto plates that were uniformly seeded with HT115 that was transformed with a specific RNAi clone. F1 and F2 generations were scored for HSN phenotypes.

2.2.10 RNA sequencing analysis

Worm synchronization

Worms were cultured at 20°C and the extractions were performed in synchronized populations at L2 stage. L4-stage worms were picked onto the plates and grown for 4 days for N2s and 5 days for *sma-3(wk30)* mutant strain. After this period, the majority of the worms on the plate were Day 1 adults. These worms were bleached using bleaching solution (1.7 M NaOH, 2.1% v/v NaOCl) and the recovered eggs were added onto the new plates. 1000 eggs per plate were used. The worms were grown for 3 days for N2s and 4 days for *sma-3 (wk30)* mutant animals. At the end of this period, worms were washed away using M9 buffer (22 mM KH_2PO_4, 50 mM Na_2HPO_4, 86 mM NaCl, 1 mM $MgSO_4$) and the left eggs on the plates were chunked onto the new plates. After 30 hours of growing period, L2-stage worms were observed on the plates. These worms were collected into a 15-ml falcon tube using M9 buffer. After washing steps,

Trizol (Ambion) was added to the worms and the tubes were instantly frozen using liquid nitrogen. Tubes were stored at -80°C until extraction.

RNA extraction

Worms were cracked using freeze/thaw cycles between liquid nitrogen and 37°C. The freeze/thaw cycles were repeated seven times After the last cycle, tubes were put on ice for 30 sec and then vortexed for 30 sec. These ice/vortex cycles were repeated six times. After the last cycle, tubes were checked under microscope to make sure all the worms were cracked open. Tubes were left at RT for 5 min. 300 µl of chloroform was added and tubes were inverted for 15 sec. The rest of the experiment was performed following the manufacturer's protocol of RNA Isolation Kit by Qiagen.

RNA sequencing

The library preparation and RNA sequencing were carried out by Micromon Sequencing Facility (Melbourne, Australia).

2.2.11 Worm lysis

Worms grown on OP50-seeded NGM plates were washed into 0.2 ml tubes using lysis buffer [50 mM KCl, 10 mM Tris pH8.3, 2.5 mM $MgCl_2$, 0.45 % NP-40, 0.45 % Tween-20, 0.01 % gelatine and 0.5 mg/ml Proteinase K (Promega)]. Tubes were frozen at -80°C for 1 h and then placed into thermal cycler using following reaction: Incubation at 65°C for 60 min and at 95°C for 15 min. Lysates were stored at -20°C.

2.2.12 Molecular Biology

General molecular biology experiments were carried out using standard techniques. Primers were designed using Serial Cloner 2.6.1 software.

Polymerase chain reaction (PCR)

PCR method was used for cloning and genotyping purposes. Primers were designed using Serial Cloner 2.6.1 software and were ordered from Merck Aldrich (Merck) in 100 uM concentrations in water. The list of primers can be found in Appendix Table 8.1.

Table 2.6. PCR contents.

Reagent	Final Concentration (uM)	Volume (µl)
Betaine	-	5
Taq Buffer	1X	2.5
Forward primer	4	2
Reverse primer	4	2
dNTP mix	2	0.4
Taq Polymerase	-	0.5
Worm lysate	-	4
Water	-	8.6

Table 2.7. PCR conditions.

Step	Temperature (°C)	No. of cycles	Length (min:sec)
Initial Denaturation	95	1	5:00
Denaturation	95	35 cycles	0:30
Annealing	Variable		0:30
Extension	72		Variable*
Final Extension	72		5:00

* 1 min per kb

Agarose gel electrophoresis

In order to visualize nucleic acid fragments, agarose gel electrophoresis method was used. Agarose gel was prepared in 1% concentration of agarose in 1X TAE buffer and mixed with ethidium bromide as an intercalating agent for nucleic acids. Samples were mixed with loading dye and run for 30 min at 120 V and then screened using ChemiDoc™ XRS+ (Bio-Rad).

Plasmid growth and plasmid isolation

Plasmid growth was carried out by transforming DH5-alfa or HT115 strains of *E. coli*. Briefly, 1 µl plasmid was added to a tube of 40 µl cells and put on ice for 30 min. After ice incubation, the tube was placed in a water bath 42°C for 30 sec. Then it was put back on ice for 5 min. 200 ml of LB was added to the tube and the tube was incubated horizontally in a shaker at 37°C for 1 h. Finally, cells were seeded on an LB-ampicillin plate and incubated at 37°C overnight. Next day, a positive colony was picked into a tube of 5 ml LB-ampicillin and grown overnight at 37°C. Using this cell suspension, plasmid DNA was extracted using QIAprep Spin Miniprep Kit (Qiagen) according to the manufacturer's instructions.

Restriction endonuclease digestion

DNA fragments were cut using restriction endonuclease (re) enzymes for cloning purposes. Digestion mix was prepared according to Table 2.8 and mixtures were incubated at 37°C for 30 min.

Table 2.8. Digestion reaction.

Component	Volume/Amount
DNA	1 ug
Restriction enzyme(s)	1 µl per enzyme
Digest buffer	4 µl
Water	Up to 40 µl

Recovery of DNA after PCR

DNA was recovered using PCR purification or gel extraction methods using QIAquick Gel Extraction Kit (Qiagen) or QIAquick PCR Purification Kit (Qiagen) according to the manufacturer's instructions.

Quantification of nucleic acids

Nucleic acids extracted from organisms or recovered from gels were quantified using Nanodrop1000 Spectrophotometer (Thermo Fisher Scientific).

2.2.13 Cell culture

Maintenance

Human embryonic kidney (HEK293T) cells were cultured in T75 flasks using DMEM (Life Technologies) with 10% FBS (Thermo Fisher Scientific) and 5 µM L-glutamine (Life Technologies) at 37°C, 5% CO_2. Cells were frozen in 10% DMSO, 40% DMEM and 50% FBS mixture and stored at -80°C. When cells reach confluency, they were dissociated from the flasks by applying 2 ml trypsin EDTA 0.25% (Life Technologies) for 2 min. After dissociation, cell culture media was added to neutralize the cell suspension and cells were counted using EVE™ Automatic Cell Counter (Alpha Metrix Biotech). 2.5 x 10^5 cells per well in 6-well plates and 1.5 x 10^5 cells per well in 12-well plates were seeded for experimental use.

Cell transfection

To deliver DNA into the cells, Lipofectamine® 2000 reagent was used. 2.5 x 10^5 cells were seeded on 6-well plates one day before the transfection. 6 µg DNA and 12 µl Lipofectamine® 2000 reagent were diluted in 350 µl Opti-MEM® I - Glutamax™-I (Thermo Fisher Scientific) in separate tubes and incubated for 5 min. After incubation, DNA and lipofectamine dilutions were mixed and incubated for 20 min and then the mixture was added to the cells. Cells were mixed by gently rotating the plates and incubated for 6 h. After the incubation, mixture was replaced with standard culture media and cells were incubated for 18h, until cell lysis.

Cell lysis

Prior to lysis, cells were placed on ice and washed with ice-cold PBS for 3 times. After removing PBS, cells were lysed with 200 µl lysis buffer (50 mM Tris pH 7.4, 150 mM NaCl, 0.01% SDS, 1% Triton X-100 and protease inhibitor) per well of a 6-well culture dish. After lysis, cells were collected into 1.5 ml Eppendorf tubes using a cell scraper. Tubes were incubated in a rotator shaker at 4°C for 10 min and centrifuged at 10000 rpm for 10 min. Supernatants were collected and stored at -20°C until use. 20 µl from each sample was put in another tube and mixed with 20 µl elution buffer [2.5X Bolt LDS Sample Buffer (Thermo Fisher Scientific), 1X Bolt™ Sample Reducing Agent (Life Technologies)] to check input expression.

Co-immunoprecipitation

For protein-protein interaction experiments, co-immunoprecipitation (co-IP) method was performed using Dynabeads Protein G (Thermo Fisher Scientific). For all washing steps, a magnetic rack was used to collect the beads. Beads were washed with ice-cold PBS for 3 times before use and resuspended with lysis buffer. Each cell lysate was incubated with 15 µl beads for 30 min to remove and see the possible unspecific bindings. Beads were collected after incubation and stored at -20°C until use. After initial incubation with beads, lysates were collected and incubated with specific antibodies (1 µl of 1µg/ml antibody per sample) using a rotator shaker at 4°C for 4 h. Then, 20 µl of beads per sample was added to the samples and they were incubated at 4°C using a rotator shaker overnight. Next day, supernatants were removed and remaining beads were washed with ice-cold washing buffer (50 mM Tris pH 7.4, 150 mM NaCl, 1% Triton X-100, 1 mM EDTA and protease inhibitor) three times. Beads were resuspended with 20 µl elution buffer and stored at -20°C until use.

Sodium dodecyl sulfate-polyacrylamide gel electrophoresis (SDS-PAGE)

Proteins were separated according to their size using sodium dodecyl sulfate-polyacrylamide gel electrophoresis (SDS-PAGE). Stacking and resolving gels were prepared using the ingredients in Table 2.9.

Table 2.9. SDS-PAGE gel contents.

Stacking gel		Resolving gel (12%)	
Component	Volume (µl)	Component	Volume (ml)
Water	1799.5	Water	2.29
1M Tris-HCl, pH 6.8	313	1.5M Tris-HCl, pH 6.8	2.5
10% SDS	25	10% SDS	0.1
30% Acrylamide/Bis Solution, 37.5:1	345	30% Acrylamide/Bis Solution, 37.5:1	5
TEMED	5	TEMED	0.01
10% APS	12.5	10% APS	0.1

Beads and input tubes mixed with elution buffer were boiled at 95°C for 10 min and loaded onto the polyacrylamide gels. SDS-PAGE was performed at 100 V for 30 min and 120 for 90 min in a Mini Gel Tank (Thermo Fisher Scientific) filled with 1X MOPS running buffer (Life Technologies).

Transfer

Proteins were transferred from gel to a PVDF membrane in iBlot™ 2 Transfer Stacks (Thermo Fisher Scientific) using iBlotTM 2 Gel Transfer Device (Thermo Fisher Scientific) according to the manufacturer's instructions.

Western blot

After transferring proteins to a PVDF membrane, the membrane was placed in a PBS 5% bovine serum albumin (BSA) solution and incubated in a rotator at room temperature for 1 h. The membrane was incubated with primary antibody diluted in 5% BSA/PBST at 4°C overnight. The membrane was washed with PBST for three times and then incubated with secondary antibody at RT for 1 h. Membrane was washed three times with PBST, and proteins were detected using EZ-ECL Chemiluminescence Detection Kit for HRP (Biological Industries) on a ChemiDoc XRS+ Gel Documentation System (Bio-Rad Laboratories). Images were taken using Image Lab™ software.

2.2.14 Statistical Analysis

Statistical analysis was conducted using GraphPad Prism® software (GraphPad Software Inc.). The specific tests used for analysis of data, error bars and number of animals or conditions were stated in each figure legend. P values lower than 0.05 were considered as statistically significant.

3. The TGF-β family pathway regulates HSN development in a non-canonical manner

3.1 Abstract

Correct development of biological systems requires strict regulation of cellular processes such as cell migration, proliferation and differentiation. The transforming growth factor beta (TGF-β) pathway is a major player in these processes, however its role in neuronal migration and axon guidance is not fully understood. The roundworm *C. elegans* is an excellent model organism for studying neurons as it has a small nervous system composed of 302 invariantly positioned neurons and its whole neuronal wiring diagram has been mapped. The hermaphrodite-specific neurons (HSN) are particularly useful to study developmental process as they undergo long-range migration and axon guidance at distinct periods of development. In a candidate gene approach, I found that the loss of SMA-6, a type I receptor of TGF-β receptor, causes dysregulation of HSN development. In contrast, loss of DAF-4, which is the only type II TGF-β family receptor in *C. elegans* and is normally required for the activation of SMA-6, does not affect HSN development. This suggests that SMA-6 may regulate HSN development in a non-canonical manner. I further investigated the role of TGF-β family pathway components in the development of the HSNs and found that a subgroup of the intracellular TGF-β family pathway molecules, SMA-2, -3 and -4 are also required for this process. To further substantiate my findings on type-II-receptor-independent action of the type I receptor SMA-6, I analyzed how recycling events that control TGF-β receptor availability affect HSN development. It has been reported that SMA-6 recycling is regulated by the endosome protein RME-1, whereas DAF-4 recycling occurs via ADP-ribosylation factor 6 (ARF-6). I found that the loss of RME-1 has adverse effects on HSN development, whereas ARF-6 is dispensable for the same process, which confirms my previous findings. Finally, I have examined other regulators of the TGF-β family pathway and found that secreted metalloprotease ADT-2, which is required for body size regulation, is also required for HSN development. These findings reveal that a specific TGF-β signaling pathway is crucial for HSN development and the regulation of this process occurs in a non-canonical manner. Here I propose, for the first time, that a type I receptor can act independently of a type II receptor in the context of neuronal development with the help of specific intracellular and extracellular signaling molecules.

3.2 Introduction

TGF-β family signaling is a crucial pathway conserved in many organisms including the roundworm *Caenorhabditis elegans*. In this organism, the TGF-β family pathway is required for diverse biological processes such as body size regulation and innate immunity [96], however its role in neurodevelopment is unclear. The TGF-β signaling pathway is composed of many molecules that act in specific spatial and temporal contexts [5]. The TGF-β pathway components include extracellular ligands, receptors and intracellular signaling molecules. (More information on the generic TGF-β signaling can be found in Chapter 1). In *C. elegans*, these molecules are categorized into two sub-pathways called the Sma/Mab and dauer pathways (Fig. 3.1). The Sma/Mab pathway is important for body size regulation and male tail development while the dauer pathway controls dauer formation and innate immunity [96]. The TGF-β family type I receptors that coordinate these developmental and immunity processes are DAF-1 for the dauer/immunity pathway and SMA-6 for the Sma/Mab pathway. These receptors are regulated by the sole TGF-β family type II receptor called DAF-4, which is common for both pathways. Intracellular signaling molecules called Smads, which regulate transcription of TGF-β-pathway target genes, are SMA-2, SMA-3, and SMA-4 for the Sma/Mab pathway and whereas DAF-3, DAF-8 and DAF-14 are part of dauer pathway. The TGF-β family ligands are DBL-1 for the Sma/Mab pathway and DAF-7 for the dauer pathway [96]. In addition, there is another TGF-β family ligand called UNC-129, causes an uncoordinated phenotype and has not been shown to control any known TGF-β receptor to date [107]. Two other ligands of the TGF-β family are TIG-2 and TIG-3, for which little mechanistic information is available.

There are intracellular and extracellular components that control the signaling pathway. One of the extracellular regulators is SMA-10/LRIG, a member of the leucine-rich repeats and immunoglobulin-like domains (LRIG) family, which interacts with the TGF-β family receptors to mediate the binding of ligands [123]. Another extracellular regulator of the pathway is LON-2/glypican, which is a heparan sulfate proteoglycan core protein. It has a negative effect on the signaling by interfering with the interaction between the receptor and the ligand, which is required for maintaining a normal body size [45] and has been shown to regulate the HSN development [86]. In contrast, a secreted metalloprotease, ADT-2, positively regulates body size and is required for

proper cuticle development [125]. At the intracellular level, SMA-9, which is a homolog of *Drosophila* Schnurri, functions as a transcription factor by associating with Smads [120]. The least characterized member of the TGF-β family pathway is TAG-68. which is hypothesized to be an inhibitory Smad (I-Smad) molecule based on its structure [96]. I-Smads are intracellular regulators of TGF-β signaling [46]. They act in number of ways to inhibit the intracellular signaling, by acting in the degradation process of the TGF-β receptors, dephosphorylation of type I receptors or competing with receptor-activated Smads (R-Smad) [46]. TAG-68 has structural similarities with the vertebrate I-Smads Smad6 and Smad7, which further suggests an inhibitory function.

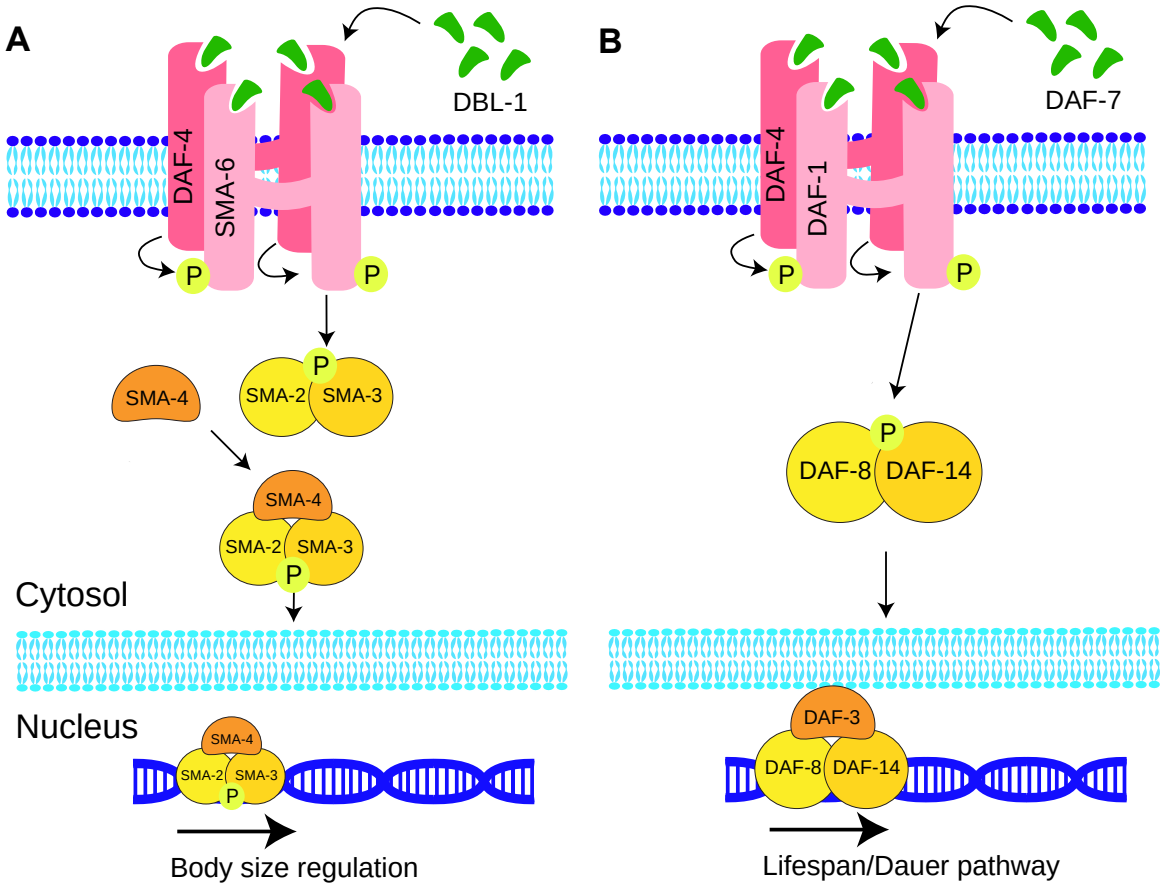

Fig. 3.1. Canonical TGF-β family pathways in *C. elegans*.

(A) illustrates the Sma/Mab pathway which is crucial for body size regulation and innate immunity while (B) illustrates the dauer pathway that controls dauer formation. These pathways share the type II receptor DAF-4, but have separate type I receptors, Smads and extracellular ligands. DBL-1 and DAF-7 are the ligands of the Sma/Mab and the dauer pathway, respectively. The Sma/Mab pathway has SMA-2 and SMA-3 as receptor-activated Smads (R-Smad) and SMA-4 as common-partner Smad (co-Smad), whereas the dauer pathway has DAF-8 and DAF-14 as R-Smads and DAF-3 as the co-Smad.

The TGF-β family signaling cascade commences with the binding of an extracellular ligand to a type II receptor (DAF-4 in *C. elegans)*, which enables the recruitment of a type I receptor (SMA-6 or DAF-1 in *C. elegans*) into the complex. Activation of the type I receptor occurs by the type II receptor. Activated type I receptor propagates signaling to the receptor-activated Smads (R-Smad) which are SMA-2, -3 or DAF-8, -14 in *C. elegans*. These molecules act with the common-partner Smad (co-Smad), SMA-4 or DAF-3 in *C. elegans*, to regulate the expression of target genes [96].

In order for signaling to occur properly, receptor recycling between the cell membrane and the cytosol is critical, and interference with this process can lead to impaired signaling [116, 117]. In the TGF-β family pathway, both type I and II receptors are targeted to the cell membrane in order to interact with extracellular ligands and intracellular Smad molecules. After this interaction, they are either recycled via endosomes or targeted to the lysosome for degradation. In *C. elegans*, this mechanism has been shown to be a complex process as the type I and type II receptors are recycled via distinct pathways [117]. According to this study, the type I receptor SMA-6 is recycled via a retromer complex. This process is regulated by the vacuolar protein sorting factor-35 (VPS-35), sorting nexin-3 (SNX-3) and RME-1, which is a receptor-mediated endocytosis protein. Conversely, type II receptor DAF-4 recycling is mediated by ADP-ribosylation factor-6 (ARF-6). These divergent recycling mechanisms makes *C. elegans* TGF-β family receptors unique from receptors in other systems.

TGF-β family signaling is associated with wide range of developmental disorders [139], however its role in the development of nervous system is poorly understood. As a model to examine this process in *C. elegans* I chose the hermaphrodite-specific neurons (HSN) which undergo long-range neuronal migration and axon guidance events in distinct temporal windows during development. The HSNs are a bilaterally

symmetric pair of motor neurons (HSNL - left and HSNR - right) that innervate vulval muscles to control egg laying through the release of serotonin [67, 87]. During embryogenesis, the HSNs are born in the presumptive tail region and migrate to the midbody, a distance of half the length of the embryo. From larval stage two (L2), the HSNs extend axons around the vulva before entering the ventral nerve cord, through which the HSNs extend anteriorly and finally terminate at the nerve ring in the head [61, 67]. HSN migration and axon guidance is strictly controlled by multiple conserved molecule mechanisms. Wnt signaling has been reported to be required for migration events, while Slit/Robo, ephrin and netrin signaling are important for axon guidance [75, 76]. In addition to these studies, it has recently been shown that the loss of *pdi-1* gene which encodes for a protein disulphide isomerase interferes with the migration of HSNs [91].

TGF-β signaling is already known for its importance in body size regulation, innate immunity and dauer formation, however its role on neurodevelopment is poorly understood. To interrogate this role, I examined the requirement of TGF-β pathway components for development of the HSNs. I propose that the outcome of this research will shed light on how TGF-β family pathway functions to control brain development.

3.3 Methods

Examination of HSN phenotypes were performed using the HSN marker strains; *zdIs13, mgIs71,* and the transgenic line *rpEx6* based on the chromosomal region of the candidate genes. To avoid confusion, these strains were written as *HSN::GFP*. For more scoring and other details, please refer to General Methods, Chapter 2.

3.3.1 Molecular Cloning

pRG62 *pelt-3::sma-6::GFP*

The plasmid was kindly donated by Richard Padgett (Rutgers University, USA). It includes 2058 bp upstream of the *elt-3* coding sequence as a hypodermal-specific promoter and unspliced genomic *sma-6* sequence without the stop codon fused to GFP coding sequence.

RJP346 *pdpy-7::sma-6*

sma-6 cDNA was amplified from N2 cDNA using Phusion DNA polymerase with the primers OFB58 and OFB64. NcoI restriction enzyme was used to insert the amplified *sma-6* cDNA into pPD49.26 *pdpy-7* expression vector which includes approximately 244 bp upstream to the *dpy-7* coding sequence.

RJP411 *ptph-1::sma-6*

sma-6 genomic sequence was amplified from pRG62 *pelt-3::sma-6::GFP* using Phusion DNA Polymerase with the primers OFB135 and OFB136. pPD49.26 *ptph-1* expression vector, which includes 1748 bp upstream to the *tph-1* coding sequence, was cut with NheI restriction enzyme and the amplified *sma-6* genomic sequence was inserted into the cut vector using the standard protocol for In-Fusion HD Cloning Kit.

3.3.2 Transgenic lines

Transgenic lines were generated as described in Chapter 2. *Pmyo-2::mCherry* was injected at 5 ng/μl final concentration as a co-injection marker along with the rescue plasmid. For endogenous and intestinal *sma-6* rescue, ZC1334 (*psma-6::sma-6*),

ZC1398 (*pelt-2::sma-6*) and ZC1573 (*pges-1::sma-6*) strains were used which were kindly donated by Yun Zhang (Harvard University, USA). For *sma-6* rescue in HSN neurons, the transgenic lines *rpEx1792* and *rpEx1793* were obtained by injection of *ptph-1::sma-6* into N2 animals at a final concentration of 10 ng/μl. For more details, please refer to Chapter 2.

3.3.3 CRISPR/Cas9 genome editing for *daf-4*

rp122 and *rp123* alleles were generated using CRISPR/Cas9 technique which uses the ability of Cas9 to introduce double-strand breaks in the genome (Chapter 2). Briefly, N2 animals were injected with two Cas9 constructs (50 ng/μl final concentration) that each includes a different single guide RNA (sgRNA) (Table 2.5, Chapter 2) targeting the first exon of *daf-4*. Candidate mutants were picked based on the dauer and/or small phenotypes. Mutations were identified by PCR and the specific lesions confirmed by Sanger sequencing.

3.4 Results

3.4.1 SMA-6, a type I receptor of TGF-β signaling, is required for HSN development

To examine the role of TGF-β signaling in neuronal development, the HSN neurons were used as a model. Initially, type I receptors of TGF-β family in *C. elegans*, DAF-1 and SMA-6 (Fig. 3.2A) were examined using previously characterized mutant strains [112, 140]. Imaging analysis of the HSN neurons in these mutant backgrounds revealed that SMA-6 but not DAF-1 is required for the development of HSNs (Fig. 3.2B). Three independent mutant alleles of *sma-6* - *wk7*, *e1482* and *ok2894* - exhibited 30-40% HSN defects, including defects in both migration and axon guidance. *wk7* and *e1482* are point mutations in the 2nd exon which cause premature stop codons and an in-frame substitution (A90V), respectively, while the *ok2894* allele includes a deletion that removes the 10th intron and part of the 11th exon [117] [141] (Fig. 3.2A). All of these alleles exhibit small body size indicating a loss of SMA-6 function [140].

To assess the specificity of defective HSN phenotype of *sma-6* mutants, I performed a rescue experiment using a transgenic line of *sma-6* mutants that carries the wild-type *sma-6* genomic region as an extrachromosomal array (*psma-6::sma-6*). This transgenic line has been shown to rescue the learning defects detected in *sma-6* mutants [102]. Furthermore, the worms that carry the extrachromosomal array were observably also longer in body size compared to the *sma-6* mutants. For examination of HSN phenotypes, *yxEx615* was crossed with an *HSN::GFP* strain. The scoring results revealed that the transgenic worms carrying wild-type genomic *sma-6* DNA in the *sma-6(wk7)* mutant background exhibited significantly reduced percentage of HSN defects compared to the non-transgenic animals (Fig. 3.2B). This indicates that the HSN defects observed in *sma-6* mutants are due to the loss of *sma-6*.

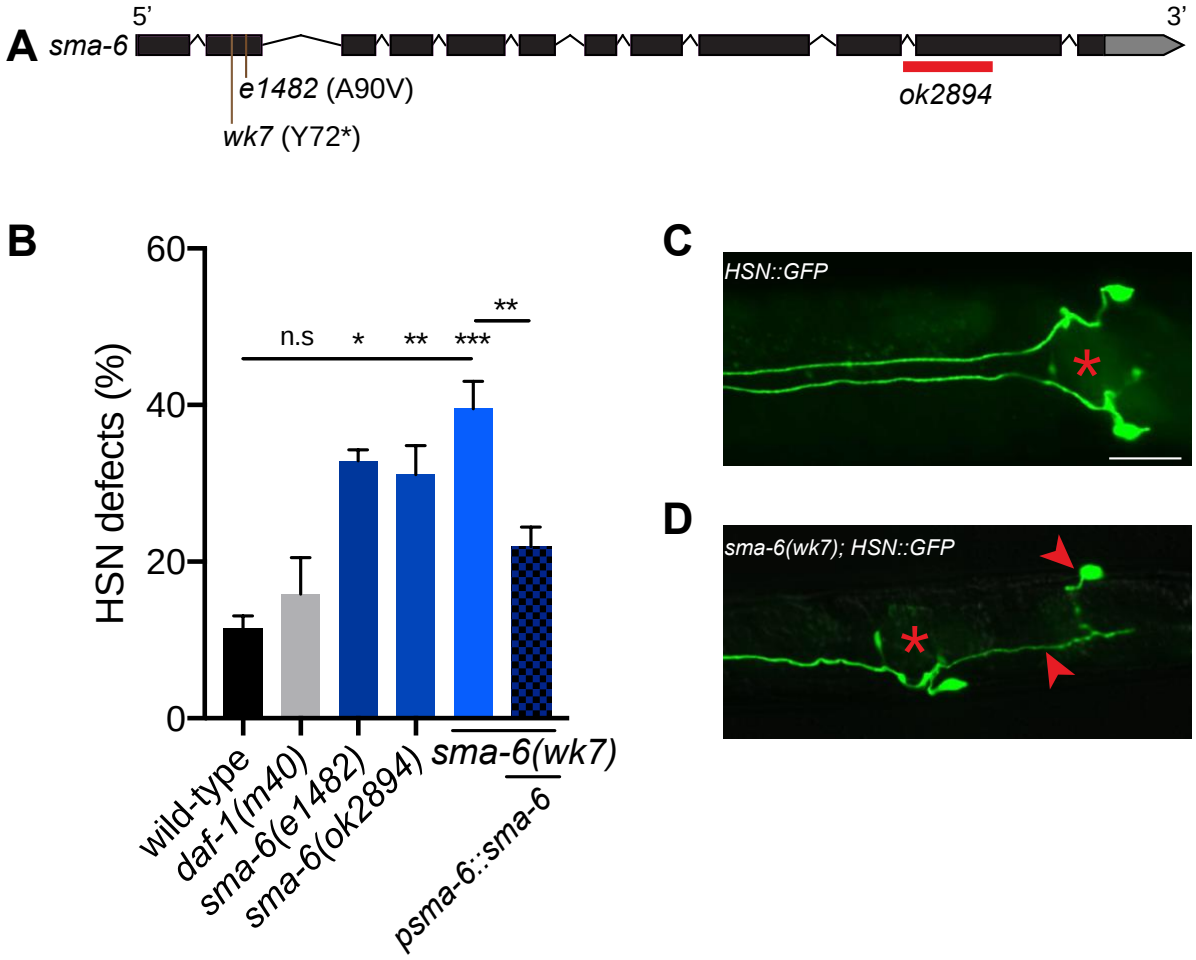

Fig. 3.2. SMA-6 regulates the HSN development.

(A) Gene structure of *sma-6* (adapted from WormBase). *wk7* and *e1482* are in-frame point mutations (Y72* and A90V, respectively), while *ok2894* is a deletion that causes a frameshift that results with a premature stop codon. Red box represents deletion and brown lines represent substitution. The black boxes indicate the exons and the black lines between them indicate the introns. Grey boxes represent the untranslated regions (UTR). (B) Scoring results of the TGF-β family type I receptors in *C. elegans*. *m40* is an in-frame point mutation (W170*) that causes a premature stop in *daf-1* transcript. Statistical analysis was performed using one-way ANOVA and Dunnett's multiple comparison test for the comparison of *daf-1* and *sma-6* mutants with wild-type, whereas the *sma-6* rescue analysis was performed via unpaired *t*-test comparing the transgenic line and *sma-6(wk7); HSN::GFP*. At least one hundred animals were scored per strain. *$p < 0.05$, **$p < 0.01$, ***$p < 0.001$, n.s., not significant. Error bars represent mean ± SEM of three biological replicates. (C) and (D) are representative images for normal and defective HSNs, respectively. Asterisk marks the vulva. Arrowheads indicate the defects in which the upper arrowhead points to an undermigration defect while the lower arrowhead points to a guidance defect where the two bilaterally symmetrical axons merged. Ventral view, anterior is to the left. Scale bar = 20 µm.

3.4.2 Examining the tissue specific function of SMA-6 in the regulation of HSN development

To better understand how the TGF-β pathway controls HSN development, I examined the tissue-specific function of SMA-6. As previously mentioned, *sma-6* is expressed in multiple tissues such as hypodermis, intestine and pharyngeal muscle. Hypodermal expression of *sma-6* is required for body size regulation, while intestinal expression might be important for innate immunity [115, 127]. To examine where SMA-6 functions to control HSN development, I focused on the hypodermis as this tissue has previously been shown to be important for non-autonomous regulation of HSN developmental decisions [86, 142]. To rescue *sma-6* expression in the hypodermis, *sma-6* cDNA was cloned into an expression vector that includes 0.2 kb upstream of *dpy-7* gene. *dpy-7* promoter is commonly used to drive expression exclusively in the hypodermis. However, the transgenic lines made with this construct caused general worm sickness and therefore, were not suitable for maintenance and scoring. This suggests that the *dpy-7* promoter drives *sma-6* expression at excessive levels and/or during inappropriate temporal windows. To circumvent these potential issues, I used an alternative hypodermal expression construct which uses the promoter region of the *elt-3* gene and *sma-6* genomic sequence (kindly supplied by Rick Padgett (Rutgers University, USA)). This construct was shown to be functional for rescuing the small phenotype of *sma-6(wk7)* worms which requires hypodermal action of the TGF-β pathway for maintaining normal body size [117]. The rescue construct was injected into N2 animals at 10 ng/µl final concentration and three independent transgenic lines (*rpEx1904*, *rpEx1905* and *rpEx1906*) were generated. These lines were crossed with *sma-6(wk7); HSN::GFP*. Resulting transgenic lines that have mutant *sma-6* in the background were identified based on the small phenotype and the presence and the absence of the transgene. *sma-6* mutants that carry the transgene exhibited longer body size than the non-transgenic animals which is an indicator of functional *sma-6* transgene. The scoring results revealed that *sma-6(wk7)* mutant animals that carry the *pelt-3::sma-6::GFP* transgene presented significantly lower HSN defects than the non-transgenic animals (Fig. 3.3), which suggest that *sma-6* expression in hypodermis is sufficient for the regulation of HSN development.

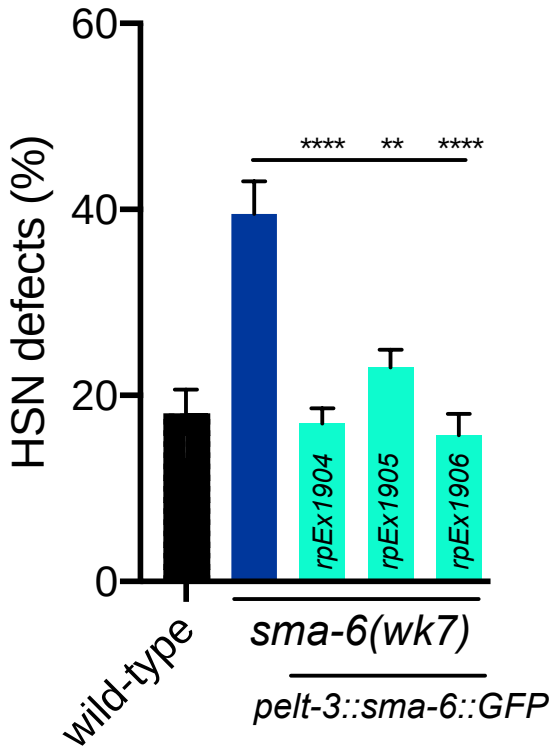

Fig. 3.3. Hypodermal expression of *sma-6* is essential for HSN development.
Quantification of HSN defects in *sma-6(wk7)* mutants and hypodermal *sma-6* rescue alleles – *rpEx1904*, *rpEx1905*, *rpEx1906*. Cyan columns indicate independent transgenic lines that carry *pelt-3::sma-6::GFP* (10 ng/µl final concentration). Statistical analysis was performed using one-way ANOVA and Dunnett's multiple comparison test, comparing the transgenic lines with *sma-6(wk7); HSN::GFP*. At least one hundred animals were scored per strain. **p < 0.01, ****p < 0.0001. Error bars represent mean ± SEM of three biological replicates.

Next, the role of intestinal *sma-6* expression on HSN development was examined. To perform this experiment, *sma-6(wk7)* mutants that carry *pelt-2::sma-6* transgene (*yxEx659*) and *pges-1::sma-6* transgene (*yxEx765*) were crossed with the *HSN::GFP* reporter strain and HSN phenotypes were scored. The *elt-2* and *ges-1* promoters are specific for the intestine and have been previously used in intestine-specific expression and/or rescue experiments [143, 144]. The transgenic worms displayed the same percentage of HSN defect as non-transgenic worms, which indicates that the intestinal expression of *sma-6* is dispensable for HSN development (Fig. 3.4)

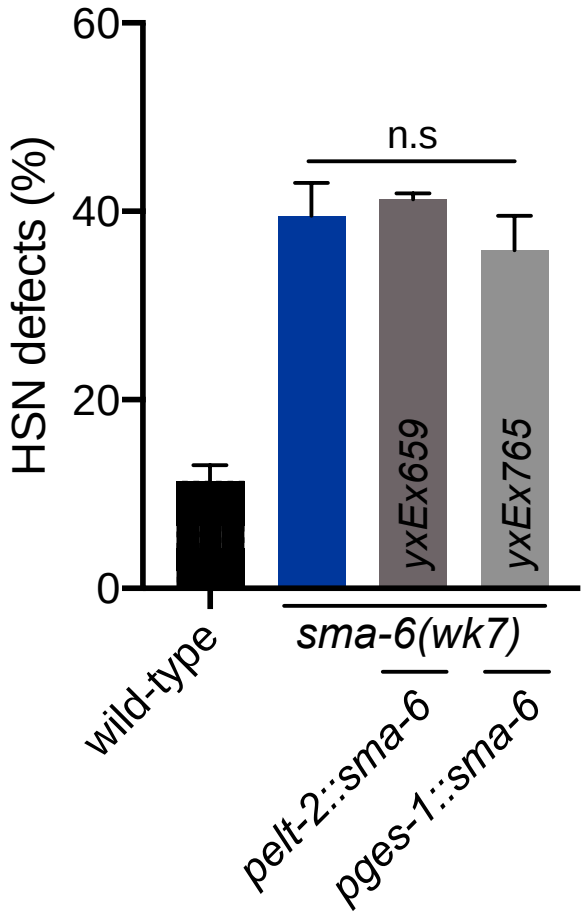

Fig. 3.4. *sma-6* expression in the intestine does not rescue the HSN defects of *sma-6* mutants. Quantification of HSN defects in *sma-6(wk7)* mutants and intestinal *sma-6* rescue lines, *yxEx659* and *yxEx765*. *sma-6* expression was rescued with two independent transgenic lines that use different intestinal promoters- *elt-2* and *ges-1*. Statistical analysis was performed using one-way ANOVA and Dunnett's multiple comparison test, comparing the transgenic lines with *sma-6(wk7); HSN::GFP*. At least one hundred animals were scored per strain. n.s., not significant. Error bars represent mean ± SEM of three biological replicates.

To date, *sma-6* expression in HSNs has not been reported. However, considering my data showing that SMA-6 function is important for HSN development, I wanted to investigate whether resupplying *sma-6* expression exclusively in the HSNs would prevent the migration and guidance defects. For this purpose, *sma-6* (genomic sequence) was cloned into a vector that carries 1.7 kb upstream of the *tph-1* gene which is expressed in HSNs and four additional neurons in the head. After confirming the cloning by Sanger sequencing, the construct was injected into N2 hermaphrodites and then the obtained transgenic lines were crossed with *sma-6(wk7); HSN::GFP* worms. This approach was used due to technical difficulties with injecting *sma-6*

mutant animals. The scoring of two independent lines revealed that *sma-6* expression in HSNs is not required for the development of HSNs as the transgenic worms did not present a reduced percentage of defects compared to non-transgenic worms (Fig. 3.5). Together with the previous tissue-specific expression analysis, the results indicate a non-cell autonomous action of SMA-6 from the hypodermis for the regulation of HSN development.

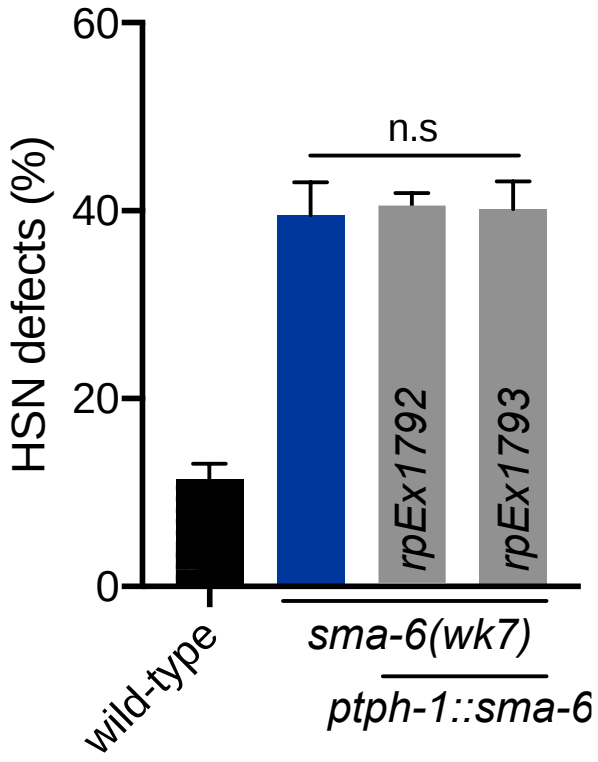

Fig. 3.5. *sma-6* expression in HSNs does not rescue the HSN defects of *sma-6* mutants.
Quantification of HSN defects in *sma-6(wk7)* mutants and intestinal *sma-6* rescue lines, *rpEx1792* and *rpEx1793*. Grey columns indicate independent transgenic lines that carries *ptph-1::sma-6::GFP* (10 ng/µl final concentration) in *sma-6(wk7)* background. Statistical analysis was performed using one-way ANOVA and Dunnett's multiple comparison test, comparing the transgenic lines with *sma-6(wk7); HSN::GFP*. At least one hundred animals were scored per strain. n.s., not significant. Error bars represent mean ± SEM of three biological replicates.

3.4.3 Intracellular signaling molecules of the Sma/Mab pathway are important for HSN development

Following the phosphorylation of TGF-β family receptors, intracellular signaling molecules, called Smads, are activated. There are two types of Smads called receptor-activated Smads (R-Smad) and common-partner Smads (co-Smad). After being phosphorylated by the type I receptors, R-Smads form a complex with a co-Smad and then translocate into the nucleus to regulate target gene expression [5]. After identifying the importance of the type I receptor, SMA-6, the involvement of Smads in HSN development was investigated. As mentioned earlier, there are two major types of canonical TGF-β family signaling - the dauer and Sma/Mab pathways. The Smad components of these pathways are DAF-3, -8, -14 and SMA-2, -3, -4, respectively. SMA-2 and -3 are the R-Smads that associate with the co-Smad SMA-4 in the Sma/Mab pathway. In the dauer pathway, the R-Smads are DAF-8 and -14 which associate with the co-Smad DAF-3.

In order to assess the importance of Smad molecules in HSN development, mutant strains for each Smad were crossed with *HSN::GFP* and their HSN phenotypes were examined. For dauer Smads, *daf-3(e1376)*, *daf-8(e1393)* and *daf-14(m77)* mutants were used. *daf-3(e1376)* mutants contain a 1-bp deletion that causes a frameshift, while *daf-8(e1393)* and *daf-14(m77)* are substitutions (S391X and Q192*, respectively) (Fig. 3.6A). Scoring results showed that none of these mutant strains exhibited HSN developmental defects (Fig. 3.6C). However, the absence of the Sma/Mab Smads caused a significant increase in HSN defects (Fig. 3.6B). For these scorings *sma-2(e502), sma-3(wk30) and sma-4(e729)* mutant strains were used. *e502* is a substitution that replaces the glycine residue with an aspartic acid at 372nd position, while *wk30* and *e729* are substitutions resulting in premature stop codons. As a result, *sma-2(e502), sma-3(wk30) and sma-4(e729)* mutant animals exhibit small phenotype, which indicates loss-of-function [55, 127, 145]. These mutants present HSN defects ranging from 30-40%. The results suggest that the Sma/Mab pathway is required for HSN development, whereas the components of the dauer pathway are dispensable for HSN development.

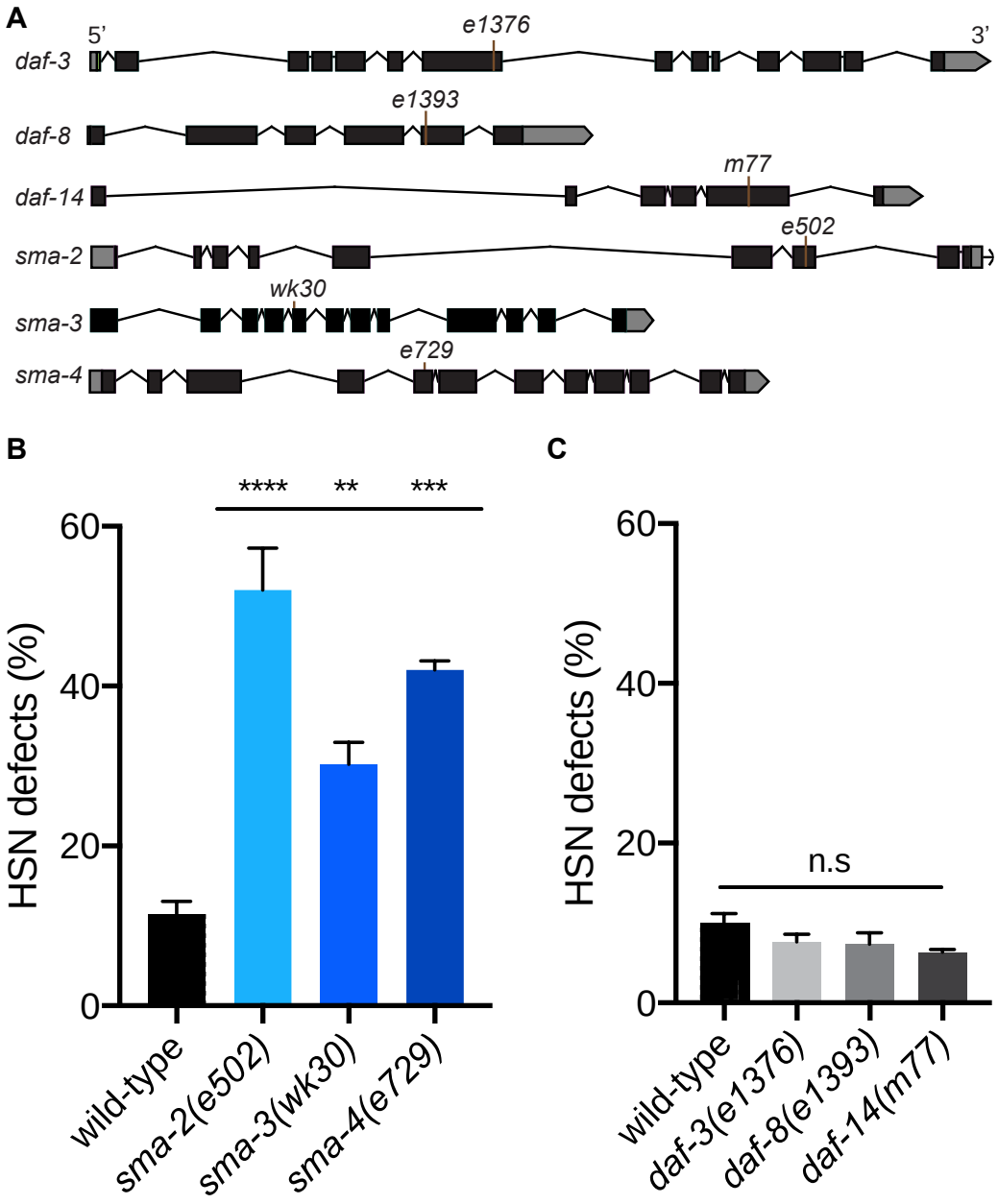

Fig. 3.6. The role of TGF-β family Smads in HSN development.

(A) Gene structures of the Smads in the Sma/Mab and dauer pathway (adapted from WormBase). *e1376* is a 1-bp deletion that causes a frameshift, while *e1393* and *m77* are substitutions (S391X and Q192*, respectively). *e502* is a substitution that replaces the glycine residue with an aspartic acid at 372nd position, while *wk30* and *e729* are substitutions resulting in premature stop codons. Brown lines represent substitutions, black boxes indicate the exons, black lines between them indicate the introns and grey boxes represent the UTRs. (B) and (C) show the quantification of HSN defects in the Sma/Mab pathway mutants and the dauer pathway mutants. Statistical analysis was performed using one-way ANOVA and Dunnett's multiple comparison test. At least one hundred animals were scored per strain. **p < 0.01, ***p < 0.001, ****p < 0.0001, n.s, not significant. Error bars represent mean ± SEM of three biological replicates.

3.4.4 The type II receptor DAF-4 is not required for HSN development

Both canonical TGF-β family signaling pathways, the Sma/Mab and the dauer pathways, require DAF-4 as it is the only type II receptor identified in the *C. elegans* genome. Because I have identified an important function for SMA-6 in controlling HSN development, I hypothesized that DAF-4 would also be required for this process, as it is necessary for SMA-6 activation. To examine this hypothesis, I used three independent deletion alleles of *daf-4* - *e1364*, *ok828 and m63*. *daf-4(m63)* has not been curated, however *daf-4(e1364)* and *daf-4(ok828)* are classical alleles of *daf-4* that have 212 and 1829 bp deletions, respectively that lead to premature stop codons. All the three alleles have been shown to cause strong dauer phenotypes [141]. These alleles were crossed with *HSN::GFP* and then scored for their HSN phenotypes. Strikingly, none of the *daf-4* mutant animals presented significant HSN defects compared to wild-type animals (Fig. 3.7B). Considering the fact that DAF-4 is the only type II receptor in *C. elegans* TGF-β family, I hypothesized that SMA-6 acts on its own to control HSN development.

To further validate that DAF-4 is not involved in this process, two additional mutant alleles of *daf-4* were generated using the clustered regularly interspaced short palindromic repeats (CRISPR)-Cas9 genome editing which uses the ability of Cas9 protein to introduce double-strand breaks in the genome. The specificity of Cas9 is determined by its recognition of small RNA molecules which can be generated *in vitro* as single guide RNAs (sgRNA). Two sgRNAs targeting the first exon of *daf-4* (Table 2.5) were designed using the CRISPR design tool [137] that is available at http://crispr.mit.edu. After the design, these sgRNAs were cloned into the CRISPR construct pDD162, which also includes the specific sequence that encodes for Cas9. Then, these constructs were injected into N2 animals at a final concentration of 50 ng/µl per construct. F2 animals were isolated into single plates based on the small and/or dauer phenotype since the loss of DAF-4 function causes both phenotypes. As a result, two independent alleles, *rp122* and *rp123*, were generated. These alleles have strong dauer phenotypes which indicates a loss of DAF-4 function. The genotypes of these alleles were identified using PCR and Sanger sequencing. *rp122* and *rp123* have 2 and 7 bp deletions in the first exon, respectively, which causes frameshifts that result

with premature stop codons (Fig. 3.7A). After characterization of these alleles, they were backcrossed with N2 animals three times and then crossed with *HSN::GFP* for the examination of HSN phenotypes. The HSN scoring results presented a wild-type phenotype for both two alleles, which further substantiate my findings on DAF-4-independent regulation of HSNs (Fig. 3.7C).

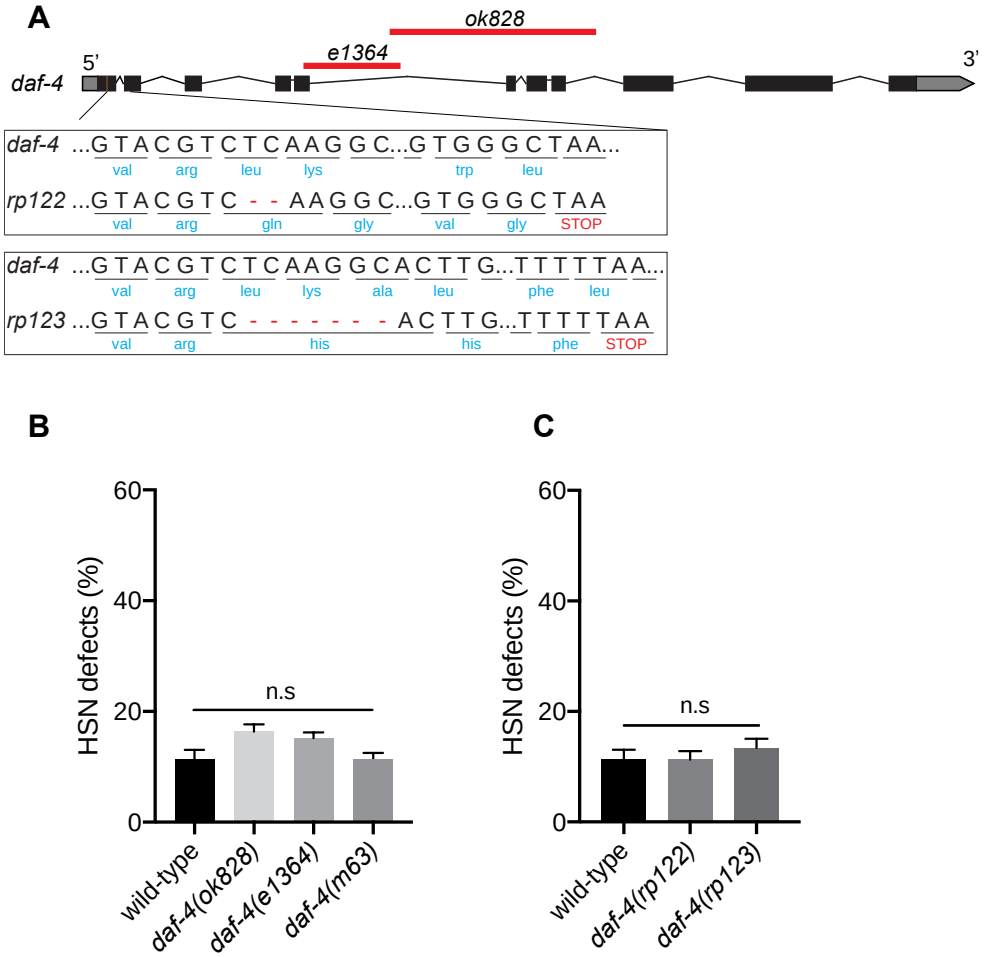

Fig. 3.7. The type II receptor DAF-4 is not required for HSN development.

(A) Schematic of the *daf-4* gene (adapted from WormBase). *e1364* and *ok828* are classical alleles that have 212 and 1829 bp deletions, respectively. *m63* has not been curated. *rp122* and *rp123* alleles were generated via CRISPR-Cas9, and are 2- and 7- bp deletions, respectively. All the mutations in these alleles, except the unknown *m63* allele, cause frameshift that results with premature stop codons. Brown lines indicate substitutions, red boxes indicate deletions, black boxes indicate the exons, black lines between them indicate the introns and grey boxes represent the UTRs. (B) and (C) represent the HSN phenotypes of the independent mutant alleles of *daf-4*. Statistical analysis was performed using one-way ANOVA and Dunnett's multiple comparison test. At least one hundred animals were scored per strain. n.s., not significant. Error bars represent mean ± SEM of three biological replicates.

3.4.5 Correct recycling of SMA-6 to the plasma membrane is crucial for HSN development

In order for receptors to function properly in the signaling pathways, their intracellular trafficking must be strictly controlled since dysregulated recycling pathways can result in the impairment of signaling [116, 117]. In *C. elegans*, it has been reported that the trafficking events of SMA-6 and DAF-4 are controlled via different mechanisms in which SMA-6 trafficking occurs via retromer-dependent receptor mediated endocytosis, whereas DAF-4 trafficking occurs independently of retromers [117]. In the same study, it was also shown that the loss of transportation molecules leads to diminished TGF-β-like BMP signaling.

Considering that SMA-6 and DAF-4 recycling are regulated by separate pathways, I hypothesized that interference of SMA-6 trafficking would lead to the dysregulation of HSN development, whereas DAF-4 trafficking would not be important. SMA-6 trafficking requires a receptor-mediated endocytosis protein RME-1, an ortholog of human Eps15 homology (EH)-domain containing 1 and 3, sorting nexin-3 (SNX-3) and the vacuolar protein sorting factor-35 (VPS-35) which is part of the retromer complex [117]. It has already been reported that the loss of VPS-35 causes migration defects for HSNs which is in concurrence with my hypothesis [90]. I subsequently examined the *rme-1(b1045)* and *snx-3(tm1595)* mutant animals to analyze the roles of *rme-1* and *snx-3* in HSN development. *b1045* allele is a 1526 bp-long deletion that removes a large portion of *rme-1*, whereas *tm1595* is a combination of a deletion that removes 420 bp and an insertion of 14 bp within the *snx-3* gene (Fig. 3.8A). The scoring results revealed that both of these mutants had significantly higher HSN migration and guidance defects than wild-type animals (Fig. 3.8B). To investigate whether RME-1 controls HSN development in the same pathway as SMA-6, I generated a compound *rme-1; sma-6* mutant and examined HSN defects. The *rme-1; sma-6* double mutant presented a similar percentage of HSN defects compared to each single mutant (Fig. 3.8B). These results suggest that RME-1 and SMA-6 acts in the same genetic pathway to regulate HSN development. However, *snx-3* mutants could not be used to examine the same hypothesis since approximately 90% of these mutant animals presented HSN defects, thus a possible additive effect on HSN defects could not be determined. As well as regulating SMA-6 trafficking, SNX-3 is also required for Wnt signaling which

has been shown to be important for HSN development [116], which may explain why loss of *snx-3* result in a higher penetrance of HSN defects than loss of *sma-6*.

DAF-4 trafficking is mediated by a retromer-independent pathway, in which ADP ribosylation factor-6 (ARF-6) plays a crucial role [117]. ARF-6 is an ortholog of human ARF6, a small GTPase that regulates the recycling between endoplasmic reticulum and the plasma membrane [146]. To investigate whether ARF-6 has a role in HSN development, I crossed *arf-6(tm1447)* mutant allele with *HSN::GFP*. These worms are missing a large portion of *arf-6* (2263 bp deletion) (Fig. 3.8A) and have been reported to cause DAF-4 accumulation in endosomes which are components of intracellular transportation [117]. The scoring results showed that these mutants did not display significant HSN defects compared to wild-type animals which indicates that ARF-6, and therefore dysregulated DAF-4 recycling, has no impact on HSN development (Fig. 3.8C). Taken together with SMA-6 recycling results, these findings further confirm DAF-4-independent SMA-6 action in the regulation of HSN development.

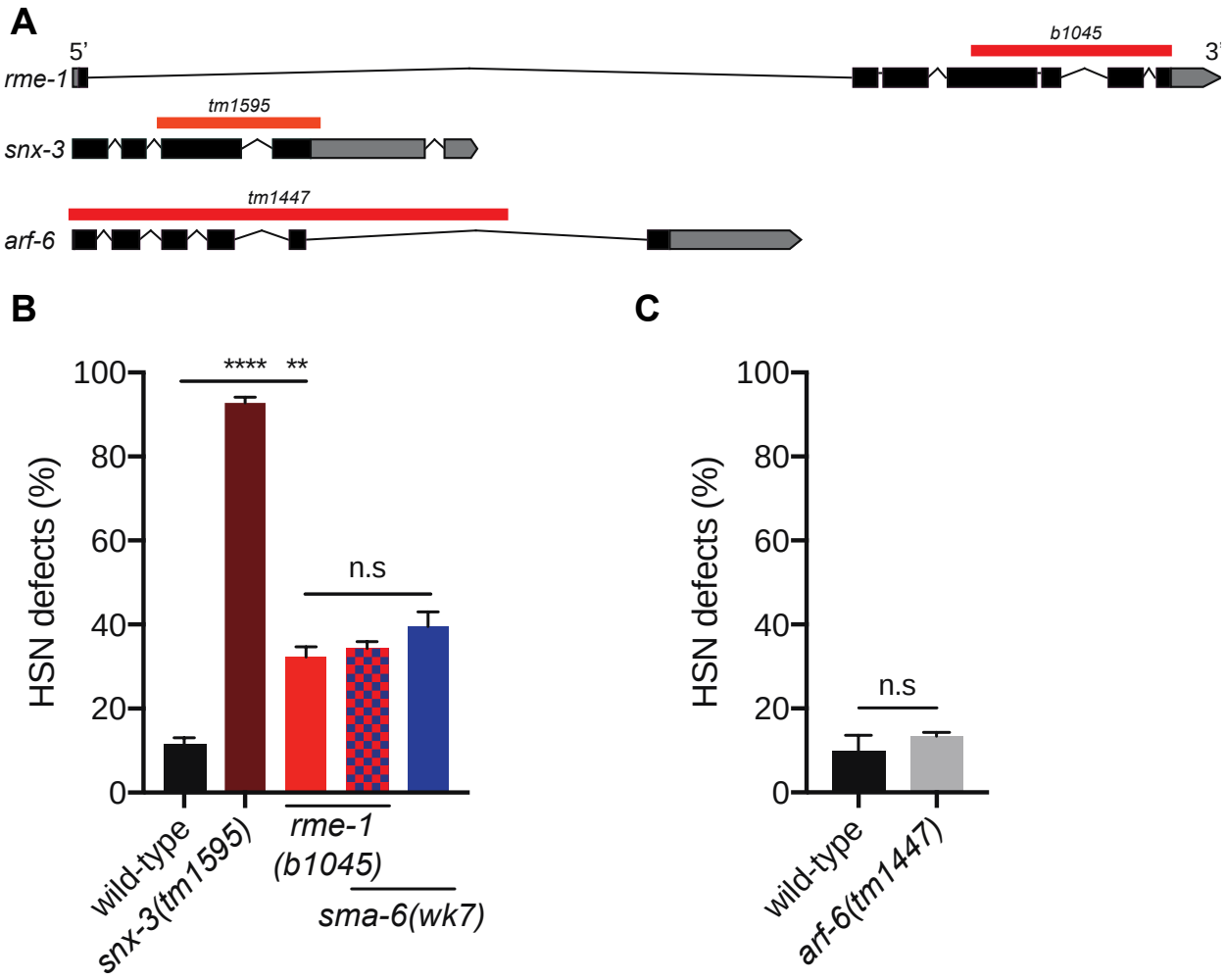

Fig. 3.8. The role of TGF-β receptor recycling in HSN development.

(A) Gene structures of *rme-1*, *snx-3* and *arf-6* (adapted from WormBase). *b1045* and *tm1447* are deletions, while *tm1595* is a combination of a deletion and insertion. Red boxes indicate deletions, black boxes indicate the exons, black lines between them indicate the introns and grey boxes represent the UTRs. Orange box indicates a combination of insertion and deletion. (B) and (C) show the quantification of HSN defects in *rme-1*, *snx-3* and *arf-6* mutants. *snx-3* mutants were compared with wild-type animals only, whereas *rme-1* mutants were compared with both wild-type and *rme-1(b1045); sma-6(wk7)* double mutants. Statistical analysis was performed using one-way ANOVA and Dunnett's multiple comparison test. *arf-6(tm1447)* was compared with wild-type and statistical analysis was performed using unpaired *t*-test. At least one hundred animals were scored per strain. **p < 0.01, ****p < 0.0001, n.s. not significant, error bars represent mean ± SEM of three biological replicates.

3.4.6 Examining intracellular and extracellular regulators of the TGF-β pathway in HSN development

SMA-10 is a member of the leucine-rich repeats and immunoglobulin-like domains (LRIG) family that is required for body size regulation [123]. *sma-10* is primarily expressed in the hypodermis and intestine [147]. SMA-10 resides on the cell surface and it can physically bind the *C. elegans* TGF-β family receptors SMA-6 and DAF-4 [123]. In another study, it was shown that loss of *sma-10* causes accumulation of SMA-6 in cells due to the reduced ubiquitin-dependent degradation [124]. Considering its regulatory effect on TGF-β family signaling, I hypothesized that SMA-10 could also be important for HSN development. To examine this, the *sma-10(ok2224)* mutant allele was crossed with *HSN::GFP*. *sma-10(ok2224)* mutants contain a 906-bp deletion in the *sma-10* locus (Fig. 3.9A) [141]. The scoring results showed that these animals did not have any significant HSN defects compared to wild-type animals (Fig. 3.9B). This could be due to the possibility that sufficient functional SMA-6 is present in these worms even though they accumulate within the cell due to defective degradation. Furthermore, it has been shown that even though SMA-6 accumulation is observed in *sma-10* mutants, the distribution of SMA-6 remained intact [124]. Therefore, SMA-6 can potentially function to regulate HSN development in the absence of SMA-10.

Another extracellular regulator of Sma/Mab pathway is ADT-2 which is a secreted metalloprotease required for cuticle development[125]. I investigated the role of ADT-2 by examining HSN development of *adt-2(wk156)* mutants. *wk156* is a substitution (Fig. 3.9A) and has been reported to cause a small phenotype [125]. The results revealed that approximately 34% of the worms scored had migration and/or guidance defects in HSN neurons (Fig. 3.9B).

SMA-9, the *C. elegans* homolog of *Drosophila* Schnurri, is an important transcription factor involved specifically in the Sma/Mab pathway, but not in the dauer pathway [120]. *sma-9* is expressed in many tissues including hypodermis, intestine and nervous system [132]. To investigate the role of SMA-9 in HSN development, *sma-9(qc3)* worms were used. These worms contain a substitution in *sma-9* locus that leads to a premature stop codon. Interestingly, these animals did not display significant HSN defects (Fig. 3.9B) This suggests that SMA-9 is not involved in the development of

HSNs and the regulation of potential target genes in this process is carried out by another factor.

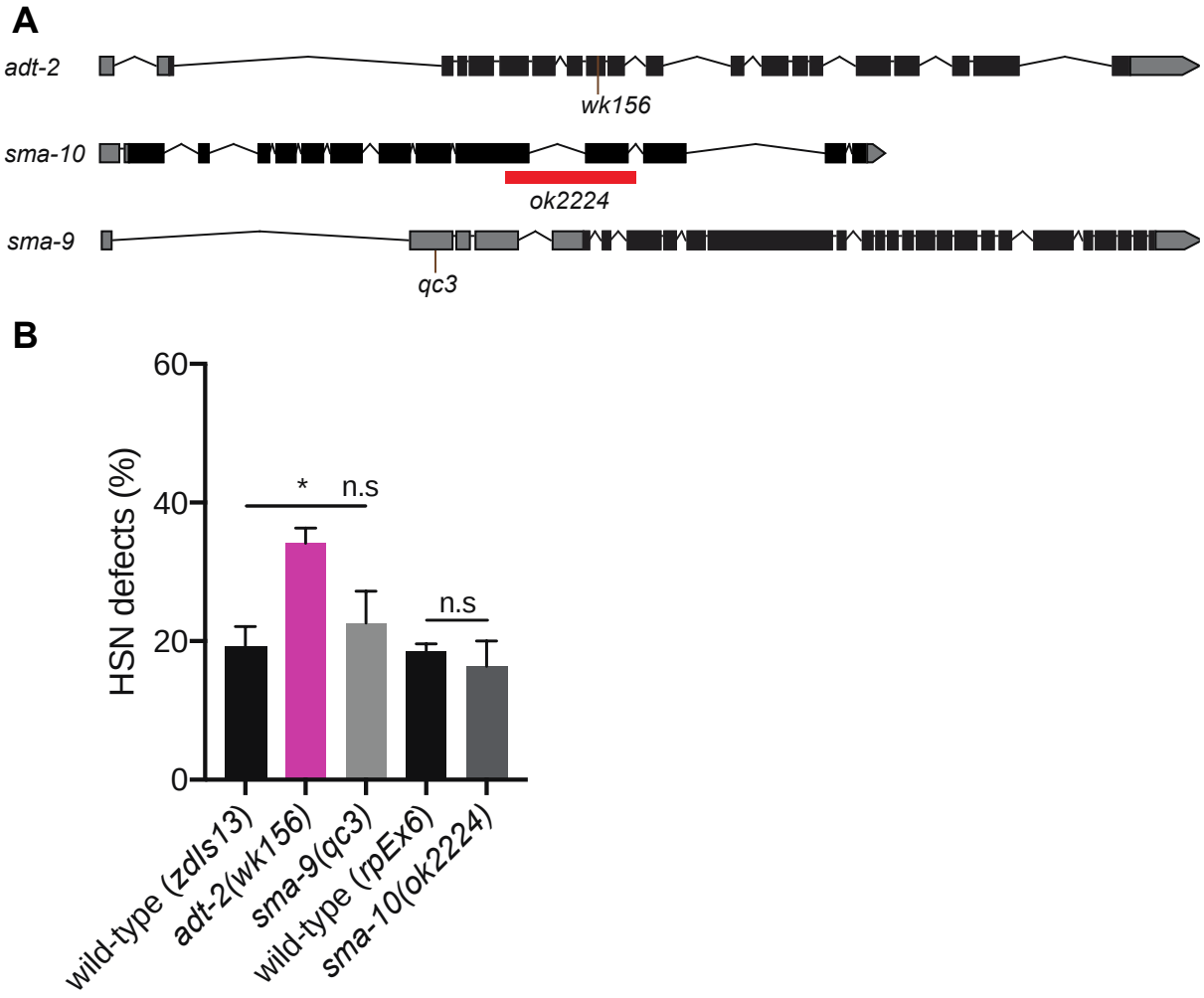

Fig. 3.9. ADT-2, but not SMA-9 and SMA-10, is important for HSN development.

(A) Gene structures of *adt-2*, *sma-10* and *sma-9* (adapted from WormBase). *wk156* and *qc3* are substitutions, while *ok2224* is a 906-bp deletion. (B) Quantification of HSN defects in *adt-2*, *sma-9* and *sma-10* mutants. Due to the chromosomal location of *sma-10*, HSN phenotype of *sma-10* mutants were examined using another reporter line (*rpEx6*) and statistical analysis was performed separately using one-way ANOVA for *adt-2* and *sma-9* and an unpaired *t*-test for *sma-10*. At least one hundred animals were scored per strain. *$p < 0.05$, n.s. not significant, error bars represent mean ± SEM of three biological replicates.

3.5 Discussion

Transforming growth factor beta (TGF-β) signaling is a highly conserved mechanism that controls vital processes during development. However, there is little evidence on how TGF-β signaling regulates the development of neurons. The roundworm *C. elegans* enables the examination of this process at single cell resolution. Using the hermaphrodite-specific neurons (HSNs) of *C. elegans*, I investigated the role of the TGF-β pathway on neuronal migration and axon guidance events. My results revealed a non-canonical mechanism in which a TGF-β family type I receptor can control the development of HSN neurons independently of the type II receptor with the help of specific intracellular and extracellular components and regulators of TGF-β signaling.

TGF-β signaling involves two different types of receptor, namely type I and type II. The function of the type I receptor requires activation by the type II receptor which leads to propagation of the signaling to the downstream molecules. In *C. elegans*, SMA-6 and DAF-1 are the type I receptors, whereas DAF-4 is the only type II receptor that acts with SMA-6 and DAF-1 in separate pathways. I found that *sma-6* mutant worms display HSN migration and guidance defects which could be rescued by resupplying *sma-6* with its endogenous promoter (Fig. 3.2B). In contrast, the other type I receptor, DAF-1, was not required for HSN development. As DAF-4 acts with SMA-6 in the canonical TGF-β family signaling, I hypothesized that the loss of DAF-4 would also cause HSN defects. Intriguingly, *daf-4* mutants displayed the wild-type HSN phenotype, indicating that DAF-4 is dispensable for HSN development (Fig. 3.7B-C). To further substantiate these findings, I examined the trafficking events of SMA-6 and DAF-4. Interestingly, SMA-6 and DAF-4 are transported via distinct mechanisms [117]. SMA-6 transportation is regulated by a retromer-dependent process mediated by sorting nexin SNX-3, vacuolar protein sorting factor VPS-35 and receptor mediated endocytosis protein RME-1, whereas DAF-4 trafficking occurs independently of retromers and is mediated by ADP ribosylation factor ARF-6. Considering the interplay between signaling and recycling events, I hypothesized that the interference with the recycling events would cause impaired TGF-β signaling leading to the dysregulation of HSN development. Interestingly, Pan *et al.* reported that the loss of VPS-35 leads to migration defects for HSNs [90]. Therefore, I examined the HSN phenotypes of *rme-1* and *snx-3* mutants and found that these mutants possess significantly higher HSN

defects than wild-type worms (Fig. 3.8B). Furthermore, *sma-6; rme-1* double mutant animals did not display increased HSN defects compared to the single mutants, suggesting they act in the same genetic pathway. This is also a great illustration of how a disturbance in intracellular transportation events can lead to impaired signaling, and thus impaired development. After investigating SMA-6 transport, I examined the HSN profile of *arf-6* mutant worms which display defective DAF-4 transport. Strikingly, these worms did not exhibit a significant HSN defect compared to wild-type worms which indicates the DAF-4 transportation is not important for HSN development (Fig. 3.8C). These findings confirm my hypothesis on DAF-4 independent action of SMA-6 on HSN development. Considering that DAF-4 is the only type II receptor identified in *C. elegans*, these results lead to three different scenarios: There might be another TGF-β family type II receptor that yet to be identified or SMA-6 can activate itself to initiate the intracellular signaling events required for HSN development. Alternatively, there might be an unknown molecule that activates SMA-6 specifically in HSN development.

In order to identify where SMA-6 acts to regulate HSN development, I performed tissue-specific rescue experiments. SMA-6 is primarily expressed in hypodermis and intestine. SMA-6 is a component of Sma/Mab pathway which is a subcategory of TGF-β family signaling involved in body size regulation and innate immunity in *C. elegans* [96]. It has been shown that the expression of *sma-6* exclusively in hypodermis is sufficient to rescue the body size defects detected in *sma-6* mutant worms [115]. I initially attempted to rescue *sma-6* in the hypodermis using a construct that drives the expression *sma-6* under the control of a hypodermis-specific promoter, *dpy-7 (pdpy-7::sma-6)*. However, the injection of the *pdpy-7::sma-6* construct in different concentrations ranging from 1 ng/µl to 10 ng/µl caused general worm sickness in the animals, thus the generated transgenic lines were not suitable for HSN development scoring. This could be due to *pdpy-7* driving excessive *sma-6* expression and/or during incorrect periods of development. The construct can be injected in lower concentrations which could prevent the worm sickness or alternatively another hypodermis-specific promoter can be utilized. I chose to generate *sma-6* rescue lines using a construct that drives the expression of *sma-6* under the control of *elt-3* promoter (*pelt-3::sma-6*), which is another hypodermis-specific promoter. After scoring of these animals for their HSN phenotypes, I found that the transgenic animals presented reduced HSN defects compared to the *sma-6* mutants (Fig. 3.3). Contrarily,

the expression of *sma-6* in intestine or HSNs did not result in reduced HSN defects in *sma-6* mutant animals (Fig. 3.4). Taken together, I concluded that SMA-6 acts non-cell autonomously from the hypodermis to regulate HSN development. This action could be via controlling the expression and/or secretion of guidance cues to the extracellular environment, to direct the migration of neuronal cell bodies and axonal outgrowth. Hypodermal regulation of neuronal development has previously been shown [86, 142]. A *C. elegans* microRNA *mir-79* controls HSN development by mediating the glycosylation state of hypodermis [86]. In addition, DAF-16/FOXO transcription factor acts from hypodermis to regulate the migration of HSNs via the insulin/IGF-1-PI3K signaling [142]. Consequently, it can be concluded that non-cell autonomous action of signaling events from hypodermis is crucial for the development of neurons.

Upon interaction with extracellular ligands, receptors propagate the signals to the intracellular signaling molecules called Smads. In *C. elegans*, there are two groups of Smads which are involved in the Sma/Mab and the dauer pathway. I found that SMA-2, -3 and -4 which are the Smads of the Sma/Mab pathway are required for HSN development (Fig. 3.6B). Conversely, the Smads of the dauer pathway, DAF-3, -8 and -14, are dispensable for this process (Fig. 3.6C), which is in concurrence with my previous findings as the type I receptor DAF-1 of the dauer pathway is not involved in HSN development. These data suggest that the components of the Sma/Mab pathway are vital for HSN development with the exception of the type II receptor. As mentioned earlier, the Sma/Mab pathway is crucial for body size regulation and the loss of any components results with decreased body size (small phenotype). This raises the question whether the HSN development and body size regulation by the Sma/Mab pathway are potentially connected. However, *daf-4* mutants have wild-type-like HSN phenotype even though they exhibit small body size. Therefore, these phenotypes that small body size and HSN development are separable.

The Smads form a complex upon activation and translocate into the nucleus for their action as transcription factors. SMA-9, a zinc-finger transcription factor in *C. elegans*, has been shown to act with the Smads as a transcription co-factor in the Sma/Mab pathway [120]. To investigate the potential role of SMA-9 in HSN development, I examined the HSN phenotype of *sma-9* mutant worms. Interestingly, these worms had no detectable HSN defects (Fig. 3.9B). This suggest that the Smads could be acting

with another cofactor to regulate the expression of potential target genes that are important for HSN development.

The activity of TGF-β family signaling is strictly controlled by extracellular regulators. An extracellular regulator of TGF-β family signaling is SMA-10/LRIG, a member of the leucine-rich repeats and immunoglobulin-like domains (LRIG) family, which positively regulates the TGF-β family pathway and interacts with the TGF-β family receptors [123]. In another study, it was shown that loss of *sma-10* causes accumulation of SMA-6 in cells due to the reduced ubiquitin-dependent degradation [124]. Because of SMA-10's role in positively regulating Sma/Mab signaling, I examined the HSN profile of *sma-10* mutant worms, however I did not observe a significant increase in HSN defects (Fig. 3.9B). This could be due to the possibility that sufficient functional SMA-6 is present in these worms even though they accumulate within the cell due to defective degradation. This hypothesis is in concurrence with another finding by Gleason *et al.* which shows that the distribution of SMA-6 remained intact in *sma-10* mutants [124]. Therefore, SMA-6 can potentially function to regulate HSN development in the absence of SMA-10.

ADT-2 is a secreted metalloprotease which regulates the Sma/Mab pathway and is required for cuticle development [125]. I investigated the role of ADT-2 in HSN development and found that approximately 34% of the worms scored had migration and/or guidance defects in HSN neurons (Fig. 3.9B). In future studies, it would be beneficial to generate *adt-2; sma-6* double mutant and examine the HSN phenotype of these animals to investigate whether these proteins act in the same genetic pathway to regulate HSN development.

3.6 Conclusion

The aim of this chapter was to investigate the role of TGF-β signaling in neuronal development. For this purpose, I used the HSN neurons of the roundworm *C. elegans* as a model and found that TGF-β signaling is crucial for the development of HSNs. I showed that this regulatory action occurs in a non-canonical manner where the type I receptor SMA-6 acts independently of the type II receptor DAF-4 (Fig. 3.10). Furthermore, I discovered that SMA-6 acts non-cell autonomously from hypodermis to regulate HSN development and its intestinal and HSN expression is not required for this function. In addition to the type I receptor, I found that the loss of an extracellular regulator of TGF-β family pathway, ADT-2, results in defective HSNs. Moreover, I examined the role of the intracellular signaling components called Smads in HSN development and found that specific receptor-activated and common Smads are necessary for HSNs to develop normally. Taken together, these findings show that TGF-β family pathway regulates neuronal development in a unique way. Further interrogation is required to decipher how this process occurs. In the next chapter, I focus on identifying the extracellular ligands required for the tuning of HSN development and important domains of SMA-6 for its regulatory action.

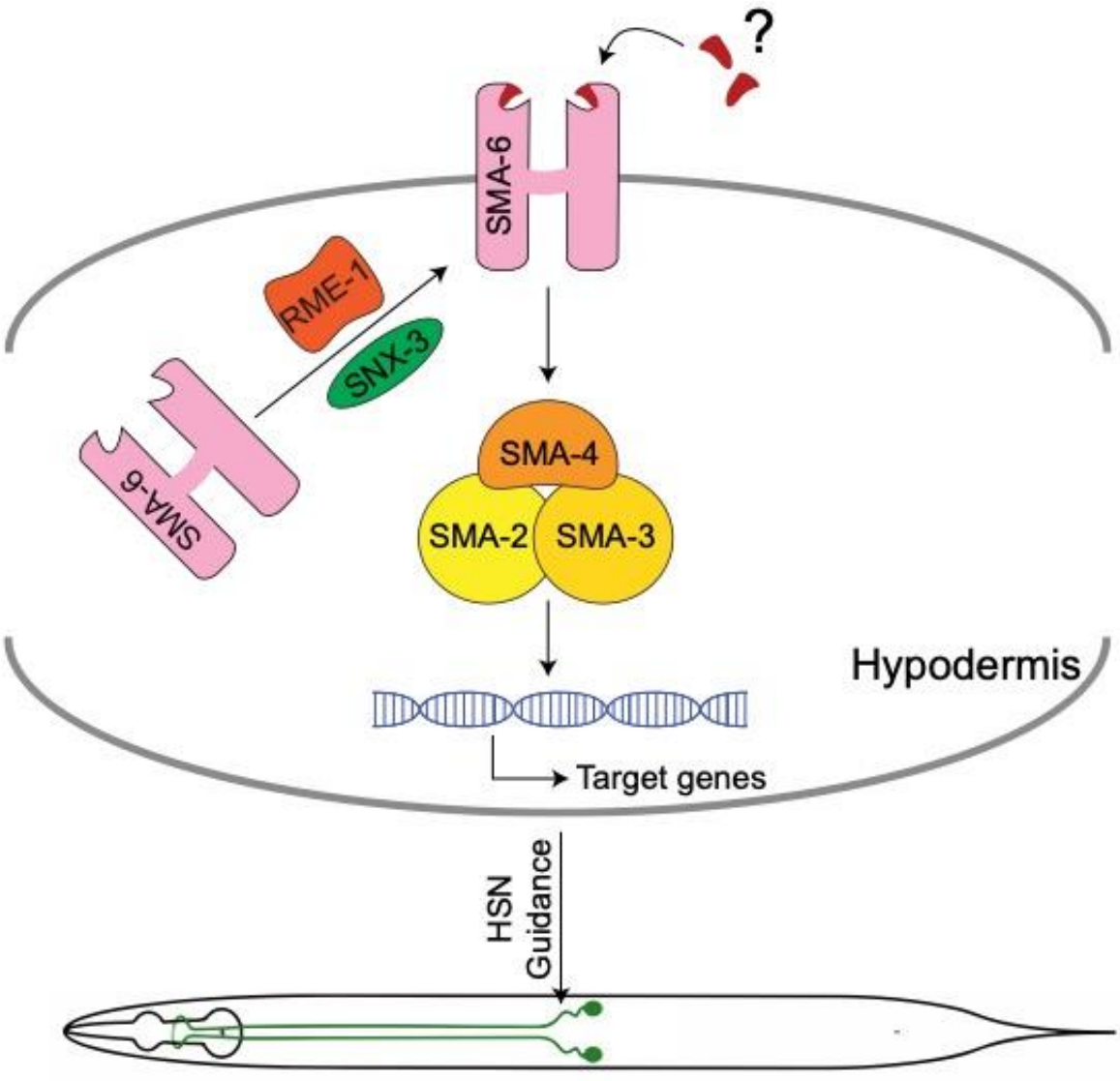

Fig. 3.10. TGF-β signaling regulates HSN development non-cell autonomously from hypodermis.

4. Structure-function analysis of TGF-β family ligands and the type I receptor SMA-6 in HSN development

4.1 Abstract

Cells require activation of receptors by extracellular ligands for generating biological response to changes in their environment. In *C. elegans*, there are five TGF-β family ligands named DBL-1, DAF-7, UNC-129, TIG-2 and TIG-3. Functions for some of these ligands have been identified in a wide range of biological functions such as the regulation of body size regulation, immunity, lifespan and neuronal development. In Chapter 3, I identified a non-canonical mechanism in which TGF-β signaling regulates the development of HSN neurons. I found that the type I receptor SMA-6 and particular SMADs - SMA-2, SMA-3 and SMA-4 - are required for HSN development, however the ligand(s) that activate SMA-6 is unclear. In this chapter, I screened the TGF-β family ligands for their roles in HSN development by examining the HSN phenotype of mutant strains as well as investigating the interactions between these ligands and the TGF-β family type I receptor SMA-6. Intriguingly, I found that the ligands of the canonical TGF-β family pathways, DBL-1 and DAF-7, were dispensable for HSN development, whereas the loss of UNC-129, TIG-2 or TIG-3 causes HSN defects. Furthermore, I found that TIG-2 and SMA-6 co-immunoprecipitate, suggesting that they interact in a protein complex. Taken together, my results revealed a non-canonical mechanism which requires multiple extracellular ligands to mediate the development of HSN neurons.

4.2 Introduction

The TGF-β family is divided into two subcategories based on their function. These are composed of TGF-β-like and the Bone Morphogenetic Proteins (BMP) group which comprises over 30 proteins in mammals. They control a wide range of processes such as cell differentiation, development and survival [148, 149] [150]. The TGF-β-like group is associated with body patterning and the formation of the three germ layers during embryogenesis, while BMPs are correlated with maintenance of epiblast pluripotency [149, 151]. The regulation of these processes by the TGF-β family requires the involvement of distinct components such as ligands, receptors and intracellular signaling molecules. This chapter will focus the on the roles of TGF-β family ligands and their association with the TGF-β family receptors.

TGF-β family ligands are produced as long precursors that include a signal peptide that determines localization and secretion, a pro-domain required for proper folding and a mature domain for its activity [10]. The precursor is cleaved by an enzyme such a proprotein convertase and then it is secreted to the extracellular space. Finally, TGF-β ligands interact target receptors in order to initiate the signaling within the receiving cell [10]. These mature forms contain a conserved cysteine knot that is composed of six cysteines that form disulfide bonds [9].

As mentioned in the previous chapters, the members of TGF-β family in *C. elegans* are subdivided into two major pathways based on the biological functions - the Sma/Mab pathway and the dauer pathway. The Sma/Mab pathway is primarily required for innate immunity, maintenance of a normal body size and male tail development, whereas the dauer pathway functions in dauer formation and the regulation of longevity [96]. There are five TGF-β family ligands encoded by the *C. elegans* genome - DBL-1, DAF-7, UNC-129, TIG-2 and TIG-3. The Sma/Mab pathway is initiated by binding of the DPP/BMP-like ligand (DBL-1) to the receptors which are SMA-6 and DAF-4 [96]. *dbl-1* is expressed in many tissues such as the pharynx and hypodermis, although its primary expression domain is in neurons [106]. DBL-1 is critical for body size regulation as *dbl-1* mutants possess a small phenotype [56]. However, it has been shown that the location of DBL-1 expression is not critical for body size regulation [103]. Furthermore, abnormal development has been reported in *dbl-1* mutant males [56, 140]. As

described in Chapter 1 and 3, DBL-1 function is strictly controlled by a transmembrane proteoglycan called LON-2/glypican which mediates the interaction between DBL-1 and its receptors [45]. In contrast, dauer pathway signaling is initiated by a TGF-β like ligand DAF-7 which is expressed during favorable environmental conditions from the ASI neurons to block dauer formation [97, 98].

The remaining three ligands in TGF-β family have not been directly associated with the canonical Sma/Mab and dauer pathways. One of these ligands is a BMP-like molecule, UNC-129. The name of this ligand comes from the uncoordinated movement displayed by the *unc-129* mutant worms [107] which is quite intriguing considering that none of the other TGF-β family member have been associated with the process of locomotion. Furthermore, *unc-129* mutant animals possess neither a variant body size nor a dauer-pathway-related phenotype which suggests a non-canonical function. UNC-129 is primarily expressed in body wall muscle and the nervous system [107] and has been shown to be important for axon guidance of specific neurons [107]. Both the absence and ectopic expression of UNC-129 can result in misguided axons, revealing that regulating the expression level of this ligand is important for correct nervous system development [107].

The ligands Transforming Growth Factor-2 and -3 (TIG-2 and TIG-3) are the least studied members of the TGF-β family of *C. elegans*. Structural similarities suggest that TIG-2 is related to BMP-like group, while TIG-3 is within the TGF-β-like group [96]. Expression of TIG-2 has been detected in body wall muscle and the pharynx [106]. Single cell sequencing data shows that TIG-3 is expressed largely in the germline and intestine [106]. To date, no phenotype has been reported in relation to this molecule.

The ligands in the TGF-β family pathway associate with two different receptors, type I and type II, via specific domains in order to initiate the signaling. When the type II receptor is activated by the ligand, it phosphorylates the type I receptor. This causes a conformational change within the type I receptor structure which then phosphorylates the intracellular signaling molecules called SMADs. Through this phosphorylation the signal is propagated to downstream effectors that regulate the expression of target genes [5]. The type I and type II receptors share similar features such as a cysteine-enriched ligand-binding domain which is conserved in the *C. elegans* TGF-β family

receptors. The sole *C. elegans* type II receptor DAF-4 possesses the conserved cysteine box within the extracellular component and has been shown to interact with human BMP2 [110]. The type I receptors DAF-1 and SMA-6 also carry the cysteine box as well as a GS domain which encompasses three repeats of serine and glycine residues. This GS domain is required for the activation of the type I receptor via phosphorylation by the type II receptor [5].

The aim of this chapter was to identify the TGF-β family ligand(s) that acts with SMA-6 to regulate HSN development. For this purpose, I examined HSN development of mutant strains for all five TGF-β family ligands as well as the double mutants generated between the mutant strains of *sma-6* and the individual ligands. Furthermore, I conducted biochemical experiments to investigate the complex formation between the TGF-β family ligands and the type I receptor SMA-6. The results of this chapter provide important information on the role of TGF-β family ligands in HSN development as well as providing insights on the structure/function relationship between these ligands and SMA-6.

4.3 Methods

Examination of HSN phenotypes were performed using the HSN marker strains; *zdIs13, mgIs71,* and the transgenic line *rpEx6* based on the chromosomal region of the candidate genes. To avoid confusion, these strains were written as *HSN::GFP*. For the maintenance and scoring details for the worms and the cell culture, please refer to Chapter 2.

4.3.1 Molecular Cloning

RJP349 *sma-6::MYC*

The construct includes *sma-6* cDNA without the stop codon fused to MYC tag (EQKLISEEDL) coding sequence.

RJP152 *tig-2::FLAG*

The construct includes *tig-2* cDNA without the stop codon fused to FLAG tag (DYKDDDDK) coding sequence.

RJP410 *tig-3::HIS*

The construct includes *tig-3* cDNA without the stop codon which was amplified from N2 cDNA with Phusion DNA Polymerase using OFB139 and OFB140 primers. OFB140 also contains the coding sequence of the HIS tag that translates into HHHHHH peptide. The vector pcDNA™ 3.1/Zeo(+) linearized by NheI and KpnI enzymes. The PCR product was digested with NheI and KpnI and inserted into the vector.

RJP409 *unc-129::V5*

The construct includes *unc-129* cDNA without the stop codon which was amplified from N2 cDNA with Phusion DNA Polymerase using OFB143 and OFB144 primers. The vector pcDNA-Wnt3A-V5 was linearized and Wnt3A sequence was removed by PCR with Phusion DNA Polymerase using OFB141 and OFB142. This vector contains the coding sequence of V5 tag that translates into GKPIPNPLLGLDST.

4.3.2 Site-Directed Mutagenesis

RJP521 *Δsma-6::MYC*

The three cysteine residues of the putative ligand-binding domain (CCYEGNYCN), which are at the 143rd, 144th and 150th position in SMA-6 protein, were replaced by alanine residues. RJP349 *sma-6::MYC* plasmid was amplified by PCR with Phusion DNA Polymerase using mismatch primers in two steps. Initially, the first two cysteines were replaced using OFB62 and OFB63, and then the resulting plasmid was amplified using OFB131 and OFB132.

4.3.3 Co-Immunoprecipitation and western blot

In order to investigate protein-protein interactions, co-immunoprecipitation (co-IP) experiments were performed using HEK293T cells. Detailed information on cell preparation, transfection, lysis, co-IP, sodium dodecyl sulfate–polyacrylamide gel electrophoresis (SDS-PAGE) and western blot can be found in Chapter 2, General Methods. Briefly, cells were transfected with the required constructs (*sma-6::MYC*, *Δsma-6::MYC*, *tig-2::FLAG*, *tig-3::HIS*, *unc-129::V5* and alternative mixture of these construct based on the experiment) and were lysed after 24 hours of incubation. To capture the proteins for co-IP, Dynabeads Protein G (Thermo Fisher Scientific) and the antibodies specific for the protein tags which are anti-MYC (ab9106, abcam), anti-FLAG (2368, Cell Signaling), anti-HIS (AD1.1.10, Bio-Rad) and anti-V5 (SV5-Pk1, Bio-Rad) were used. Proteins were separated using SDS-PAGE and then they were transferred to a PVDF membrane using iBlot™ 2 transfer system (Thermo Fisher Scientific). Proteins were visualized by ChemiDoc™ XRS+ (Bio-Rad) using the antibodies specific for the protein tags.

4.4 Results

4.4.1 Screen for TGF-β ligands that regulate HSN development

In Chapter 3, I showed that TGF-β signaling regulates HSN development via a non-canonical mechanism. I showed that the type I receptor SMA-6 acts independently of the type II receptor DAF-4 along with the intracellular signaling SMADs, however the extracellular ligands necessary for the initiation of signaling remain unclear. For this purpose, I investigated the role of the five TGF-β family ligands of *C. elegans* which are DPP/BMP-like ligand (DBL-1), DAF-7/TGF-β-like, UNC-129/BMP-like, Transforming Growth Factor-2 and -3 (TIG-2 and TIG-3). DBL-1 and DAF-7 are the ligands of the two canonical TGF-β family signaling in *C. elegans*, the Sma/Mab and the dauer pathway, respectively, whereas UNC-129 acts in a non-canonical manner regulating axon guidance events [96]. TIG-2 and TIG-3, however, have not been studied extensively and their biological roles are unclear.

To interrogate the role of these ligands in HSN development, I crossed the following mutant strains with the *HSN::GFP* reporter - *daf-7(e1372)*, *tig-2(ok3416)*, *tig-3(tm2092)*, *dbl-1(wk70)* and *unc-129(ev554)*. *dbl-1(wk70)* and *unc-129(ev554)* contain substitutions that introduce premature stop codons [56, 107], while *daf-7(e1372)* contains a substitution at a conserved intron splicing site and has been shown to cause dauer formation [152]. *tig-2(ok3146)* and *tig-3(tm2092)* contain 467-bp and 703-bp deletions, respectively that result with frameshifts and premature stop codons.[141]. *tig-3(tm2092)* and *tig-2(ok3416)* alleles have not been fully characterized, however the rest of the mutants for the other genes cause gene-specific phenotypes. My phenotypic analysis of these strains revealed a very sophisticated mechanism, detailed below, in which there are multiple ligands acting in the same pathway as SMA-6 to control the development of HSNs (Fig. 4.1B).

DAF-7, the ligand of the dauer pathway, was found to be dispensable for HSN development, which is in concurrence with my previous findings on the components of the dauer pathway (Fig. 4.1B). Interestingly, the loss of DBL-1, the ligand of Sma/Mab

pathway, also did not cause HSN developmental defects (Fig. 4.1B). DBL-1 is a known interactor of SMA-6 for the control of body size regulation, therefore this result further suggests a non-canonical mode-of-action action for TGF-β signaling on HSN development. The third TGF-β family ligand UNC-129 was found to be an important molecule for HSN development, as approximately 45% of *unc-129* mutant animals had defective HSNs (Fig. 4.1B). UNC-129 has previously been reported to regulate the migration of mesodermal cells and the axon guidance events of motor neurons [107]. My finding shows this regulatory function of UNC-129 is not limited to these cells, but is also required by the HSNs, which are also motor neurons. Lastly, the least studied ligands of TGF-β family in *C. elegans*, TIG-2 and TIG-3, were also found to be required for HSN development. TIG-2 and TIG-3 had not been associated with any other mechanisms, thus the HSN-defective phenotype is the first evidence that sheds light on the function of these ligands.

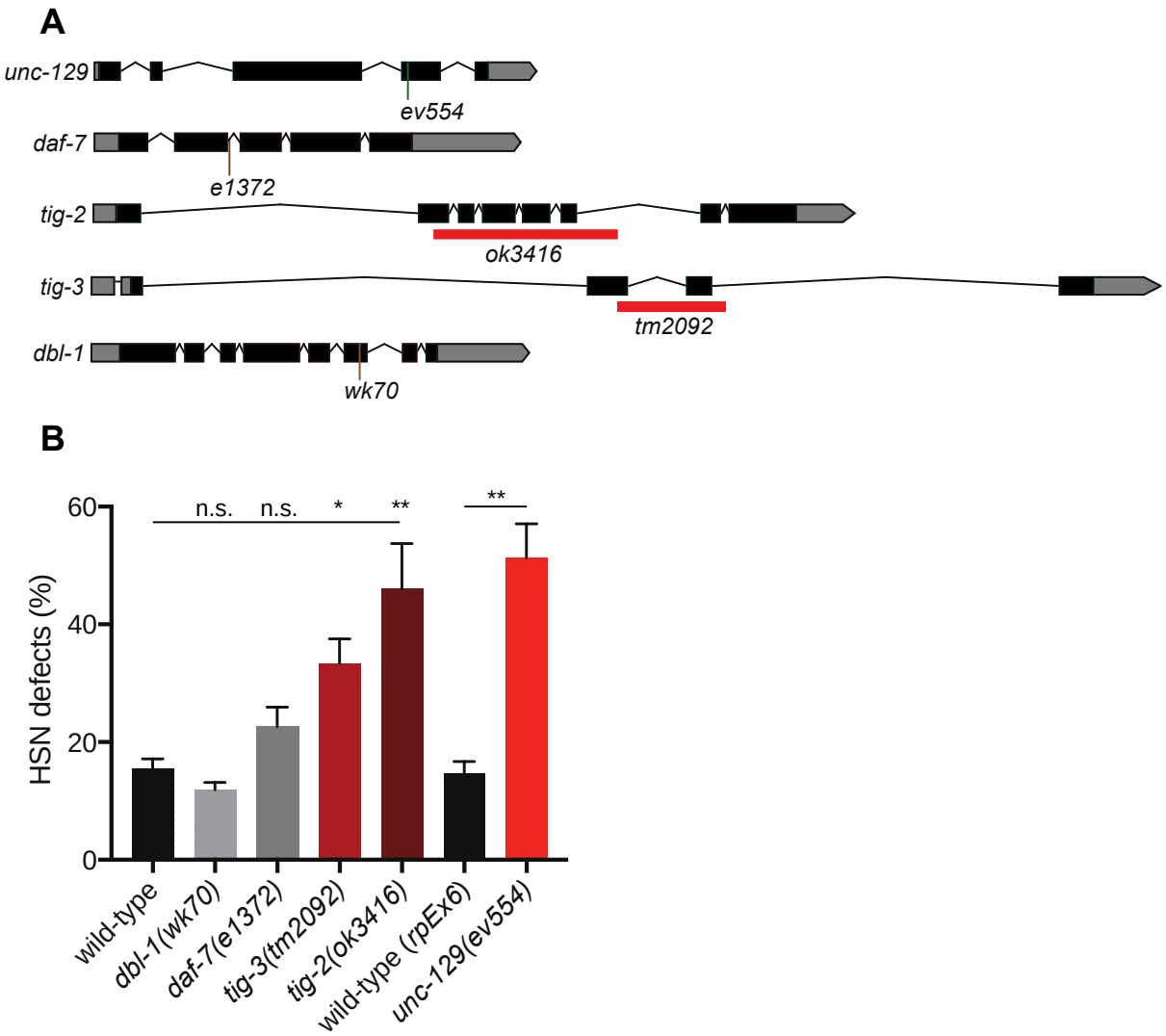

Fig. 4.1. The screen of TGF-β family ligands in HSN development.

(A) Gene structure of TGF-β family ligands. Black boxes represent exons, black lines represent introns and grey boxes represent UTRs. For the mutations, red boxes represent deletions and brown lines represent substitutions. *ok3146* and *tm2092* are 467-bp and 703-bp deletions, respectively that result with frameshifts and premature stop codons. *wk70* is a substitution that introduces a premature stop codon (Q314*), while *e1372* is a G>A substitution at a conserved intron splicing site. *ev554* causes a premature stop codon (D327*), however the change in the DNA sequence has not been reported, therefore was shown with a green line. (B) Quantification of HSN defects in wild-type and mutant worms of TGF-β family ligands. Statistical analysis was performed using one-way ANOVA and Dunnett's multiple comparison test. Due to chromosomal location of *unc-129*, HSN development of *unc-129* mutant animals have been examined with another HSN marker strain, *rpEx6*, which carries *HSN::GFP* as an extrachromosomal array. Statistical analysis of these data was performed using an unpaired *t*-test. At least one hundred animals were scored per strain. n.s., not significant, *$p < 0.05$, **$p < 0.01$, error bars represent mean ± SEM of three biological replicates.

Based on these data, it can be concluded that the extracellular ligand requirement for TGF-β signaling to control HSN development is quite complex, therefore requires further interrogation. To understand which of these ligands act with SMA-6, the mutant strain for each ligand was crossed with *sma-6(wk7)* mutants and HSN development of the resulting double mutants were examined. Interestingly, all the three double mutants showed similar defects as the single mutants (Fig. 4.2) which suggests that these ligands act in the same genetic pathway with SMA-6 for regulation of HSN development. To date, an action of multiple TGF-β ligands on the same receptor has not been reported in *C. elegans*. However, growth and differentiation factor 1 (GDF1) and Nodal - members of TGF-β family ligands - have been shown to function together in body pattering of mouse embryos [153]. Therefore, it is possible that action of multiple ligands is required for TGF-β-mediated HSN development.

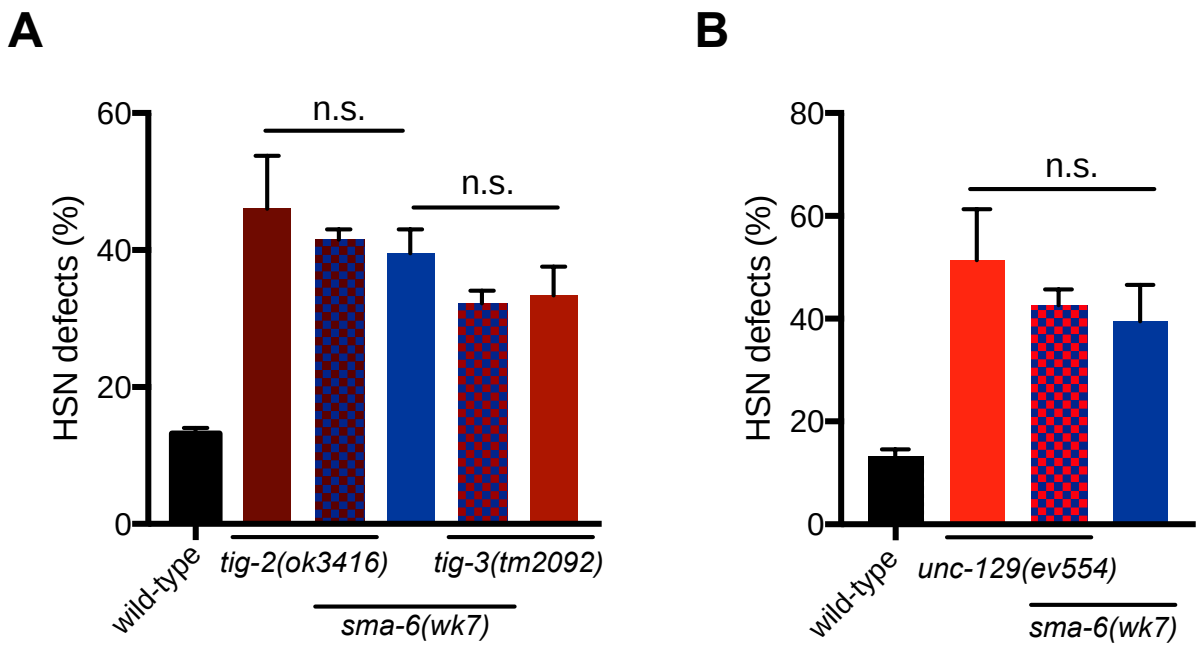

Fig. 4.2. SMA-6 acts with multiple ligands to regulate HSN development.

The role of TIG-2 and TIG-3 (A) and UNC-129 (B) in SMA-6-regulated HSN development. *wk7* is a missense point mutation that results with a premature stop codon. Statistical analysis was performed using one-way ANOVA and Dunnett's multiple comparison test. The test was performed separately for each ligand comparing the single mutants with the double mutants. At least one hundred animals were scored per strain. n.s., not significant, error bars represent mean ± SEM of three biological replicates.

To further investigate the hypothesis of multiple TGF-β family ligand action in HSN development, I generated double mutant combinations of *unc-129*, *tig-2* and *tig-3* mutants as well as the *unc-129; tig-2; tig-3* triple mutant. Strikingly, I did not detect a further increase in the HSN defects of these double and triple mutants compared to the single mutants (Fig. 4.3). Although the severity of the defects was slightly lower in *tig-3* mutants, statistical analysis revealed no difference. Taken together with the *sma-6* double mutant analysis, these data indicate that UNC-129, TIG-2 and TIG-3 act in the same genetic pathway as SMA-6 to regulate HSN development.

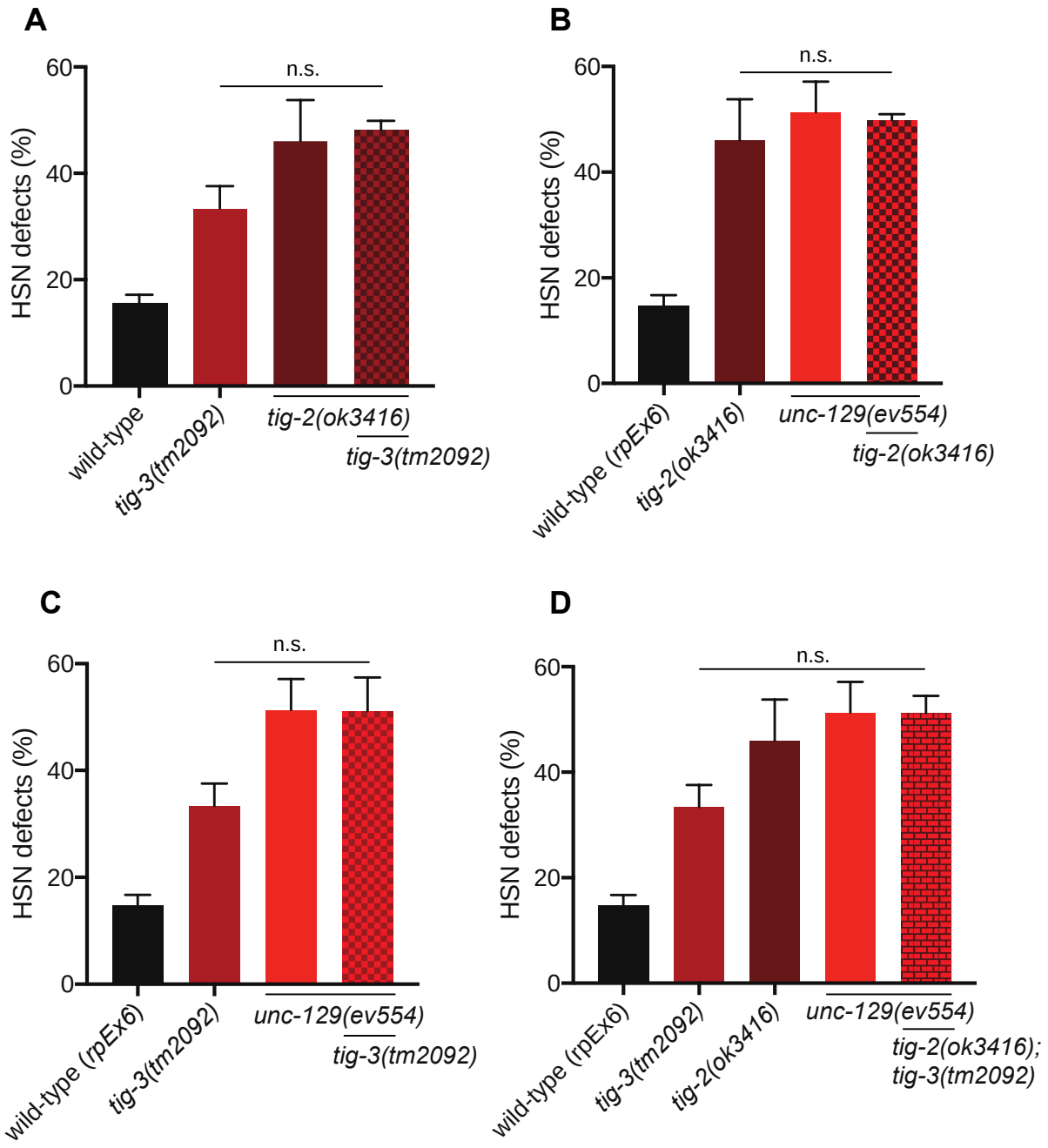

Fig. 4.3. UNC-129, TIG-2 and TIG-3 act in the same pathway to regulate HSN development.
(A), (B) and (C) show the quantification of HSN defects in the *unc-129; tig-2; tig-3* triple mutant as well as the double mutant combinations of *unc-129*, *tig-2* and *tig-3* mutants. For the ease of presentation of the data, these combinations were plotted separately, however statistical analysis was performed using one-way ANOVA and Tukey's multiple comparison tests analyzing all the data together. At least one hundred animals were scored per strain. n.s., not significant, error bars represent mean ± SEM of three biological replicates.

4.4.2 Analysis of interactions between the TGF-β ligands and SMA-6, the TGF-β type I receptor

The extracellular ligands of the TGF-β family typically act by interacting with the type I and the type II receptors. The type I receptors in *C. elegans* are SMA-6 and DAF-1, while DAF-4 is the only type II receptor. So far, I have identified that among the five TGF-β family ligands, UNC-129, TIG-2 and TIG-3 are required for HSN development (Fig. 4.1). Furthermore, I showed that these ligands act with SMA-6 in the same genetic pathway (Fig. 4.2). To further investigate this complex mechanism, I examined the interaction between these ligands and the type I receptor SMA-6 using co-immunoprecipitation experiments in mammalian cells.

The unavailability of the antibodies for *C. elegans* makes the protein studies challenging. In previous studies, it has been shown that the mammalian HEK293T cells can be used for testing interactions between *C. elegans* proteins [45]. Thus, I decided to use these cells to test the potential interaction between the TGF-β ligands and SMA-6. In order to express these genes in the HEK293T cells, coding sequences of these genes were cloned into an expression vector as described in Section 4.3. Each gene was cloned into a vector that has a different protein tag at the C-termini of the proteins so that they could be detected using a specific antibody against the tags (*tig-2::FLAG*, *tig-3::HIS*, *unc-129::V5*). After cloning, the constructs were tested for expression before proceeding to the interaction experiments. Initially, the cells were transfected with *tig-2::FLAG* as described in Section 4.3 and the detection of the proteins was performed using SDS-PAGE and western blot. TIG-2 protein has only one isoform and its estimated molecular weight is 41.3 kD. Examination of the membrane showed that there is a strong band between the 36 and 50 kD bands on the protein standard which was not present in the non-transfected cells, thus the identified band is TIG-2 (Fig. 4.4). Furthermore, there was no observable difference between the different conditions in which the cells expressed the construct for 24 hours and 48 hours. Based on these data, I decided to use 3 μg of *tig-2::FLAG* construct and 24 hours incubation time. The same conditions were applied to all the other ligands.

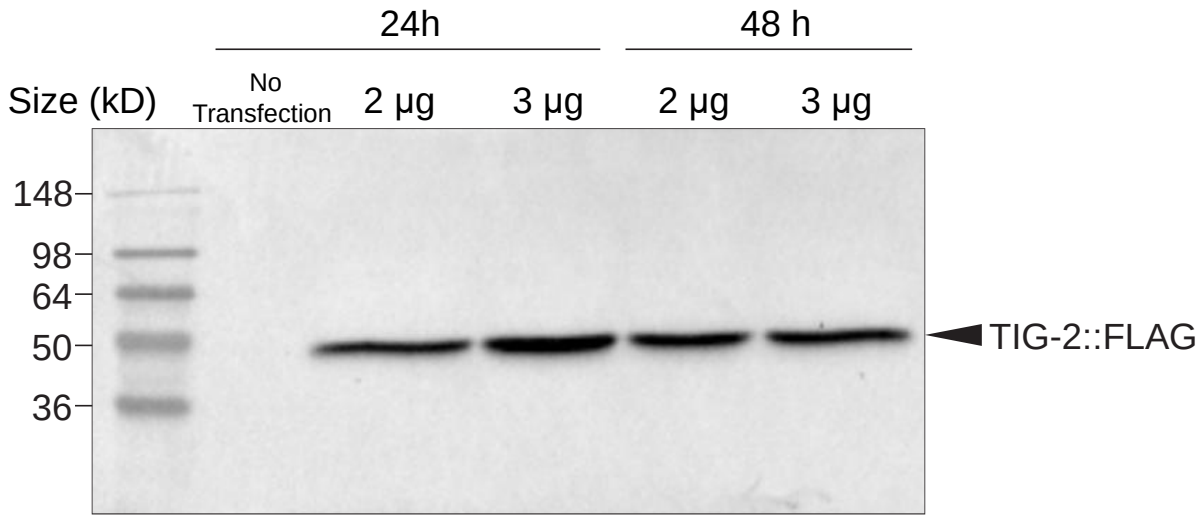

Fig. 4.4. TIG-2::FLAG expression in HEK293T cells.

Western blot analysis of TIG-2::FLAG using HEK293T cell lysates. Cells were incubated with 2 µg or 3 µg *tig-2::FLAG* for 24 hours or 48 hours before lysis. The membrane was incubated with anti-FLAG antibody (Cell Signaling) to detect TIG-2::FLAG. No band was detected in the control lysate.

After successfully expressing *tig-2::FLAG* in the HEK293T cells, I proceeded to the interaction experiment. First, I tested the interaction between TIG-2-FLAG and SMA-6 which was fused with a MYC tag in the expression vector. The experiment was carried out using co-immunoprecipitation (co-IP) followed by a western blot. In this experiment, one of the proteins is used as a "bait" and is captured using magnetic beads with a specific antibody against one of the proteins. Then, during the western blot experiment another antibody which is specific to the second protein (prey) is used for detection. For the SMA-6/TIG-2 interaction, reciprocal experiments were performed using each protein as bait and prey in different conditions and these experiments were repeated at least three times. The results of these experiments revealed that TIG-2 was able to co-immunoprecipitate with SMA-6 (Fig. 4.5A). In the experiment shown in Fig. 4.7, SMA-6::MYC was precipitated using Protein G magnetic beads and anti-MYC (abcam) antibody as bait. Then, proteins were visualized using anti-MYC and anti-FLAG antibodies in a western blot experiment. TIG-2::FLAG (indicated by a red arrowhead), which was the prey, was detected after the precipitation of SMA-6::MYC (indicated by a blue arrowhead) which was the bait. Furthermore, TIG-2::FLAG was not detected in the control lysates which indicates the specificity of this interaction. Interestingly, another band (indicated by a brown arrowhead) was detected in the SMA-6/TIG-2 co-IP lane which is between 16 kD and 36 kD in size. I hypothesized that this could be the

cleaved form of TIG-2 considering that TGF-β family ligands are synthesized in large precursor forms and they are cleaved to a mature form prior to being secreted to the extracellular environment [10]. In another study, I have shown that TIG-2 indeed has long and short forms where the long precursor form was detected in the cell lysate, while the short mature form was detected in the cell culture media [91]. The short form was not detected in the previous western blot experiment, since the cell culture media was not examined. Next, I performed another co-IP in which the bait and the prey were reversed to TIG-2 and SMA-6, respectively (Fig. 4.5B). TIG-2::FLAG was precipitated using Protein G magnetic beads and anti-FLAG antibody. Then, proteins were visualized using anti-MYC and anti-FLAG antibodies in a western blot experiment. SMA-6::MYC (indicated by a blue arrowhead) was detected after the precipitation of TIG-2::FLAG (indicated by a red arrowhead). Furthermore, SMA-6::MYC was not detected in the TIG-2::FLAG-only control lysate which indicates the specificity of this interaction. Taken together, these data show that TIG-2 and SMA-6 co-immunoprecipitate which suggests that these proteins interact with each other and/or they are part of the same protein complex. Moreover, these findings further substantiate my hypothesis on TIG-2 acting in the same genetic pathway as SMA-6.

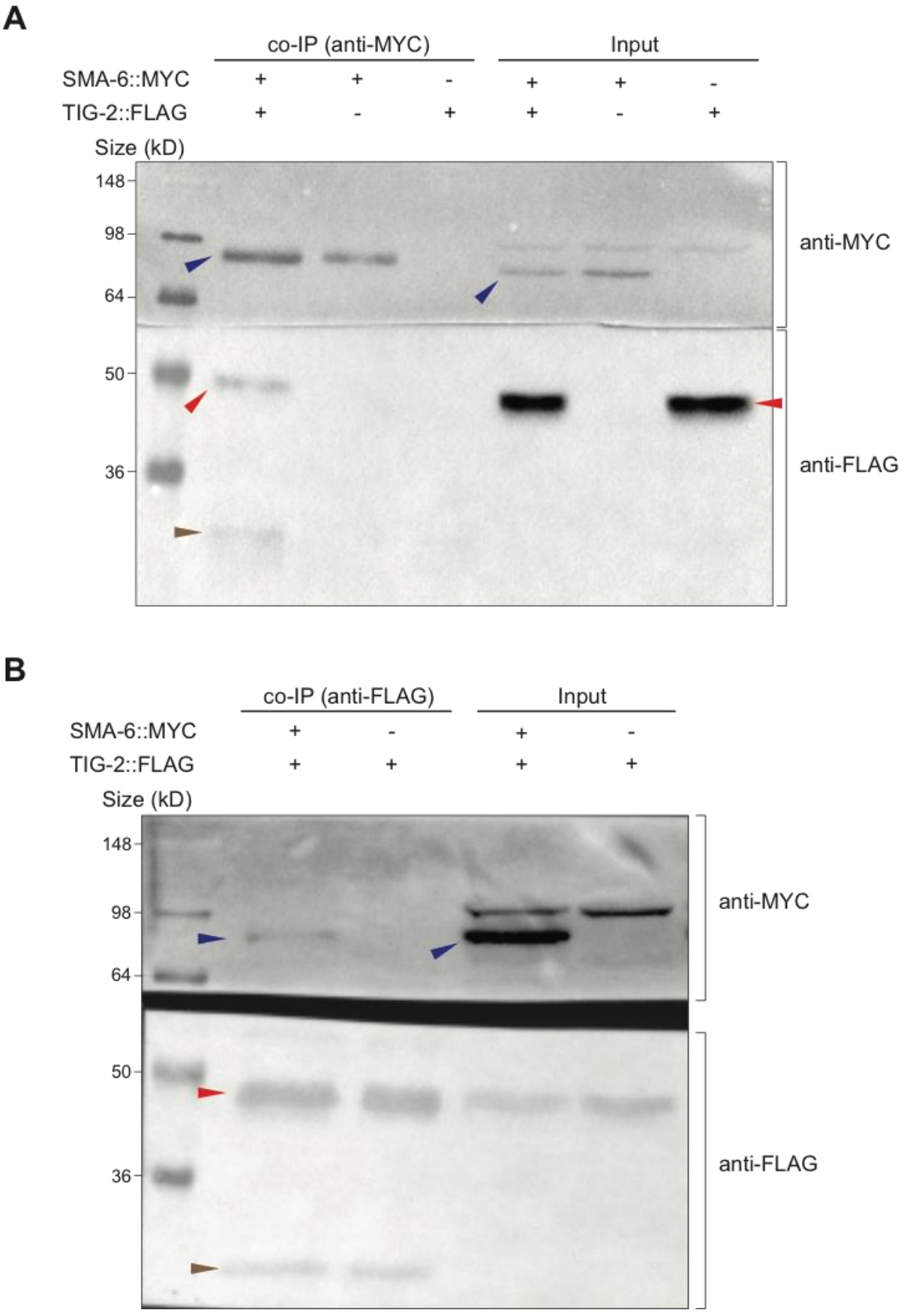
A
co-IP (anti-MYC)
Input
SMA-6::MYC + + - + + -
TIG-2::FLAG + - + + - +
Size (kD)
148
98
64
50
36
anti-MYC
anti-FLAG
B
co-IP (anti-FLAG)
Input
SMA-6::MYC + - + -
TIG-2::FLAG + + + +
Size (kD)
148
98
64
50
36
anti-MYC
anti-FLAG

Fig. 4.5. TIG-2 and SMA-6 co-immunoprecipitate in HEK293T cells.

(A) and (B) show the western blot analysis of the co-IP experiments between SMA-6::MYC and TIG-2::FLAG. In (A), co-IP was performed targeting SMA-6::MYC (bait) using magnetic beads (Dynabeads Protein G) and anti-MYC antibody, whereas in (B), co-IP was performed targeting TIG-2::FLAG (bait) using magnetic beads (Dynabeads Protein G) and anti-FLAG antibody. WB refers to the western blot experiment which allows visualization of both SMA-6::MYC and TIG-2::FLAG. The estimated size of SMA-6 and TIG-2 are 72.2 and 41.3 kD, respectively. In order to prevent non-specific binding to the antibodies, the membrane was cut horizontally between 50 kD and 64 kD bands. The upper band was incubated with anti-MYC, whereas the lower band was incubated with anti-FLAG. Input refers to the cell lysates without co-IP step which were prepared to ensure that SMA-6::MYC and TIG-2::FLAG were expressed properly. Arrowheads indicate SMA-6 and TIG-2 in blue and red, respectively. Brown arrowhead indicates the putative cleaved form of TIG-2. It was not detected in the input samples as this cleaved TIG-2 is secreted to the cell culture media. *sma-6::MYC* only and *tig-2::FLAG* only transfections were performed to ensure the detected interaction was not due to an unspecific binding of the prey to the beads or to the antibody.

Next, the interaction between SMA-6 and TIG-3 was investigated. The coding sequence of *tig-3* was fused with the HIS protein tag and cloned into an expression vector (Section 4.3.1). Prior the examination of the interaction, a western blot experiment was performed to visualize the expression of *tig-3::HIS*. HEK293T cells were incubated with 3 ug of *tig-3::HIS* for 24 hours before lysis. After the cells were lysed, an SDS-PAGE and western blot experiment were performed. Since multiple bands were detected for TIG-2 expression, both the cell lysate and the cell culture media of *tig-3::HIS*-transfected cells were analyzed. After examining the cell lysates, I detected a band between the 16 and 36 kD protein standard bands (Fig. 4.6, green arrowhead) which was not present in the non-transfected cells. TIG-3 protein has only one isoform and its estimated molecular weight is 28.4 kD, therefore I concluded that the detected band is of TIG-3. Interestingly, no bands were detected in the cell culture media of neither *tig-3::HIS*-transfected nor non-transfected cells which could be due to its potential low expression.

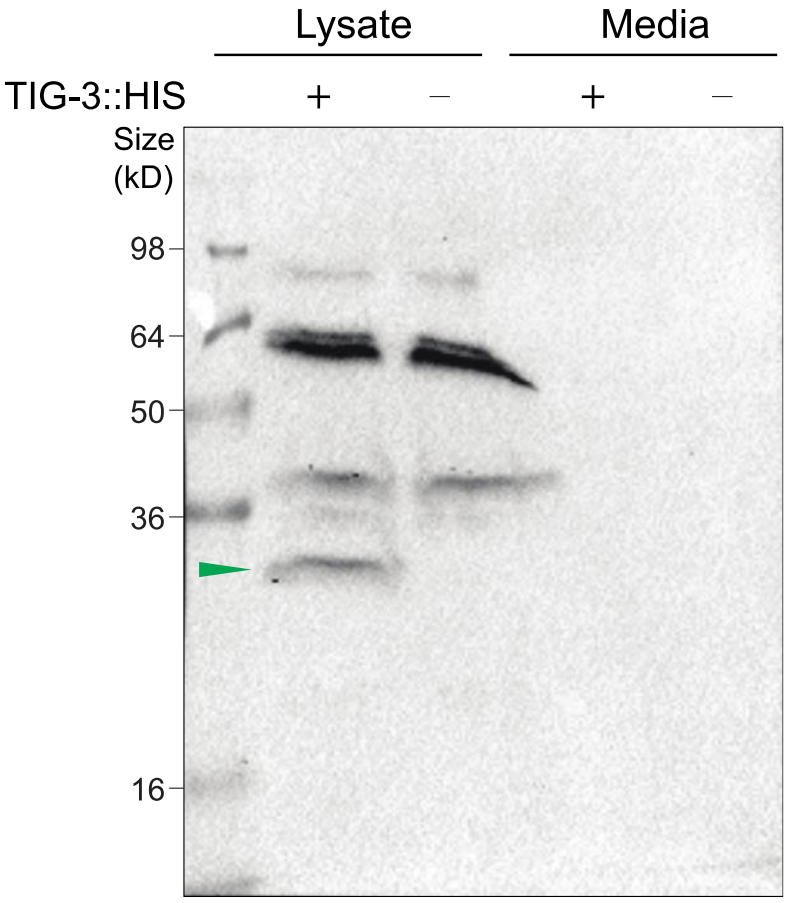

Fig. 4.6. TIG-3::HIS expression detected in HEK293T cells.

Western blot analysis of TIG-3 using HEK293T cell and cell culture media lysates. The estimated size of TIG-3 protein is 28.4 kD. Green arrowhead indicates the TIG-3::HIS band which is not present in the non-transfected cells. No band was detected in the media of either *tig-3::HIS* transfected cells or non-transfected cells. The specific protein detection was achieved using anti-HIS (Bio-Rad) primary antibody.

After confirming the TIG-3::HIS production in HEK293T cells, I interrogated the potential interaction between SMA-6 and TIG-3 by conducting a co-IP experiment followed by a western blot. The bands in the input lanes show a successful TIG-3 and SMA-6 expression marked with green and blue bands, respectively (Fig. 4.7) In the co-IP experiment, SMA-6 (bait) was pulled down using anti-MYC antibody and Protein G magnetic beads which could also be seen specifically in the SMA-6::MYC/TIG-3::HIS- and SMA-6::MYC-only-transfected cell lysates. However, there were unspecific bands in each co-IP lanes between 36 and 16 kD. Considering that these bands were present in all of the lanes, I concluded that these bands cannot be of TIG-3::HIS. Furthermore, the sizes of these unspecific bands were very similar to the size of TIG-3 in comparison with the TIG-3 bands in the input lanes. Thus, a potential co-immunoprecipitation of

TIG-3 with SMA-6 would overlap with the unspecific bands. Consequently, I was not able to conclude whether TIG-3 interacts with SMA-6.

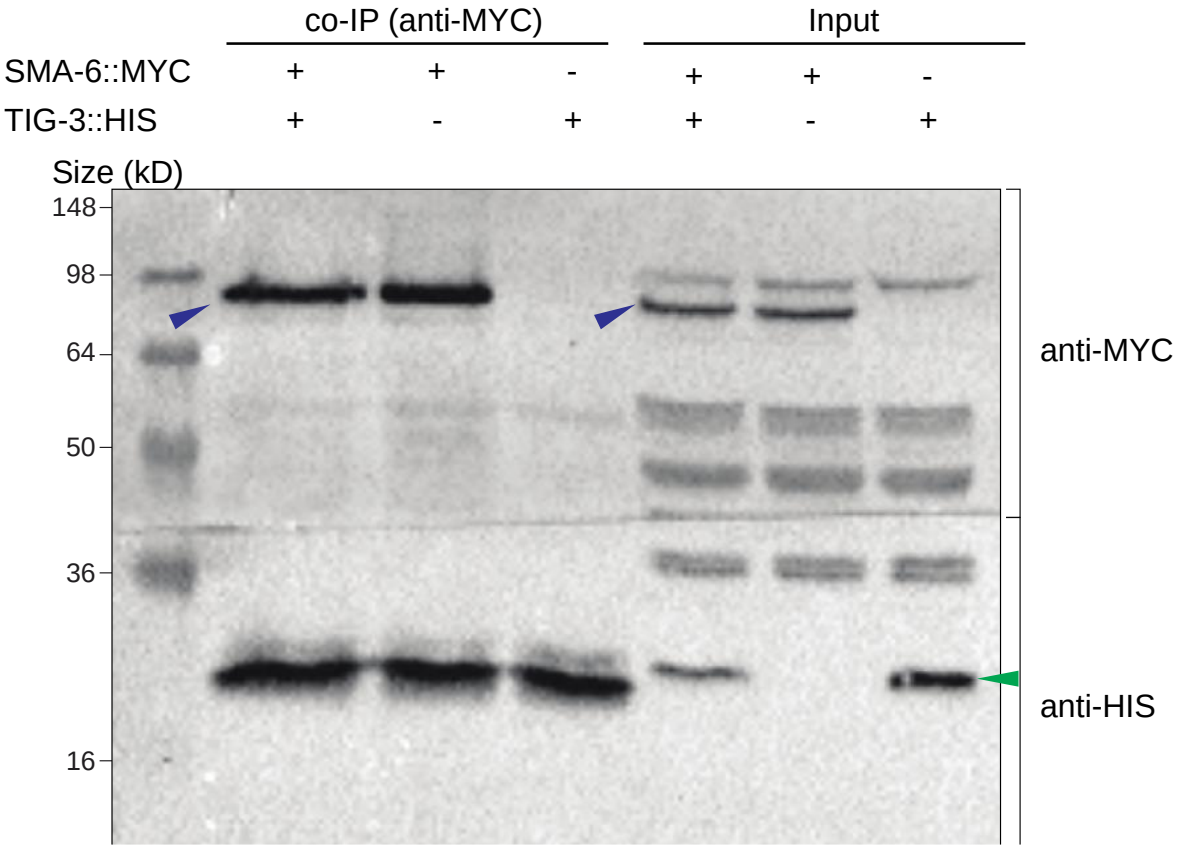

Fig. 4.7. Analysis of TIG-3 and SMA-6 interaction in HEK293T cells

Western blot analysis of the co-IP experiment between SMA-6::MYC and TIG-3::HIS. Co-IP was performed targeting SMA-6::MYC (bait) using magnetic beads (Dynabeads Protein G) and anti-MYC antibody. WB refers to the western blot experiment which allows visualization of both SMA-6::MYC and TIG-3::HIS (prey). The estimated size of SMA-6 and TIG-3 are 72.2 and 28.4 kD, respectively. In order to prevent non-specific bindings to the antibodies, the membrane was cut horizontally between 64 kD and 50 kD indicators. The upper band was incubated with anti-MYC, whereas the lower band was incubated with anti-HIS. Input refers to the cell lysates without co-IP step which were prepared to ensure that SMA-6::MYC and TIG-3::HIS were expressed properly. Arrowheads indicate SMA-6 and TIG-3 in blue and green, respectively.

Finally, I have investigated the expression of BMP-like ligand UNC-129. The coding sequence of *unc-129* was fused with the V5 protein tag and cloned into an expression vector (Section 4.3.1). Prior the examination of the interaction, a western blot experiment was performed to visualize the expression of *unc-129::V5*. HEK293T cells were incubated with 3 µg of *unc-129::V5* for 24 hours before lysis. Cell culture media

was collected before cell lysis to examine if UNC-129 released to the extracellular space. After the cells were lysed, an SDS-PAGE and western blot experiment were performed using anti-V5 antibody (Bio-Rad) to detect UNC-129::V5. Interestingly, two different bands were detected the cell lysate of *unc-129::V5*-transfected cells which could be large precursor and short mature form of UNC-129 protein (Fig. 4.8).One of these bands was between 50 kD and 64 kD, while the other band was between 16 kD and 36 kD, indicated by dark and light blue arrowheads in Fig. 4.8, respectively. These bands were absent in the non-transfected cells which suggests that they are related to UNC-129. UNC-129 protein has only one isoform and its estimated size is 47.3 kD, thus the larger protein detected in *unc-129::V5*-transfected cells is most likely to be the large precursor form of UNC-129 protein. In addition, the cell culture media of *unc-129::V5*-transfected cells presented a strong band between 16 kD and 36 kD having the same size with the short band detected in the cell lysates. However, this band was observably much stronger in the cell culture media than in the lysates. Taken together, these findings suggest that like other TGF-β family ligands, UNC-129 has two alternative forms which are likely to be a long precursor form and short secreted mature form.

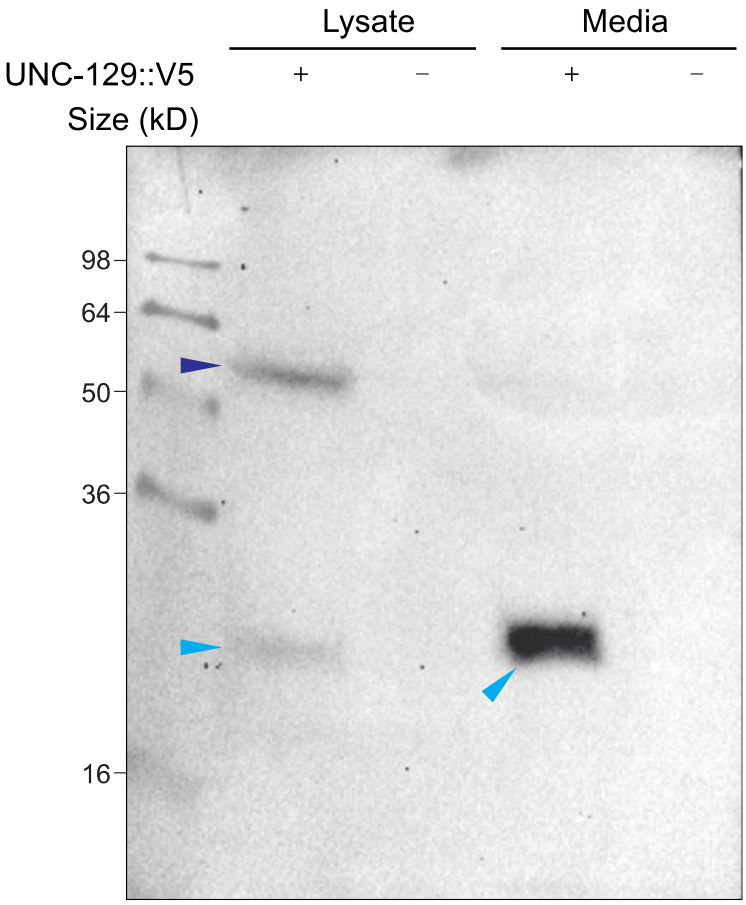

Fig. 4.8. UNC-129::V5 expression detected in HEK293T cells.

Western blot analysis of UNC-129 using HEK293T cell and cell culture media lysates. The estimated size of UNC-129 protein is 47.3 kD. Dark and light blue arrowheads indicate the potential precursor and mature forms of UNC-129, respectively. No bands were detected in the cell and cell culture media lysates of non-transfected cells. The specific protein detection was achieved using anti-V5 (Bio-Rad) primary antibody.

After successfully expressing UNC-129::V5 in HEK293T cells, I examined the potential interaction between SMA-6 and UNC-129 by performing a co-IP experiment followed by a western blot. However, I was not able to detect any proteins due to experimental problems, therefore data was not shown. To fully understand how UNC-129 works in the same pathway as SMA-6 in HSN development, this experiment needs to be repeated.

4.4.3 Investigation of the structural requirements of SMA-6/TIG-2 interaction

SMA-6 is a single-pass receptor that has a conserved cysteine box ($CCX_{4-5}CN$) which is likely to be the ligand-binding domain. To investigate whether this region is required for its interaction with TIG-2, the cysteine residues in the domain were replaced with alanine residues via site-directed mutagenesis. After confirmation of the mutation with Sanger sequencing, HEK293T cells were transfected in separate wells with the mutated (*Δsma-6::MYC*) and wild-type form of *sma-6::MYC* along with *tig-2::FLAG*. The interaction experiment was conducted using co-IP followed by SDS-PAGE and western blot. The bands in input lanes show that all the proteins were produced normally including ΔSMA-6::MYC which indicates that the substitution of cysteines with alanines in the putative ligand-binding domain did not affect expression or stability of the protein (Fig. 4.9). Surprisingly, TIG-2 was co-immunoprecipitated with ΔSMA-6::MYC as well as wild-type SMA-6::MYC. This suggests that the putative-ligand binding domain is not required for the complex formation between SMA-6 and TIG-2.

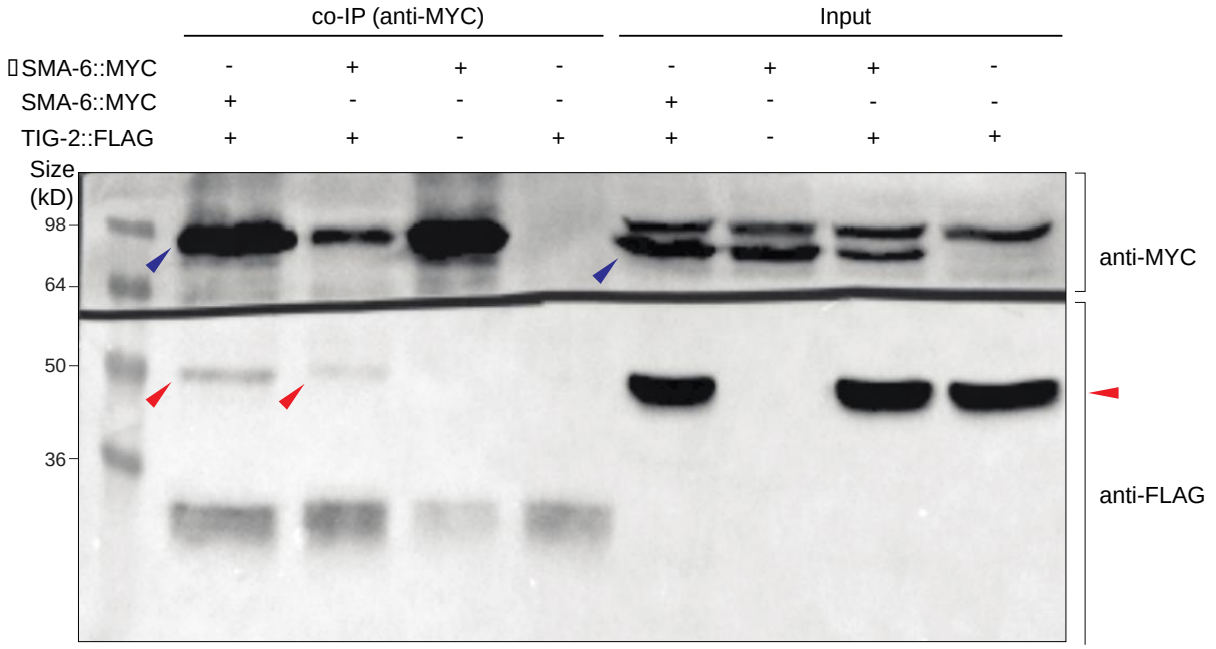

Fig. 4.9. TIG-2 co-immunoprecipitates with ΔSMA-6.

Western blot analysis of the co-IP experiment between SMA-6::MYC and TIG-2::FLAG. Co-IP was performed targeting SMA-6::MYC or ΔSMA-6::MYC (baits) using magnetic beads and anti-MYC antibody. ΔSMA-6 refers to the mutated SMA-6 of which the cysteine residues in the putative ligand-binding domain were substituted with alanine residues. The western blot experiment was performed using anti-MYC and anti-FLAG primary antibodies. In order to prevent non-specific binding to the antibodies, the membrane was cut horizontally between 64 kD and 50 kD indicators. Input refers to the cell lysates without co-IP step which were prepared to ensure that *sma-6::MYC*, *⊿sma-6::MYC* and *tig-2::FLAG* were expressed properly. The upper band was incubated with anti-MYC, whereas the lower band was incubated with anti-FLAG. Blue arrowheads indicate SMA-6::MYC, while red arrowheads indicate TIG-2::FLAG (prey). The interaction was detected in both combinations in which the cells expressed wild-type-SMA-6 or mutant-SMA-6.

4.5 Discussion

In this chapter, I aimed to identify the TGF-β family ligand(s) involved in HSN development. I found that the loss of UNC-129, TIG-2 and TIG-3 result with increased HSN defects, whereas DBL-1 and DAF-7 were dispensable for HSN development (Fig. 4.1B). Intriguingly, my double mutant analysis showed that all three ligands act in the same genetic pathway as SMA-6 (Fig. 4.2, Fig. 4.3). I therefore hypothesize that these ligands act in a complex for activating SMA-6 in the regulation of HSN development.

In Chapter 3, I showed that TGF-β family signaling acts in a non-canonical mechanism to drive HSN guidance. This mechanism includes the components of Sma/Mab pathway with the exception of the type II receptor DAF-4, whereas the components of the dauer pathway were found to have no impact on HSN development. DAF-7, the ligand acting in the dauer pathway, was found dispensable for the regulation of HSN development which is in concurrence with my previous findings. However, it was surprising to find that the loss of DBL-1 did not cause a defective HSN phenotype considering its role in the canonical Sma/Mab pathway. This is another indicator on how my proposed mechanism functions in a non-canonical manner.

UNC-129 acts neither in the Sma/Mab nor the dauer pathway. Instead, it is involved in the axon guidance events of specific motor neurons [107]. Interestingly, this process occurs independently of the canonical TGF-β family type I and type II receptors which makes UNC-129 unusual among the TGF-β family members in *C. elegans*. However, my results showed that UNC-129 is required for HSN development (Fig. 4.1) and it acts in the same genetic pathway as SMA-6 (Fig. 4.2B). The remaining two ligands are TIG-2 and TIG-3 which are BMP-like and TGF-β-like members of the *C. elegans* TGF-β family, respectively. Unlike DBL-1, DAF-7 and UNC-129, these molecules have not been extensively studied. To date, no function has been described for TIG-3, therefore my findings in HSN development were the first evidence on the function of the protein. I also found that TIG-2 is very important for the development of HSNs and it acts in the same pathway as SMA-6 as well as the other ligands. The loss of TIG-2 has been reported to weakly enhance the dauer formation [96]. This shows that TIG-2 can act on both two canonical TGF-β family pathways in *C. elegans*. In order to understand how these ligands act in HSN development, it could be useful to perform temporal and

tissue-specific rescue experiments. However, considering that these ligands are potentially secreted to the extracellular space, they could act from different tissues.

Use of mammalian cells to investigating the interactions among the *C. elegans* proteins have previously been reported [45]. Using HEK293T cells, I performed co-IP and western blot experiments to examine the interactions between TGF-β family ligands and SMA-6 which is a TGF-β family type I receptor in *C. elegans*. I showed that TIG-2 and SMA-6 co-immunoprecipitate (Fig. 4.5) which suggests that they are part of the same protein complex. Considering that the experiment was performed in mammalian cells, TIG-2 and SMA-6 were the only *C. elegans* proteins, therefore it could be argued that there is a physical interaction between these molecules. However, due to the homology between the TGF-β family members of *C. elegans* and mammalian cells, an unknown third molecule that is present in the cell lysates could have potentially mediated formation of this complex. Consequently, further experiments such as mass spectrometry are required to show the potential physical interaction between TIG-2 and SMA-6 in worms.

After showing a complex formation between TIG-2 and SMA-6, I investigated TIG-3 and UNC-129 as they are the other two ligands that act with SMA-6 in HSN development. However, I could not draw conclusions on the potential interaction of these ligands with SMA-6 due to experimental issues. In the SMA-6/TIG-3 co-IP experiment, I detected unspecific bands which were very similarly sized as TIG-3, thus I could not comment on the presence or absence of the protein after the pulldown of SMA-6. In future experiments, this experiment can be performed using an alternative antibody for the detection of TIG-3 which could potentially remove the unspecific bands. Alternatively, TIG-3 can be immunoprecipitated as the bait and SMA-6 can be detected as the prey. In SMA-6/UNC-129 co-IP experiment, detection of the specific proteins including SMA-6 and UNC-129 was failed which could be due to a wide range of experimental problems. In future experiments, higher concentrations of SMA-6 and UNC-129 expression constructs can be used in the co-IP experiments. Furthermore, the potential interaction between SMA-6 and UNC-129 might require the presence of other ligands, therefore co-expression of TIG-2 and TIG-3 as well as SMA-6 and UNC-129 could promote this process.

The C-terminus of the SMA-6 protein contains serine and tyrosine residues are important for kinase activity while the N-terminus contains a conserved cysteine box with $CCX_{4-5}CN$ amino acid consensus which has been shown to be the ligand-binding domain in mammalian systems. To investigate whether this domain facilitates the complex formation between SMA-6 and TIG-2, I mutated the cysteines with alanine residues (ΔSMA-6) and repeated the co-IP experiment. Surprisingly, TIG-2 was co-immunoprecipitated with ΔSMA-6 (Fig. 4.9) which shows that the putative ligand-binding domain is dispensable for the complex formation between SMA-6 and TIG-2. In future studies, targeting different regions of SMA-6 for mutagenesis and performing co-IP experiments are needed to discover the important domain required for the SMA-6-TIG-2 complex formation. Given the fact that the function of the conserved ligand-binding domain has not specifically been shown in *C. elegans* TGF-β family receptors, it is also likely that another ligand-binding domain is required for the interaction of SMA-6 with other TGF-β family ligands. Thus, it is important to perform further experiments on all the ligands to fully understand the structural requirements of the interaction between the TGF-β family receptors and ligands.

Prior to being secreted to the extracellular space, TGF-β ligands are generated as long precursors which include a localization signal, a prodomain and a mature domain [10]. These precursors are cleaved by a proteolytic enzyme and then are secreted to the extracellular space for their action on the receptors. However, this process has not been shown in TGF-β family ligands of *C. elegans*. In my SMA-6/TIG-2 co-IP experiment, I detected two differently sized TIG-2 bands that co-immunoprecipitated with SMA-6 (Fig. 4.5). The smaller band, which I hypothesized to be the secreted mature form of TIG-2, was not present in my initial western blot experiment as this mature form was secreted to the extracellular space. In another study, I performed western blot experiments on both the cell lysate and and cell culture media of *tig-2::FLAG*-transfected cells and also detected two TIG-2 bands [91] which were at the same size as in the SMA-6/TIG-2 co-IP experiment. Taken together, these findings show that production in long precursors and proteolytic cleavage processes of TGF-β family ligands are also conserved in *C. elegans*. UNC-129, which is also required for HSN development, was also detected in two differently sized bands (Fig. 4.8). Interestingly, the longer band was detected between 50 and 64 kD indicators, while the predicted protein size for UNC-129 is 47.3 kD. This could be due to the presence of

the 14-amino acid long V5 tag that has a mass of approximately 1.1 kD and potential post-translational modifications. The absence of this band in the control lysate indicates that this band is UNC-129. The shorter band, potentially the mature form of UNC-129, was between 16 and 36 kD indicators. Furthermore, most of this protein was secreted to the extracellular space considering the observable density difference between the cell lysate and cell culture media. Therefore, this smaller, processed form of UNC-129 is likely the functional form. Finally, TIG-3 expression was examined using HEK293T cells. Surprisingly, I found a specific band only in the cell lysate, but not in the cell culture media of *tig-3::HIS*-transfected cells (Fig. 4.6). The density of the detected TIG-3 band was observably lower than of TIG-2, therefore, TIG-3 expression was possibly too low to be detected in the culture media. Furthermore, the protein could be sensitive, thus could have been degraded in the cell culture media during the experimental process. Alternatively, there could be a problem in the cleavage process of the protein which could affect its maturation and secretion to the extracellular environment. In the future studies, immunoprecipitation experiments can be performed which could potentially enable stronger detection of the potential mature form of TIG-3.

By performing co-IP and western blot experiments in this chapter, I investigated the secretion of the TGF-β family ligands and their interaction with the type I receptor SMA-6. The reason that these experiments were conducted in mammalian cells rather than worms was the unavailability of the specific antibodies for these molecules. In future studies, these interactions can also be analyzed in worms thanks to emergent CRISPR/Cas9 techniques. Using this technique, knock-in mutants for the ligands as well as for SMA-6 can be generated by inserting protein tags next to the N or C terminus of the proteins. Although this may cause issues on the functionality of the proteins, my results suggest that the tagged ligands were structurally stable in HEK293T cells. Therefore, it is highly likely that the proteins after knock-in insertions would remain stable and could be used for interaction experiments. For this experiments, precursor and mature forms of the ligands should be taken into consideration as tagging the N termini of ligands could interfere with their localization signals and a potential cleavage could result with the loss of the tagged regions of ligands, thus their detection would not be possible.

TGF-β family signaling in *C. elegans* is, at present, divided into two canonical pathways which are Sma/Mab and dauer pathways. Both of these pathways require a single ligand to initiate the signaling which are DBL-1 and DAF-7, respectively. Therefore, it was surprising to identify multiple ligands acting with a single receptor in a non-canonical manner. However, the concept of multiple ligand action in the same TGF-β family signaling has previously been reported in different organisms [153]. Growth and differentiation factor 1 (GDF1) and Nodal - members of TGF-β family ligands - have been shown to function together during embryonic development of frogs and mice [153]. According to this study, GDF1 acts as a co-ligand for Nodal and regulates the activity of Nodal signaling. In the same study, these proteins have been shown to co-immunoprecipitate together and thus, are hypothesized to form heterodimers [153]. This concept could be also present in *C. elegans*. Specifically, UNC-129, TIG-2 and TIG-3 could potentially form a large complex with SMA-6, which could be via direct binding of ligands to SMA-6 individually. Alternatively, ligands could bind to each other and then bind to SMA-6 as a heterotrimer complex. If any of these molecules are removed, it could perturb the mechanism regulating the HSN development. This hypothesis could also explain the results of my triple and double mutant analysis among the ligands (Fig. 4.3) and SMA-6 (Fig. 4.2). In the future studies, this hypothesis can be interrogated by conducting co-IP experiments among UNC-129, TIG-2 and TIG-3 to examine a potential formation of a heterodimerization complexes. Furthermore, using a SMAD-specific reporter, the signaling strength of *unc-129*, *tig-2* and *tig-3* mutants can be compared with the double mutants which could give insights on the action of multiple TGF-β family ligands on the same pathway.

4.6 Conclusion

I found that the regulation of HSN development by the TGF-β family requires multiple ligands acting with the type I receptor SMA-6 (Fig. 4.10). In this mechanism, I showed that TIG-2 and SMA-6 form a protein complex, however further studies are required to investigate the biochemical interactions among SMA-6, UNC-129 and TIG-3. Furthermore, my results provide the first evidence on the function of previously uncharacterized TGF-β family ligands, TIG-2 and TIG-3, mediating HSN development through SMA-6. Taken together, my findings provide insight into the role of TGF-β family ligands in neuronal development as well as their alternative structural forms which could be critical for their function.

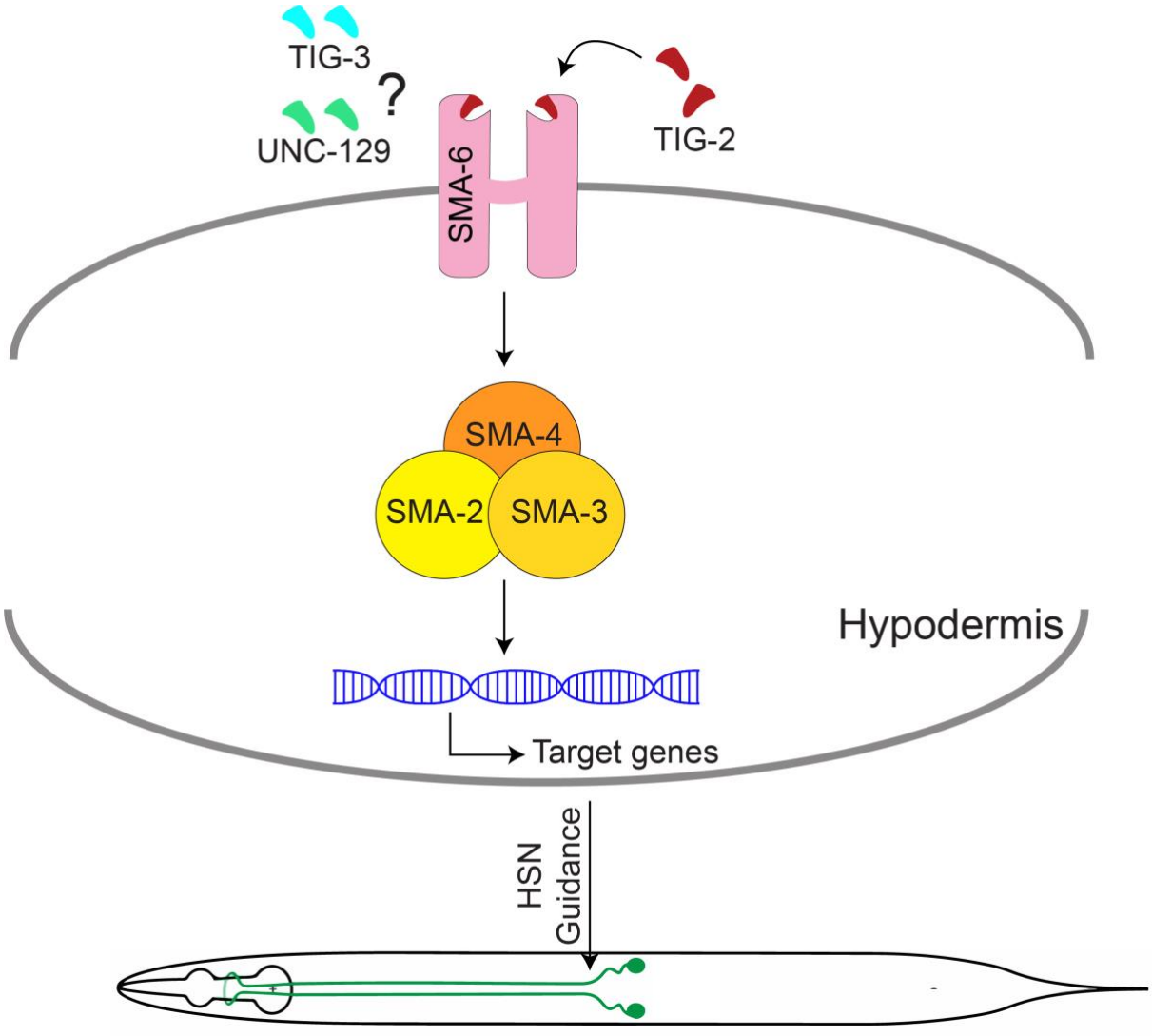

Fig. 4.10. Illustration of TGF-β ligand action in HSN development.

My model proposes that multiple ligands act with a single TGF-β type I receptor in the same pathway to regulate HSN development.

5. Identification of TGF-β pathway target genes that control HSN development

5.1 Abstract

In the previous chapters, I identified a non-canonical TGF-β family signaling pathway required for the development of hermaphrodite specific motor neurons. This mechanism involves a TGF-β family receptor type I receptor, SMA-6, acting with multiple extracellular ligands independently of the type II receptor. I have also shown that specific intracellular SMADs that act as transcriptional regulators - SMA-2, SMA-3 and SMA-4 - are required for HSN development. However, the targets of these molecules in the regulation of HSN development are unclear. In order to identify these downstream targets, I conducted RNA sequencing from synchronized *sma-3* mutants and wild-type worms to compare their transcriptomes. After analyzing the RNA sequencing data, I selected twelve differentially expressed candidate genes and performed an RNAi screen to uncover the potential role of these candidates in the context of HSN development. As a result, I found that the knockdown of *neurexin like receptor-1 (nlr-1)* partially suppresses the HSN defects of *sma-3* mutants, suggesting that transcriptional regulation of *nlr-1* by SMA-3 is important for HSN development. *nlr-1* is an ortholog of human *contactin associated protein like 2* (*CTNAP2*) gene which has been implicated in neurodevelopmental disease.

5.2 Introduction

Correct development of complex tissues relies on the capability of receiving, interpreting and responding to environmental cues at a cellular level. The production and action of these environmental cues is strictly controlled by a cascade of interactions between an extracellular effector molecule and its target cell which leads to initiation of intracellular signaling mechanisms. Collectively, these processes are known as signaling pathways. Dysregulation of these pathways can result with catastrophic effects for the organism such as cancer, diabetes and skeletal malformation [139].

As mentioned in the previous chapters, the Sma/Mab pathway, a sub-category of TGF-β family signaling in *C. elegans*, regulates many biological processes such as body size regulation. As such, loss-of-function mutations in any of the components of this pathway can cause altered body size [96]. In this thesis, I identified a non-canonical mechanism where TGF-β signaling controls the development of HSN neurons. In this complex mechanism, a TGF-β family type I receptor, SMA-6, acts independently of the type II receptor, DAF-4 (Fig. 3.2, Fig. 3.7). Furthermore, multiple BMP- and TGF-β-like extracellular ligands; TIG-2, TIG-3 and UNC-129, are required (Fig. 4.1). In addition, specific intracellular signaling SMAD molecules; SMA-2, -3 and -4, which are known to function as transcriptional regulators, act to control HSN development (Fig. 3.6). However, the downstream targets of these SMADs and, therefore the entire signaling pathway in relation to HSN development, remain unknown. RNA sequencing is an important tool to study transcriptional regulation and can help us identify the transcriptional changes in different conditions by comparing the transcriptome of a wild-type organism with an organism that carries a mutation in a specific gene.

In this chapter, I aimed to identify the downstream target(s) of the TGF-β pathway in the context of HSN development. For this purpose, I performed RNA sequencing on *sma-3* mutant worms as well as wild-type (N2) worms and conducted an RNAi screen on the dysregulated genes to examine their role in HSN development. The outcome of this chapter will provide insights on the function downstream targets of signaling pathways in neuronal development.

5.3 Methods

5.3.1 RNA sequencing

Worm synchronization

All strains were grown at 20°C. Worms were synchronized to be at L2 stage for RNA extraction. Briefly, L4 stage worms were picked onto OP50-seeded NGM plates. One-day adults of the F1 generation were bleached and the obtained eggs were plated. After the worms reached adulthood and laid eggs, they were washed away from the plates and the remaining eggs were placed onto fresh plates. When these worms reached to L2 stage, they were collected with M9 solution and frozen in Trizol (Invitrogen) solution at -80°C.

RNA extraction

Worms were cracked with freeze/thaw cycles using liquid nitrogen. RNA was extracted using RNeasy® Mini Kit (Qiagen) according to the manufacturer's instructions. Five replicates of RNA extraction per strain were performed.

RNA sequencing analysis

RNA sequencing and raw data analysis were carried out by Micromon Sequencing Facility (Melbourne, Australia). The sequencing data was analyzed using edgeR quasi-likelihood method comparing *sma-3(wk30)* and wild-type data. Differentially expressed genes that have a false discovery rate (FDR) lower than 0.05 were described as statistically significant.

5.3.2 RNA interference (RNAi)

RNAi knockdown was performed via feeding method [138]. Briefly, L4 stage wild-type (*HSN::GFP*) or *sma-3(wk30); HSN::GFP* mutant animals were picked onto empty NGM plates to prevent the carriage of OP50 bacteria to the RNAi plates. After five minutes, these worms were placed onto the RNAi plates seeded with HT115 bacteria that carry the specific RNAi clone for gene of interest. Worms were grown in RNAi plates for two

generations at 20°C and one-day adults of F1 and F2 generations were scored. For detailed information, please refer to Chapter 2.

5.3.3 Molecular Cloning

RJP430 L4440 *mboa-6* RNAi

The sequence between 4130th and 4636th positions in *mboa-6* coding sequence were amplified from N2 genomic DNA by PCR with Phusion DNA polymerase using OFB150 and OFB151 primers. Amplified product was cloned into L4440 plasmid that was digested with HindIII enzyme.

RJP428 L4440 *mec-1* RNAi

The region between 1163rd and 2488th position in the *mec-1* coding sequence were amplified from N2 genomic DNA by PCR with Phusion DNA polymerase using OFB152 and OFB153 primers. Amplified product was cloned into L4440 plasmid that was digested with NheI enzyme.

For more details, please refer to Chapter 2.

5.4 Results

In the previous chapters, I identified a non-canonical mechanism that involves a TGF-β family type I receptor acting independently of the type II receptor, multiple extracellular ligands and intracellular signaling molecules. However, the downstream targets of the identified non-canonical pathway required for HSN development remain unclear. To identify these target genes, I conducted RNA sequencing analysis using wild-type worms and *sma-3(wk30)* mutants. Worms were synchronized at the L2 stage as explained in the methods section. The sequencing data was analyzed using edgeR quasi-likelihood method comparing *sma-3(wk30)* data with wild-type data. Genes were filtered using a cut-off of false discovery rate (FDR) < 0.05 and the resulting genes were listed as differentially expressed genes (DEG). I then tested a dozen candidate target genes and validated *nlr-1* as a target gene that plays a role in HSN development.

5.4.1 Analysis of RNA sequencing data

For both wild-type (N2) animals and *sma-3* mutants, I used five independent biological replicates. In order to observe the similarity of these independent replicates, I conducted a Principal Component Analysis (PCA) which can reduce a multidimensional data such as RNA sequencing data from multiple samples, into a low dimensional graph to extract the relevant information. The PCA analysis demonstrated that the RNA samples obtained from *sma-3* mutants and wild-type worms were distributed separately (Fig. 5.1). Furthermore, each biological replicate within the same strain [*sma-3(wk30)* or wild-type] were able to be grouped together. This indicates that *sma-3* and wild-type samples displayed differential gene expression patterns.

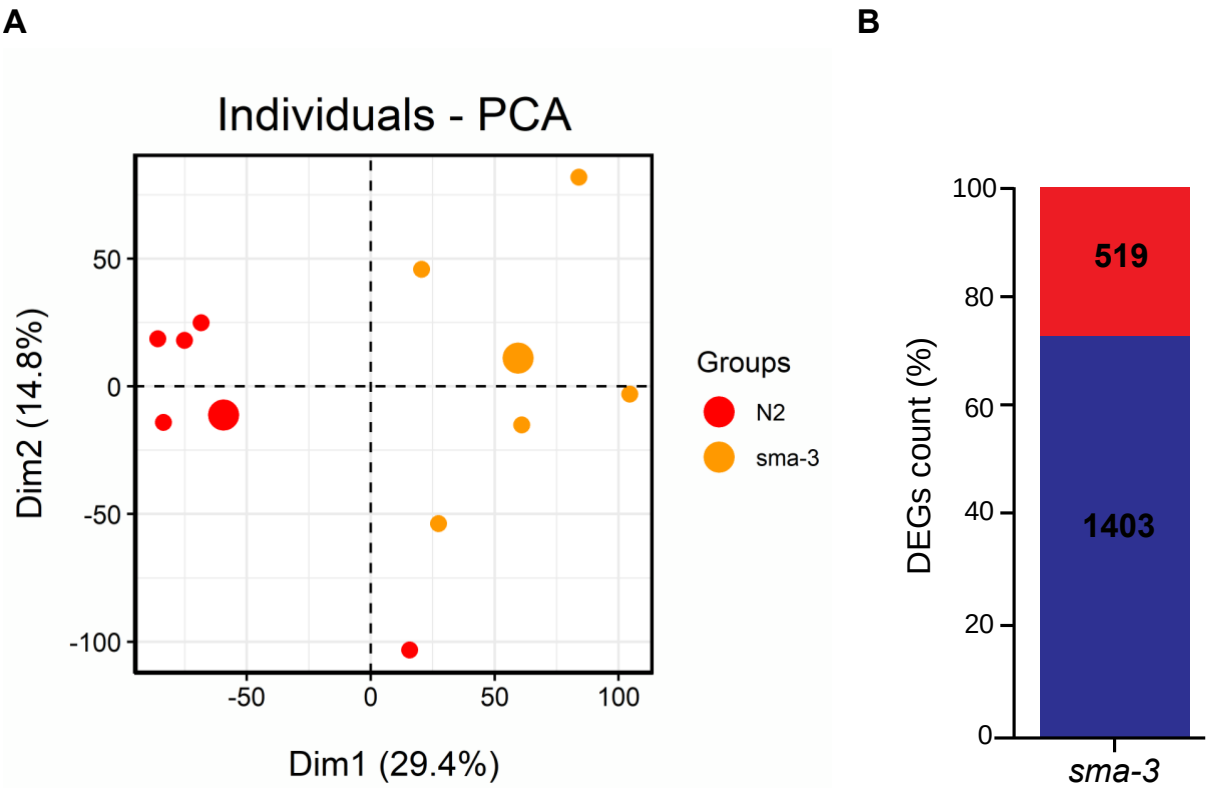

Fig. 5.1. Transcriptome analysis of *sma-3* mutants and wild-type animals.
(A) PCA analysis of *sma-3* mutants and wild-type animals. Red circles represent N2 replicates, while orange circles represent *sma-3* replicates. Five small circles represent each replicate and the large circles represent the mean of replicates. Dim1 and Dim2 represent the Dimension 1 and 2. The percentages in brackets represent the percentages of the variables that could cloud the total variability. (B) A bar graph of the number of DEGs in *sma-3* mutant animals relative to N2. Red bar represents the percentage of upregulated genes, whereas blue bar represents the percentage of downregulated genes. The numbers in the red and blue boxes show the number of upregulated and downregulated genes, respectively.

As expected, I obtained a large number of DEGs due to the importance of TGF-β pathway in a wide range of biological functions. Specifically, *sma-3* mutants possessed 1,922 differentially expressed genes (DEG) compared to wild-type animals. Due to the large number of DEGs, I selected a group of twelve genes (Table 5.1) according to their putative biological relevance in neuronal development and analyzed their role in TGF-β-mediated HSN development.

Table 5.1 Candidate dysregulated genes in *sma-3* mutants.

Gene	Product	Log_2Fold Change (relative to wild-type)	False Discovery Rate	*P* value
sgk-1	Kinase	-0.36	$2.24e^{-3}$	$2.43e^{-5}$
kpc-1	Proprotein convertase	-0.25	0.05	$6.70e^{-3}$
mboa-6	Acyl transferase	-0.28	$5.00e^{-3}$	$9.99e^{-5}$
vab-8	Kinesin-like	0.22	0.02	$1.11e^{-3}$
slt-1	Ligand	0.27	0.02	$1.32e^{-3}$
smp-1	Semaphorin	0.21	0.02	$8.96e^{-4}$
max-1	Pleckstrin homology domain-containing	0.28	0.01	4.14_{e-4}
lad-2	Adhesion molecule	0.32	0.02	1.07_{e-3}
vab-19	KN motif and ankyrin repeat domain-containing	0.28	0.01	4.67_{e-4}
mec-1	Extracellular matrix protein	0.32	0.01	3.82_{e-4}
sdn-1	Proteoglycan	0.26	0.01	5.40_{e-4}
nlr-1	Neurexin-like	0.27	7.06_{e-3}	2.04_{e-4}

In order to investigate the role of these genes in HSN development, RNAi knockdown experiments were performed by feeding worms with bacteria that produce double-stranded RNA which are specific to the corresponding mRNAs of the target genes. I hypothesized that if the HSN development defects in *sma-3* mutants were attributable to upregulation of downstream molecules, knockdown of these molecules could suppress the HSN defects of *sma-3* mutant animals. Similarly, if these defects were attributable to the downregulated target molecules of SMA-3, I hypothesized that knockdown of these molecules in the wild-type worms could phenocopy the HSN defects of *sma-3* mutants. Therefore, knockdown of upregulated downstream targets was conducted in *sma-3* mutants, whereas knockdown of downregulated downstream targets was conducted in wild-type (*HSN::GFP*) worms. Worms were picked onto the RNAi plates at L4 stage and resulting F1 and F2 generations were examined for their HSN profiles (Fig. 5.2).

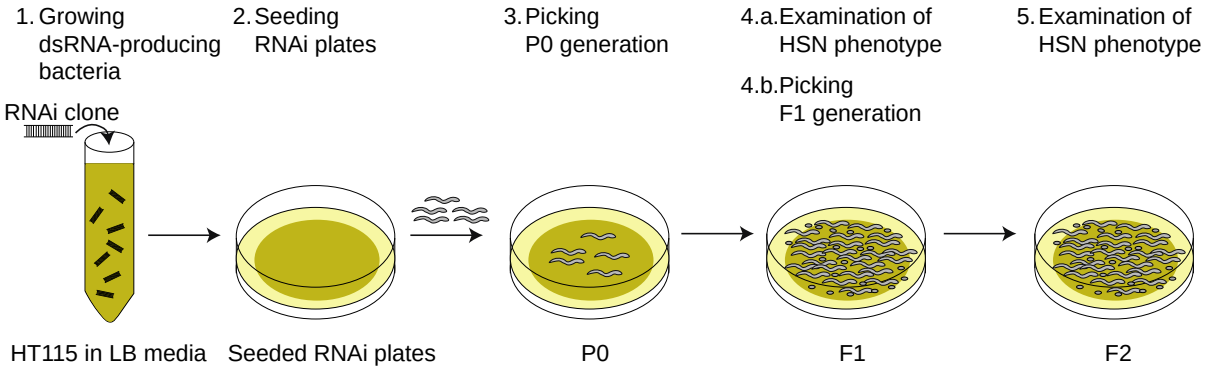

Fig. 5.2. RNAi by feeding.

5.4.2 Examination of downregulated candidate genes in HSN development

sgk-1

Serum- and Glucocorticoid-inducible Kinase-1 (SGK-1) is a kinase that is primarily expressed in intestine and nervous system. SGK-1 is implicated in a wide-range of biological processes in *C. elegans* such as development, metabolism, lifespan, endoplasmic reticulum (ER) stress, protein trafficking and egg laying [154, 155]. Furthermore, it mediates *Rictor*/TORC2 kinase in body size regulation [156]. To date,

no data have been published with regards to the role of SGK-1 in neuronal development in *C. elegans*. My RNA sequencing shows that *sgk-1* expression is significantly downregulated in *sma-3* mutants compared to the wild-type (Log_2Fold change: -0.37). Considering the role of SMA-3 in HSN development, I asked whether the HSN defects detected in *sma-3* mutants arise due to the downregulation of *sgk-1*. In order to investigate this hypothesis, I performed an *sgk-1*-specific RNAi knockdown experiment in *wild-type* (*HSN::GFP*) worms and examined the HSN neurons. The *sgk-1*-specific RNAi clone targets the last two exons of *sgk-1* which encodes for two isoforms (Fig. 5.3A). Scoring results revealed that knockdown of *sgk-1* did not have a detrimental effect on HSNs (Fig. 5.3B), which suggests that SGK-1 is not involved in the regulation of HSN development. However, further analysis such as examining the null mutants of *sgk-1* is needed confirm this finding.

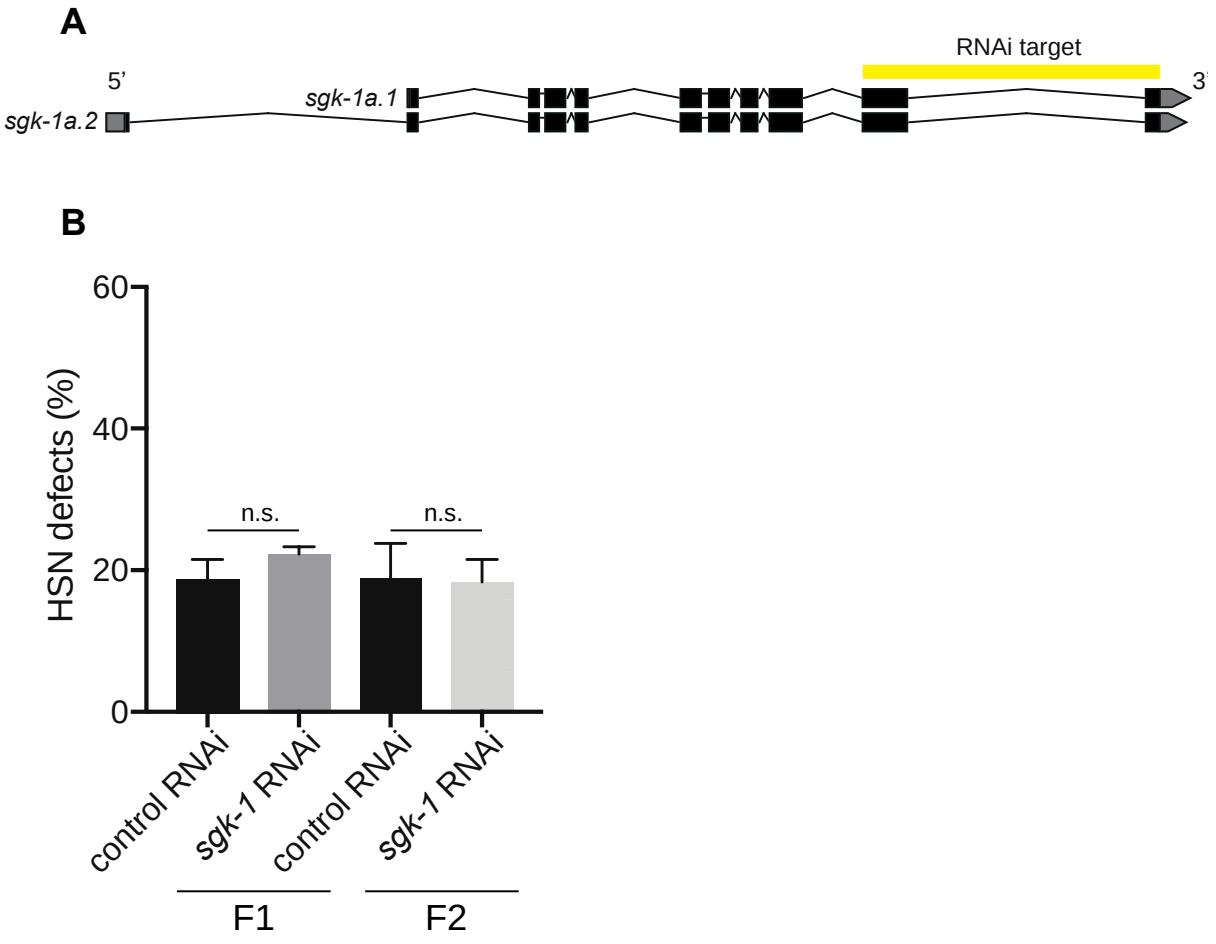

Fig. 5.3. Knockdown of *sgk-1* does not cause HSN defects.

(A) Gene structure of *sgk-1* (adapted from WormBase). The RNAi target (yellow box) targets a common sequence between the two *sgk-1* transcripts. Black boxes represent exons, black lines represent introns

and grey boxes represent UTRs. (B) Quantification of HSN defects in wild-type worms fed with *sgk-1*-specific or control vector RNAi. Statistical analysis of F1 and F2 scoring was performed separately using an unpaired *t*-test. At least one hundred animals were scored per condition. n.s., not significant. Error bars represent mean ± SEM of three biological replicates.

kpc-1

The Kex-2 Proprotein Convertase family (*kpc-1*) gene encodes an ortholog of human furin protein which is an enzyme that cleaves the precursor form of proteins for their activation. *kpc-1* is primarily expressed in the nervous system and associated with neurogenesis, dauer formation and protein maturation [157, 158]. It has been shown that KPC-1 regulates the level of DMA-1 receptor which is critical for dendritic branching [157]. The mutation in *kpc-1* mutants causes upregulation of DMA-1 receptor which leads to trapped dendrites in the sensory PVD neurons [157]. Furthermore, KPC-1 plays a role in *C. elegans* brain assembly by acting in guidance-cue trafficking in glia [158]. Therefore, it is clear that KPC-1 is an important player in the development of the *C elegans* nervous system. My RNA sequencing data indicates that the level of *kpc-1* is reduced in *sma-3* mutants (Log_2Fold Change: -0.25). Thus, I hypothesized that this reduction could be critical for HSN development. To investigate this hypothesis, I conducted *kpc-1*-specific RNAi knockdown in wild-type (*HSN::GFP*) worms and examined the HSN phenotype. The *kpc-1*-specific RNAi clone targets the last four exons of *kpc-1* which encodes for two isoforms (Fig. 5.4A). Scoring results showed that knockdown of *kpc-1* did not cause a significant HSN defects (Fig. 5.4B), which suggests that KPC-1 is not involved in the regulation of HSN development. *kpc-1* null mutant needs to be tested to validate this finding.

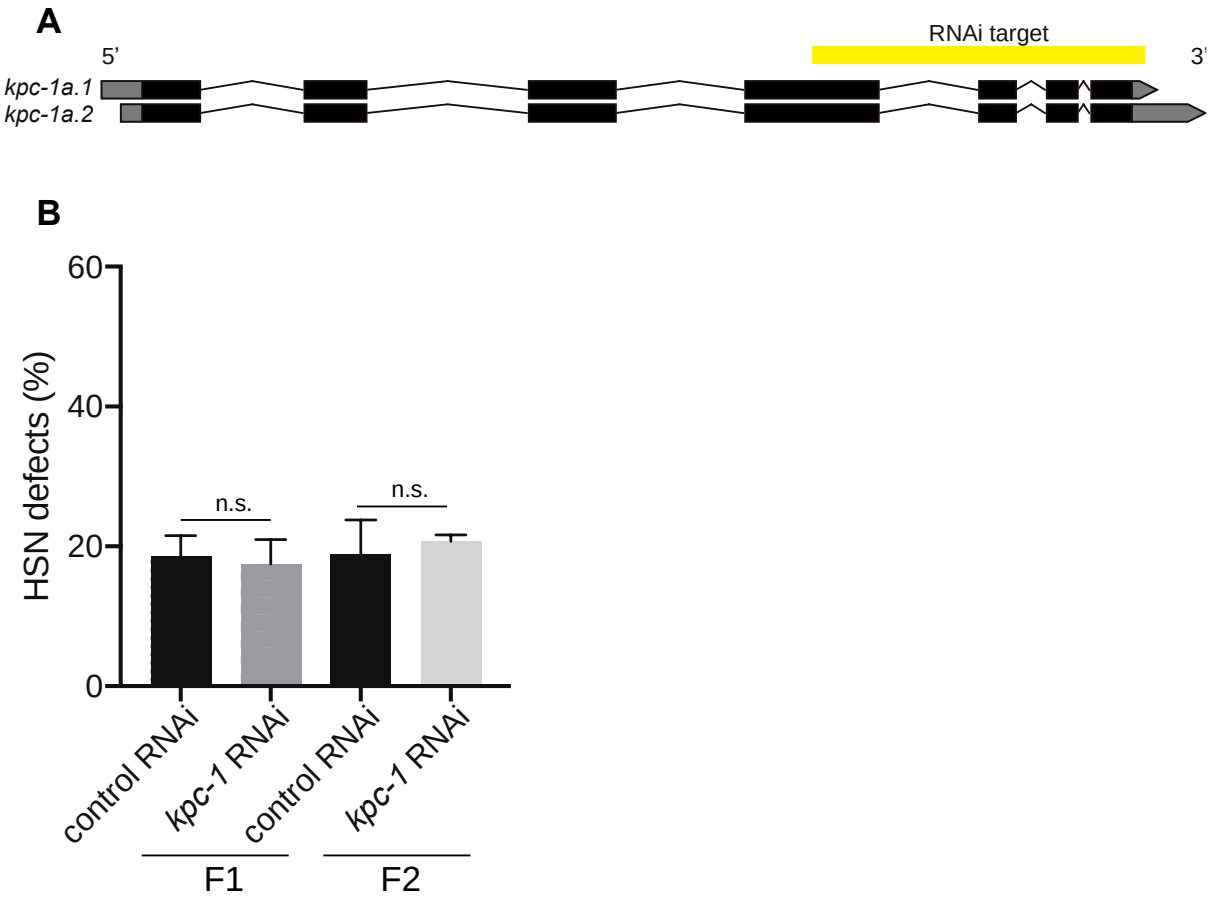

Fig. 5.4. Knockdown of *kpc-1* does not cause HSN defects.

(A) Gene structure of *kpc-1* (adapted from WormBase). The RNAi target (yellow box) targets a common sequence between the two *kpc-1* transcripts. Black boxes represent exons, black lines represent introns and grey boxes represent UTRs. (B) Quantification of HSN defects in wild-type worms fed with *kpc-1*-specific or control vector RNAi. Statistical analysis of F1 and F2 scoring was performed separately using an unpaired *t*-test. At least one hundred animals were scored per condition. n.s., not significant. Error bars represent mean ± SEM of three biological replicates.

mboa-6

MBOA-6 is a member of the conserved MBOAT (Membrane Bound O-Acyl Transferase) family which is associated with glycerophospholipid production. *mboa-6* is expressed in pharynx and tail. It has been shown that reduced level of *mboa-6* leads to slow growth, early larval arrest and dumpiness [159]. According to my RNA sequencing data, *mboa-6* expression is significantly downregulated in *sma-3* (Log_2Fold change: -0.28). To investigate whether this reduction in *mboa-6* expression interferes with the HSN development, I performed *mboa-6*-specific RNAi knockdown experiment in *HSN::GFP* worms and examined the HSN phenotype of these worms. Due to the

unavailability of *mboa-6*-specific RNAi clone, I performed a cloning experiment for generation of an RNAi clone that targets all ten isoforms encoded by *mboa-6* (Fig. 5.5A). The growth of worms upon being fed with *mboa-6*-specific RNAi bacteria was delayed which is in concurrent with previous studies and thus indicates that RNAi knockdown worked. However, examination of HSN neurons revealed inconsistency between the biological replicates ranging from 20% to 32% (Fig. 5.5B) and as a result, the phenotype of these worms was not significantly different than the wild-type worms. This suggest that *mboa-6* is not involved in the regulation of HSN development. To further confirm this finding and to avoid inconsistency in the scoring data, the null mutant of *mboa-6* can be examined in the future studies.

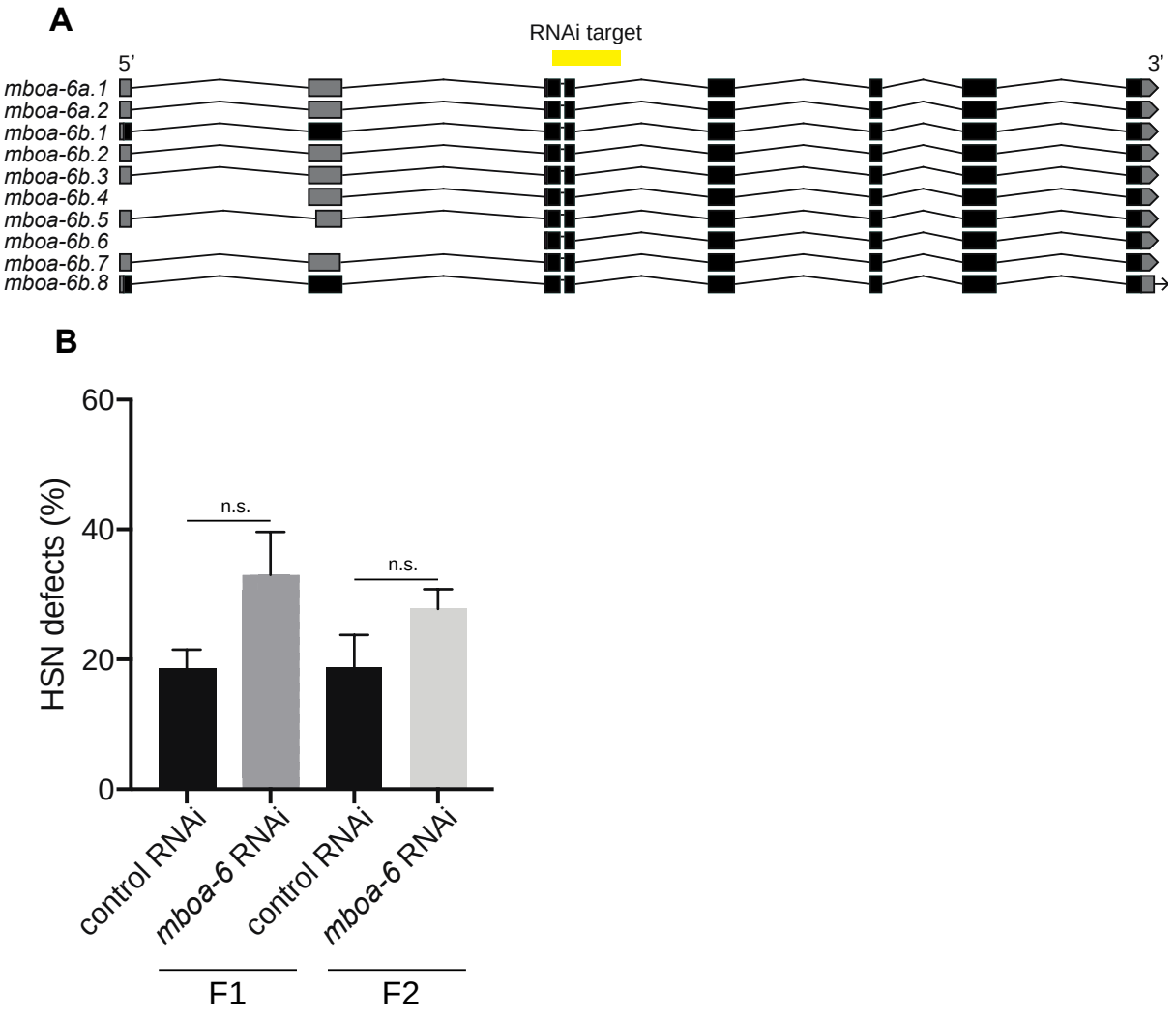

Fig. 5.5. Knockdown of *mboa-6* does not interfere with HSN development.
(A) Gene structure of *mboa-6* (adapted from WormBase). The RNAi target (yellow box) targets a common sequence among the ten *mboa-6* transcripts. Black boxes represent exons, black lines represent introns and grey boxes represent UTRs. (B) Quantification of HSN defects in wild-type worms fed with *mboa-6*-specific or control vector RNAi. Statistical analysis of F1 and F2 scoring was performed separately using an unpaired *t*-test. At least one hundred animals were scored per condition. n.s., not significant. Error bars represent mean ± SEM of three biological replicates.

5.4.3 Examination of upregulated candidate genes in HSN development

vab-8

VAB-8 is predicted to be a member of the kinesin family which directs cell migration and growth cone protrusion [88, 89, 95]. *vab-8* encodes one long isoform, VAB-8L, and two short isoforms, collectively called VAB-8S. VAB-8L contains a kinesin-like domain and functions in directing growth cones. VAB-8S does not include the kinesin-like domain and functions in cell migration [95]. *vab-8* is primarily expressed in musculature and nervous system [95]. It has been shown that mutations in *vab-8* lead to cell migration and axon guidance defects in many neurons including HSNs [88, 95] which is associated with the increased activity of EGL-20/Wnt signaling. Intriguingly, *vab-8* is upregulated (Log_2Fold change: 0.22) in *sma-3* mutant animals. Considering that the HSN migration defects of *sma-3* mutants are mostly undermigration defects (Fig. 5.7C), I hypothesized that this could be due to increased activity of VAB-8 in *sma-3* mutant animals. To investigate whether these phenotypes are correlated, I performed an RNAi knockdown of *vab-8* in *sma-3* mutants and examined the HSN phenotype. The *vab-8*-specific RNAi clone targets the last three exons of *vab-8* which would potentially affect all the isoforms (Fig. 5.6A). The scoring results showed that the knockdown of *vab-8* in sma-3 mutant animals did not cause a reduction in the percentage of worms that have defective HSNs (Fig. 5.6B).

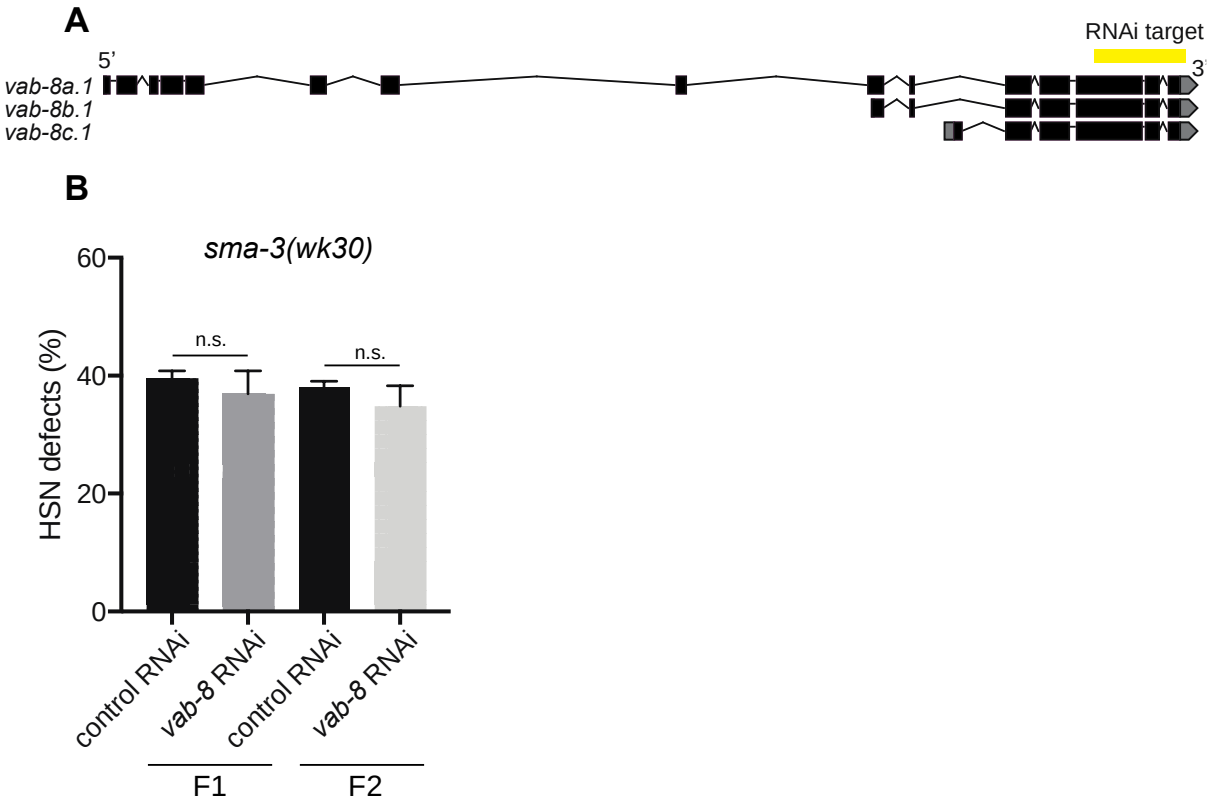

Fig. 5.6. Knockdown of *vab-8* does not change the HSN phenotype of *sma-3* mutants.
(A) Gene structure of *vab-8* (adapted from WormBase). The RNAi target (yellow box) targets a common sequence between the three *vab-8* transcripts. Black boxes represent exons, black lines represent introns and grey boxes represent UTRs. (B) Quantification of HSN defects in *sma-3(wk30)* mutants fed with *vab-8*-specific or control vector RNAi. Statistical analysis of F1 and F2 scoring was performed separately using an unpaired *t*-test. At least one hundred animals were scored per condition. n.s., not significant. Error bars represent mean ± SEM of three biological replicates.

To further substantiate this finding, I generated the compound *sma-3; vab-8* double mutant using the *wk30* allele of *sma-3* and *ev411* of *vab-8*. *ev411* is a substitution in the splicing site, which has been shown to cause uncoordinated behavior as well as overmigration and axon guidance defects in HSN neurons [95]. To validate these findings, I also scored the *vab-8(ev411)* single mutant animals (Fig. 5.7B). *vab-8* mutant animals exhibited significantly higher HSN defects compared to wild-type (*HSN::GFP*) worms which is in concurrence with previous studies. Furthermore, *sma-3; vab-8* double mutants displayed the same penetrance of HSN defects as *vab-8* mutants (Fig. 5.7B). Among these defects, I specifically analyzed the undermigration defects as the predominant type of defects detected in *sma-3* mutants. However, these results demonstrated that the *vab-8* mutation did not reduce the undermigration

defects of *sma-3* mutants (Fig. 5.7C) which indicates that upregulation of *vab-8* is not related to the HSN phenotype of *sma-3* mutants.

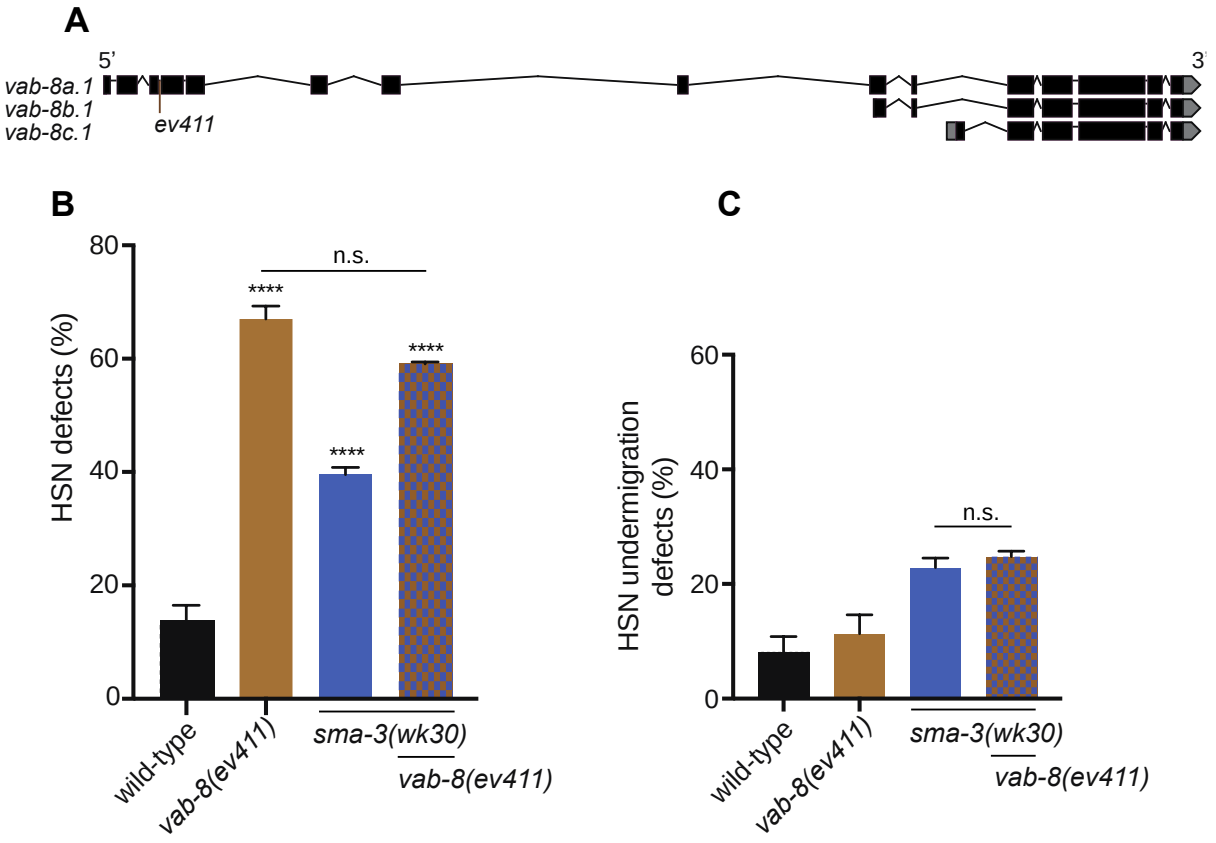

Fig. 5.7. VAB-8 is not involved in SMA-3-mediated HSN development.

(A) Gene structure of *vab-8* (adapted from WormBase). *ev411* (brown line) is a substitution in the splicing site (904th position in the coding transcript, G>A). (B) and (C) show the quantification of total and undermigration only HSN defects, respectively in *vab-8(ev411)* and *sma-3(wk30)* mutants as well as the *vab-8; sma-3* double mutant. Statistical analysis of (B) was performed using one-way ANOVA and Tukey's multiple comparison test, comparing the mean of all the columns with every other column. Statistical analysis of (C) was performed using one-way ANOVA and Dunnet's multiple comparison test, comparing the mean of *sma-3(wk30)* and of *sma-3; vab-8* double mutant. At least one hundred animals were scored per strain. ****p < 0.0001 (compared to wild-type); n.s., not significant. Error bars represent mean ± SEM of three biological replicates.

slt-1

SLT-1 is a ligand member of the conserved Slit/Robo signaling which acts as a guidance cue for axons [74]. SLT-1 acts as a ligand to activate the Robo receptor SAX-3. *slt-1* is primarily expressed in musculature, nervous system and hypodermis [77]. It

has been shown that the mutations in *slt-1* results with weak HSN migration defects and guidance defects in AVM neurons [160-162]. Considering its involvement in HSN development and upregulated expression (Log_2Fold change: 0.27) in *sma-3* mutants I interrogated the possible role of SLT-1 with SMA-3. The *slt-1*-specific RNAi clone targets the last exon of *slt-1* which encodes one isoform (Fig. 5.8A). Scoring results revealed that knockdown of *slt-1* in *sma-3* mutant worms did not cause a significant change in the HSN phenotype of *sma-3* mutants (Fig. 5.8B). This suggest that the upregulation of *slt-1* in *sma-3* mutants is not the direct cause of HSN defects displayed in *sma-3* mutants. To further investigate the potential relation between SMA-3 and SLT-1, I generated a compound *sma-3(wk30); slt-1(eh15)* mutant and examined the HSN profile of these animals. *eh15* is a 1945-bp deletion which causes a frameshift in the transcript leading to a premature stop codon and has been shown to cause HSN migration defects [163]. Examination of the *sma-3(wk30); slt-1(eh15)* double mutant revealed that these animals did not display a reduced penetrance of HSN defects compared to the *sma-3* single mutant (Fig. 5.8C). Taken together, these data show that the HSN phenotype of *sma-3* mutants is not attributable to the upregulation of *slt-1* in these animals.

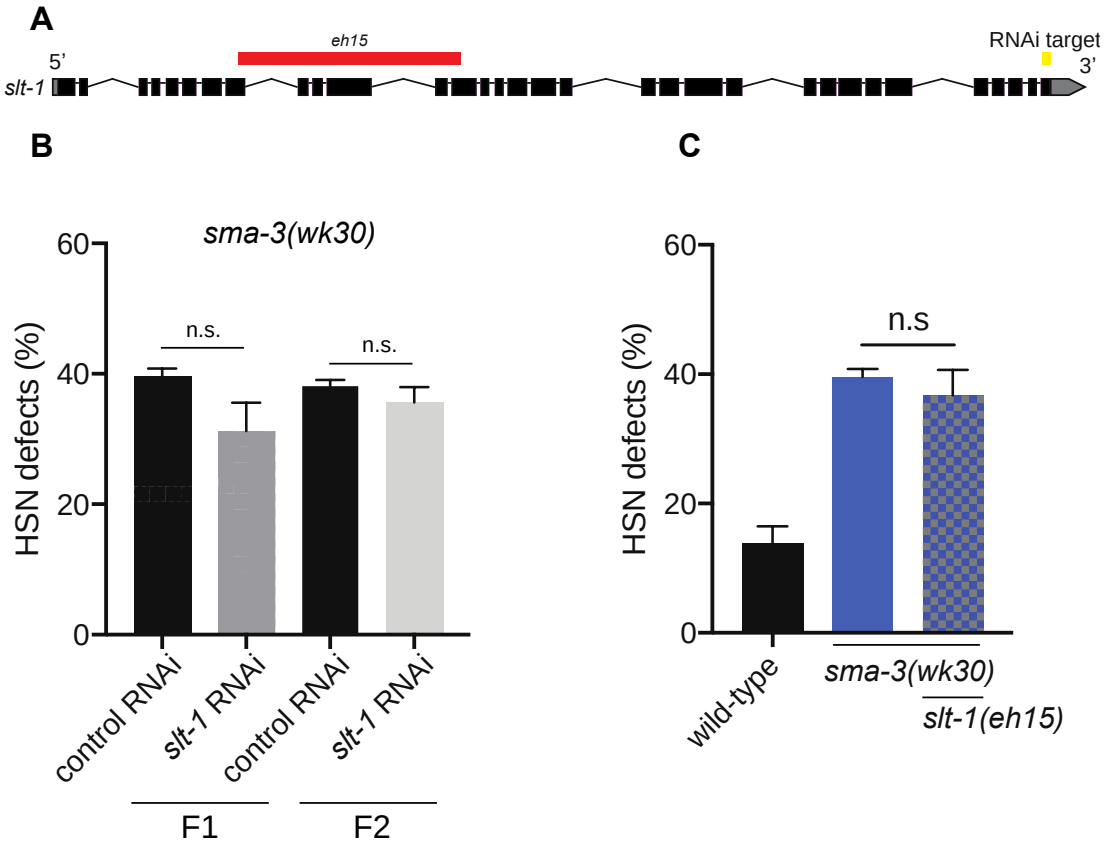

Fig. 5.8. SLT-1 is not involved in SMA-3-mediated HSN development.

(A) Gene structure of *slt-1* (adapted from WormBase). The RNAi target (yellow box) targets the exon of the *slt-1* transcript. Black boxes represent exons, black lines represent introns and grey boxes represent UTRs. *eh15* (red box) is a 1945-bp deletion which causes a frameshift in the transcript leading to a premature stop codon. (B) Quantification of HSN defects in wild-type worms fed with *slt-1*-specific or control vector RNAi. Statistical analysis of F1 and F2 scoring was performed separately using an unpaired *t*-test. (C) Quantification of HSN defects in *slt-1; sma-3* double mutant. Statistical analysis was performed using an unpaired *t*-test comparing *sma-3(wk30)* and *sma-3(wk30); slt-1(eh15)* double mutants. At least one hundred animals were scored per condition. n.s., not significant. Error bars represent mean ± SEM of three biological replicates.

smp-1

SMP-1 is a member of transmembrane semaphorins, which have been shown to play roles in synapse formation, axonal outgrowth, vulva and male tail development [164-166]. *smp-1* is primarily expressed in nervous system, musculature and hypodermis [166]. *smp-1* expression was significantly upregulated (Log_2Fold change: 0.21) in *sma-3* mutants. To investigate whether this upregulation is correlated with HSN defects of *sma-3* mutants, I performed an *smp-1*-specific RNAi experiment in *sma-3* using an

RNAi clone that targets all five isoforms encoded by *smp-1* (Fig. 5.9A). The examination of the HSN phenotype of *sma-3* mutants upon *smp-1* knockdown revealed no difference compared to the *sma-3* mutants that were fed with control RNAi bacteria (Fig. 5.9B). This suggests that SMP-1 is not involved in SMA-3-mediated HSN development. However, further studies such as *smp-1* null mutant and *smp-1; sma-3* double mutant analysis are required to have a better understanding on whether SMP-1 plays a role in HSN development.

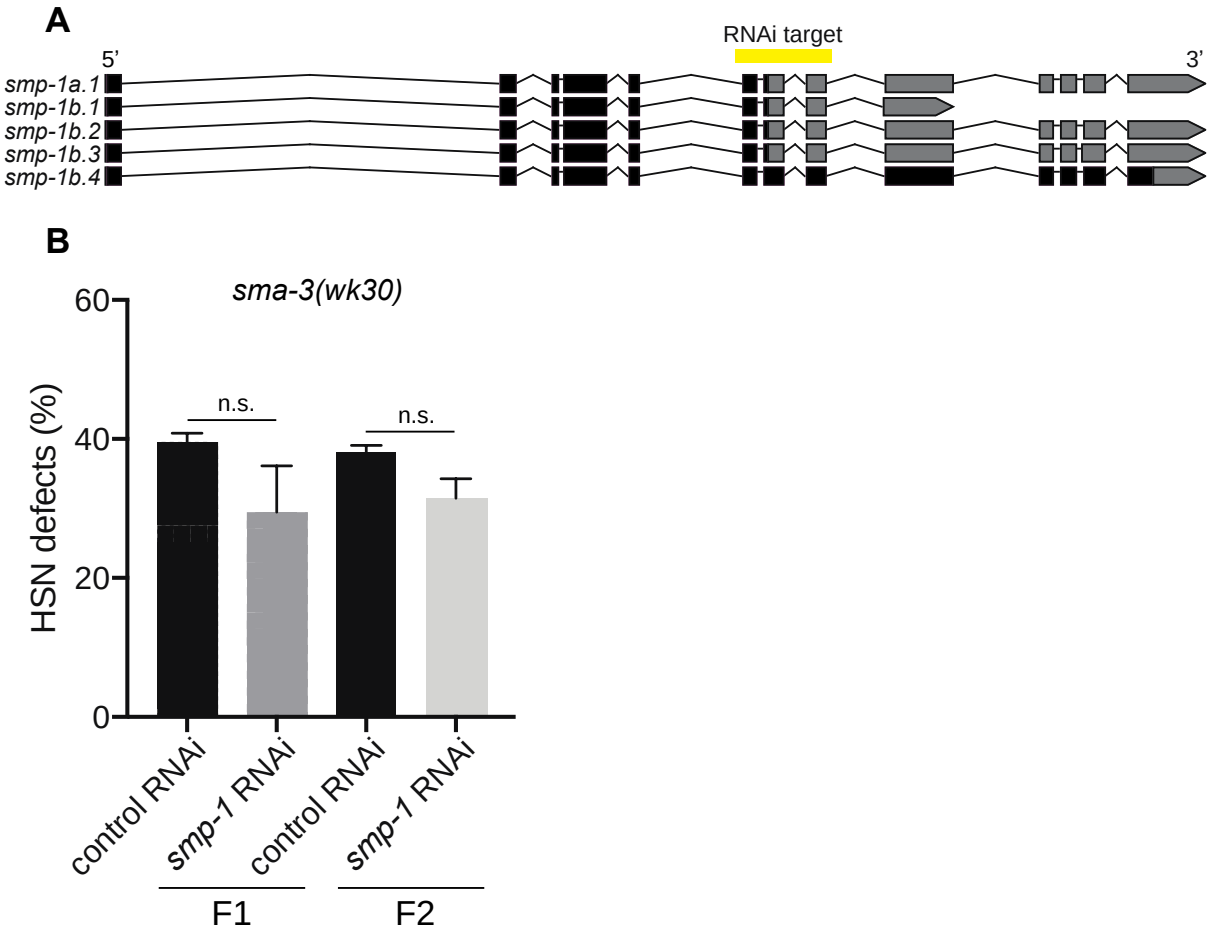

Fig. 5.9. Knockdown of *smp-1* does not change the HSN phenotype of *sma-3* mutants.
(A) Gene structure of *smp-1* (adapted from WormBase). The RNAi target (yellow box) targets a common sequence between the five *smp-1* transcripts. Black boxes represent exons, black lines represent introns and grey boxes represent UTRs. (B) Quantification of HSN defects in *sma-3(wk30)* mutants fed with *smp-1*-specific or control vector RNAi. Statistical analysis of F1 and F2 scoring was performed separately using an unpaired *t*-test. At least one hundred animals were scored per condition. n.s., not significant. Error bars represent mean ± SEM of three biological replicates.

max-1

max-1 encodes a modulator protein of the netrin pathway that is involved in motor axon guidance [167]. It is primarily expressed in the nervous system and the null mutations in *max-1* results with variable axon guidance defects, specifically in the type D motor neurons [167]. My RNA sequencing showed that *max-1* expression was significantly upregulated (Log_2Fold change: 0.28) in *sma-3* mutants. To investigate whether *max-1* plays a role in SMA-3-mediated HSN development, *max-1* expression was knocked down by RNAi in *sma-3* mutants using a *max-1*-specific RNAi clone that targets both two isoforms encoded by *max-1* (Fig. 5.10A). However, *max-1* knockdown did not cause a significant change in the HSN phenotype of *sma-3* mutants (Fig. 5.10B), which suggests that MAX-1 does not act with SMA-3 in the regulation of HSN development. However, further experiments are needed to draw a final conclusion considering the role of MAX-1 on neuronal development.

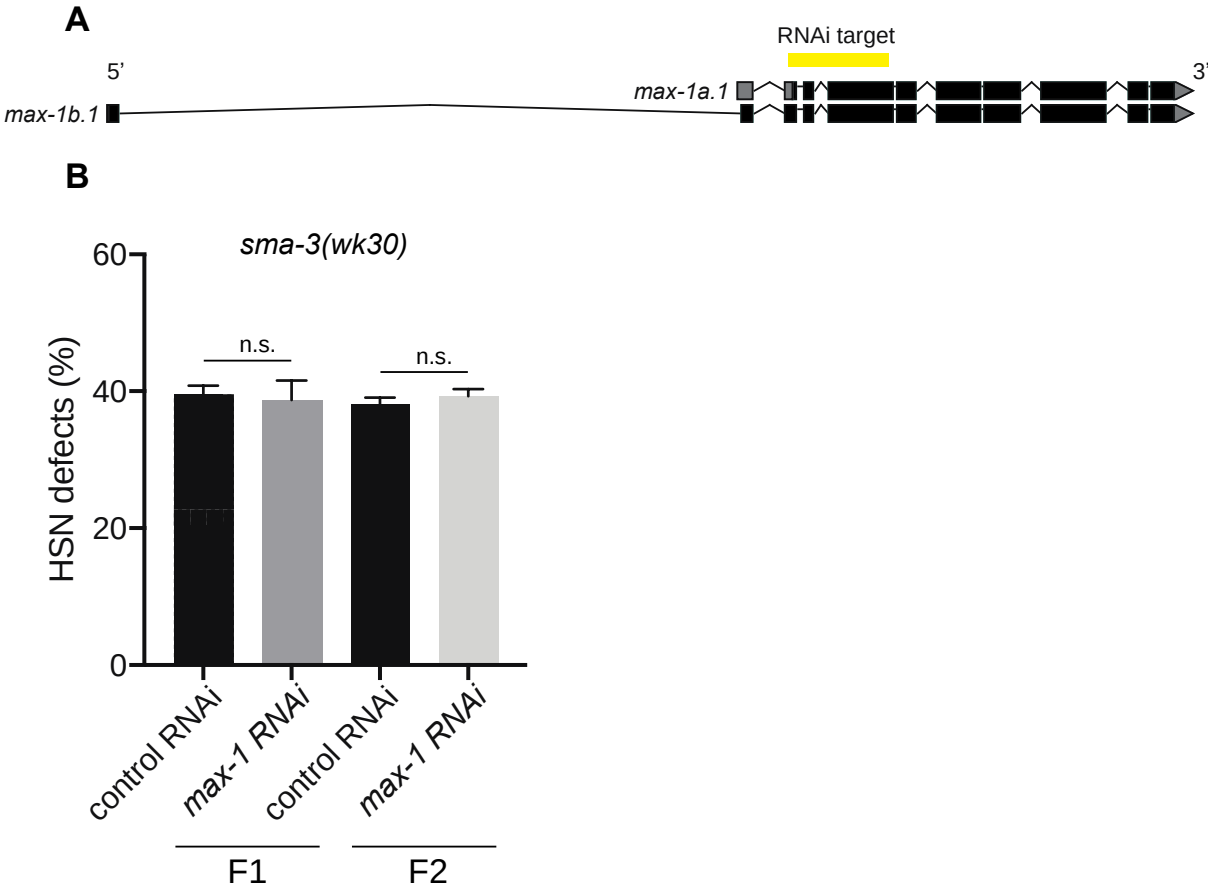

Fig. 5.10. Knockdown of *max-1* does not change the HSN phenotype of *sma-3* mutants.
(A) Gene structure of *max-1* (adapted from WormBase). The RNAi target (yellow box) targets a common sequence between the two *max-1* transcripts. Blue boxes represent exons, black lines represent introns and grey boxes represent UTRs. (B) Quantification of HSN defects in *sma-3(wk30)* mutants fed with *max-1*-specific or control vector RNAi. Statistical analysis of F1 and F2 scoring was performed separately using an unpaired *t*-test. At least one hundred animals were scored per condition. n.s., not significant. Error bars represent mean ± SEM of three biological replicates.

lad-2

L1-like adhesion gene 2 (lad-2) encodes an L1 cell adhesion molecule expressed in the nervous system. It acts in axon pathfinding of specific motor and sensory neurons by mediating semaphorin and ephrin signaling [168, 169]. These neurons include SMD, PLN and SDQ, however no study has been reported about the role of LAD-2 in HSN development. Interestingly, *lad-2* expression is upregulated (Log_2Fold change: 0.28) in *sma-3* mutants according to my RNA sequencing data (Table 5.1). Furthermore, LAD-2 acts as a non-canonical ephrin receptor that is required for proper HSN development. Taken together, I hypothesized that LAD-2 could play a role in HSN development via SMA-3-mediated pathway. To investigate this hypothesis, I conducted an RNAi knockdown experiment in *sma-3* mutant to ask if preventing the upregulation of *lad-2* can suppress the HSN defects of *sma-3* mutants. The *lad-2*-specific RNAi clone targets the last six exons of the long *lad-2* transcript which encodes for LAD-2L isoform, however the transcript of LAD-2S isoform is outside the RNAi clone target (Fig. 5.11A). Interestingly, the examination of HSN phenotypes of these animals revealed that HSN penetrance of *sma-3* mutants did not change which suggests that LAD-2L is not involved in the SMA-3-mediated pathway (Fig. 5.11B). To further investigate the role of LAD-2 in HSN development, I examined the HSN profile of the *lad-2(tm3056)* mutant. *tm3056* is a 1064-bp deletion which causes a frameshift that leads to a premature stop codon in the transcript. This mutation affects both LAD-2L and LAD-2S isoforms and has been shown to be a null mutation [168]. My scoring results revealed that *lad-2* mutants did not present significant HSN defects compared to wild-type animals (Fig. 5.11C). Taken together, these data suggest that LAD-2 is not involved in the regulation of HSN development.

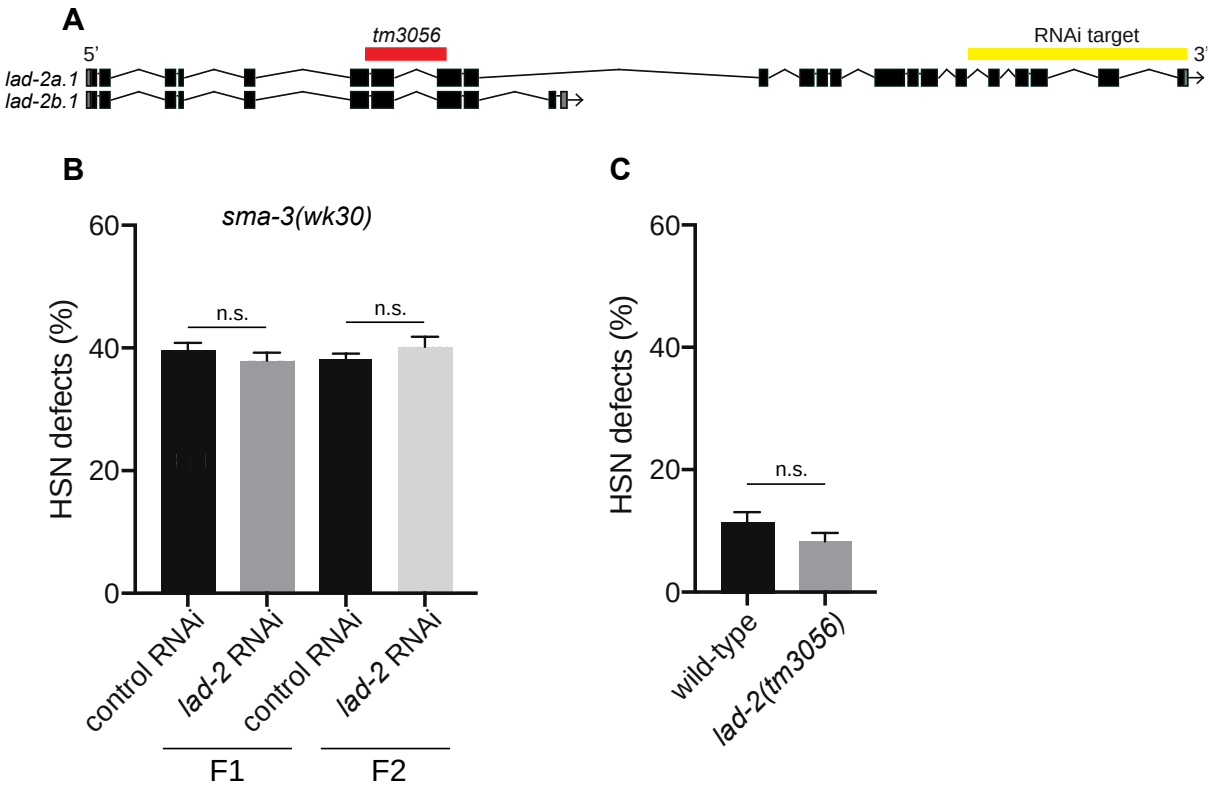

Fig. 5.11. LAD-2 is not involved in HSN development.

(A) Gene structure of *lad-2* (adapted from WormBase). The RNAi target (yellow box) targets the *lad-2a.1* transcript which encodes LAD-2L protein isoform. *tm3056* (red box) is a 1064-bp deletion which causes a frameshift that leads to a premature stop codon in both of the transcripts. Black boxes represent exons, black lines represent introns and grey boxes represent UTRs. (B) Quantification of HSN defects in *sma-3(wk30)* mutants fed with *lad-2*-specific or control vector RNAi. (C) Quantification of HSN defects in *lad-2(tm3056)* mutants. Statistical analysis of both (B) and (C) scorings were performed using an unpaired *t*-test. F1 and F2 scorings in (B) were analyzed independently of each other. At least one hundred animals were scored per condition. n.s., not significant. Error bars represent mean ± SEM of three biological replicates.

vab-19

vab-19 encodes an ankyrin-repeat containing protein which is the *C. elegans* ortholog of human Kank (KN motif and ankyrin domains) family. It is expressed in hypodermis, uterus, marginal cell and adult vulval toroid cell and is vital for the worm as the null mutants do not survive [170, 171]. However, *vab-19(e1036)* is a commonly used substitution allele and 90% of the worms survive at 20°C. This mutation in *vab-19* has been shown to cause defects in actin cytoskeleton organization and in the attachments between muscle and hypodermis [170, 171]. Furthermore, the localization of the netrin

receptor UNC-40 is altered which leads to axon outgrowth defects in the HSN neurons [172]. My RNA sequencing data shows that *vab-19* expression is upregulated in *sma-3* mutants (Log_2Fold change: 0.28). To investigate the role of VAB-19 in SMA-3-mediated HSN development, *vab-19* expression was knocked down by RNAi in *sma-3* mutants using a *vab-19*-specific RNAi clone that targets the 9th and 10th exon of *vab-19* (Fig. 5.12A). However, this knockdown did not cause a significant change in the HSN phenotype of *sma-3* mutants (Fig. 5.12B), which suggest that the upregulation of *vab-19* is not the major cause of HSN defects occurs in *sma-3* mutants. Considering that the loss of *vab-19* leads to HSN defects, future studies on the HSN profile of the compound *vab-19; sma-3* double mutant could be valuable to understand whether the HSN phenotypes of *vab-19* and *sma-3* mutants are correlated.

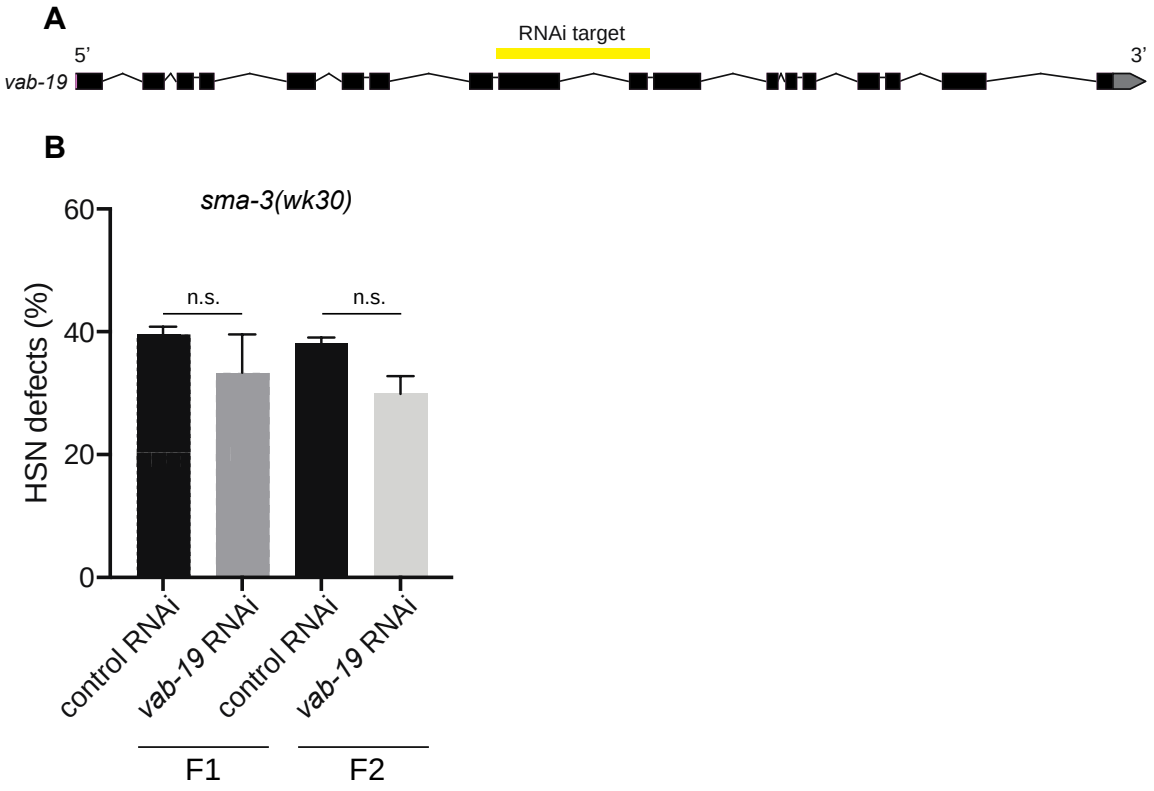

Fig. 5.12. Knockdown of *vab-19* does not change the HSN phenotype of *sma-3* mutants.
(A) Gene structure of *vab-19* (adapted from WormBase). The RNAi target (yellow box) targets the 9th and 10th exons in the *vab-19* transcript. Black boxes represent exons, black lines represent introns and grey boxes represent UTRs. (B) Quantification of HSN defects in *sma-3(wk30)* mutants fed with *vab-19*-specific or control vector RNAi. Statistical analysis of F1 and F2 scoring was performed separately using an unpaired *t*-test. At least one hundred animals were scored per condition. n.s., not significant. Error bars represent mean ± SEM of three biological replicates.

mec-1

mec-1 encodes an extracellular matrix protein that possess EGF and Kunitz domains which are required for protease inhibitory function [173]. It is primarily expressed in nervous system and muscle and is involved in locomotion, neuronal development and mechanosensation [173, 174]. It has been shown that NSM neurons of *mec-1* mutants have absent and/or short processes and displaced ALM cell bodies [175]. However, no study has been reported about the role of MEC-1 on HSN development. According to my RNA sequencing *mec-1* expression is upregulated in *sma-3* mutants (Log_2Fold change: 0.32). To examine a potential role of MEC-1 in SMA-3-mediated HSN development I performed RNAi knockdown of *mec-1* in *sma-3* mutants. I designed an RNAi clone targeting a specific region in the gene which would potentially reduce the production of all ten isoforms encoded by *mec-1* (Fig. 5.13A). Examination of HSNs showed that the knockdown of *mec-1* in *sma-3* mutants did not cause a significant change in the HSN phenotype of *sma-3* mutants (Fig. 5.13B). This suggests that the HSN defects of *sma-3* mutants are not attributable to *mec-1* upregulation. For validation of this finding, further experiments on *mec-1* such as examination of *sma-3; mec-1* double mutant are required.

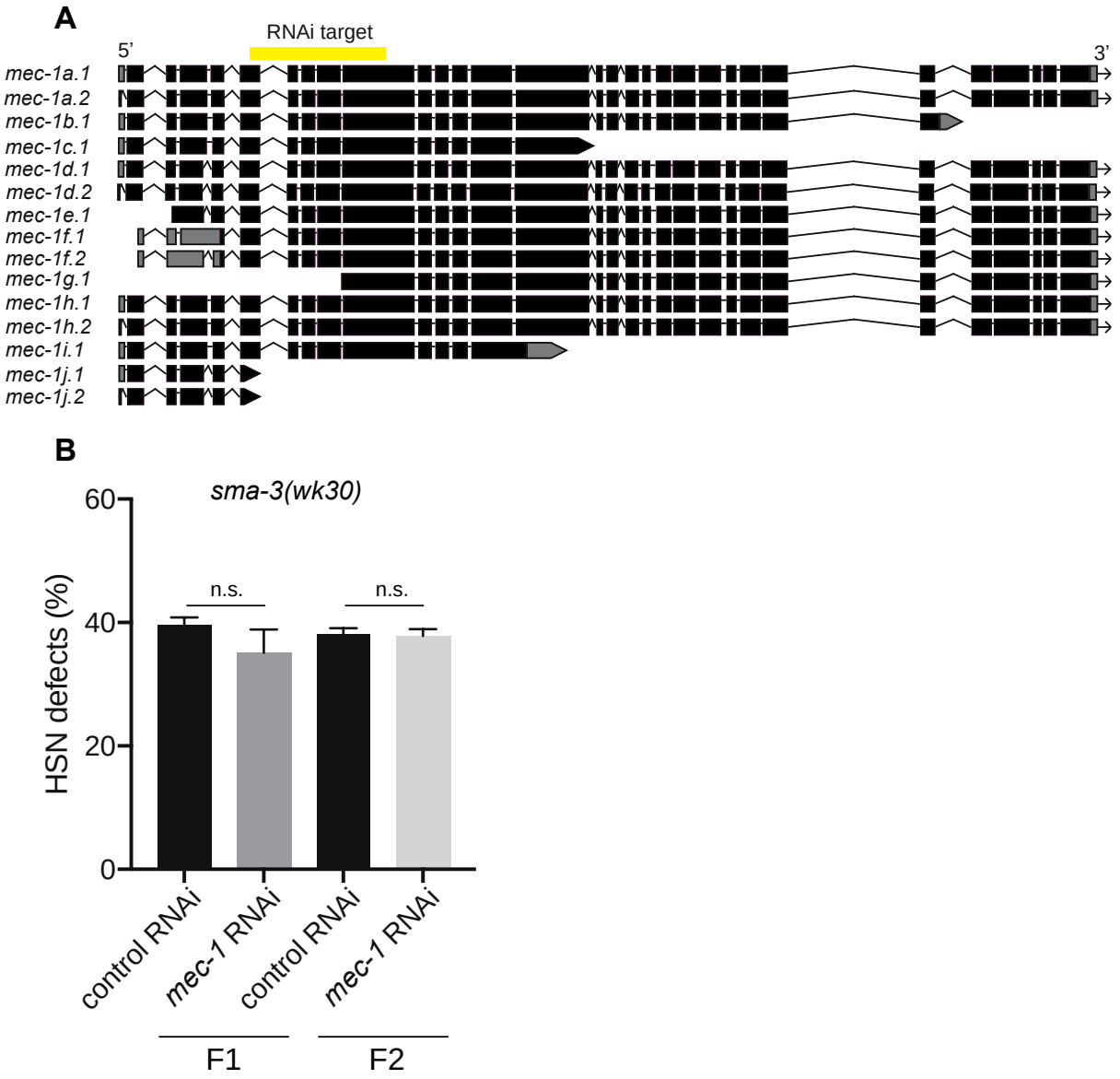

Fig. 5.13. Knockdown of *mec-1* does not change the HSN phenotype of *sma-3* mutants.
(A) Gene structure of *mec-1* (adapted from WormBase). The RNAi target (yellow box) targets a common sequence among the fifteen *mec-1* transcripts. Black boxes represent exons, black lines represent introns and grey boxes represent UTRs. (B) Quantification of HSN defects in *sma-3(wk30)* mutants fed with *mec-1*-specific or control vector RNAi. Statistical analysis of F1 and F2 scoring was performed separately using an unpaired *t*-test. At least one hundred animals were scored per condition. n.s., not significant. Error bars represent mean ± SEM of three biological replicates.

sdn-1

sdn-1 encodes the sole *C. elegans* ortholog of human syndecans which are transmembrane proteoglycans required for activation of signaling pathways via interacting with extracellular ligands [94]. SDN-1 is involved in a wide-range of

biological processes such as embryonic and larval development as well as neurodevelopment [94]. Interestingly, the mutation in *sdn-1* leads to severe migration and guidance defects in HSN neurons [92, 93]. Furthermore, removal of calcium transport channels (TRP-1 and TRP-2) in an *sdn-1* mutant background rescues the HSN defects [94]. Therefore, it has been suggested that the role of SDN-1 in HSN development is through mediating the function of TRP channels. In addition to HSN defects, *sdn-1* mutants display migration and guidance defects in many other neurons such as ALM, PVQ and AVK [94]. *sdn-1* expression is present in many different tissues in the worm including hypodermis, body wall muscle neurons and glia [92, 93, 106]. Interestingly, *sdn-1* was upregulated in *sma-3* mutants (Log_2Fold change: 0.27) according to my RNA sequencing data (Table 5.1). As stated earlier, it has been established that SDN-1 is crucial for proper HSN development, however it is unclear that whether SDN-1 mediation of HSN development is correlated with SMA-3-mediated HSN development. In order to answer this question, I performed *sdn-1*-specific RNAi experiment in *sma-3* mutants using an RNAi clone that targets both two isoforms encoded by *sdn-1* (Fig. 5.14A). The scoring results revealed that the knockdown of *sdn-1* does not affect the severity of the HSN defects of *sma-3* mutants (Fig. 5.14B). This suggest that the upregulation of *sdn-1* is not correlated with the HSN defects identified in *sma-3* mutants. To further investigate the correlation between SDN-1- and TGF-β-mediated HSN development, I generated compound *sma-6; sdn-1* double mutants. I used the *zh20* null allele of *sdn-1*, which is a 1258-bp deletion that causes a frameshift which results with a premature stop codon in the transcript [92]. Examination of the *sdn-1(zh20)* single mutant showed that these worms displayed severe HSN defects (Fig. 5.14C) which is in concurrence with previous studies [92, 93]. Next, I examined the HSN profiles of *sma-6; sdn-1* mutants and found that these animals displayed significantly increased HSN defects compared to the *sdn-1* single mutant (Fig. 5.14C). This indicates that SDN-1 and TGF-β signaling controls HSN development via parallel pathways.

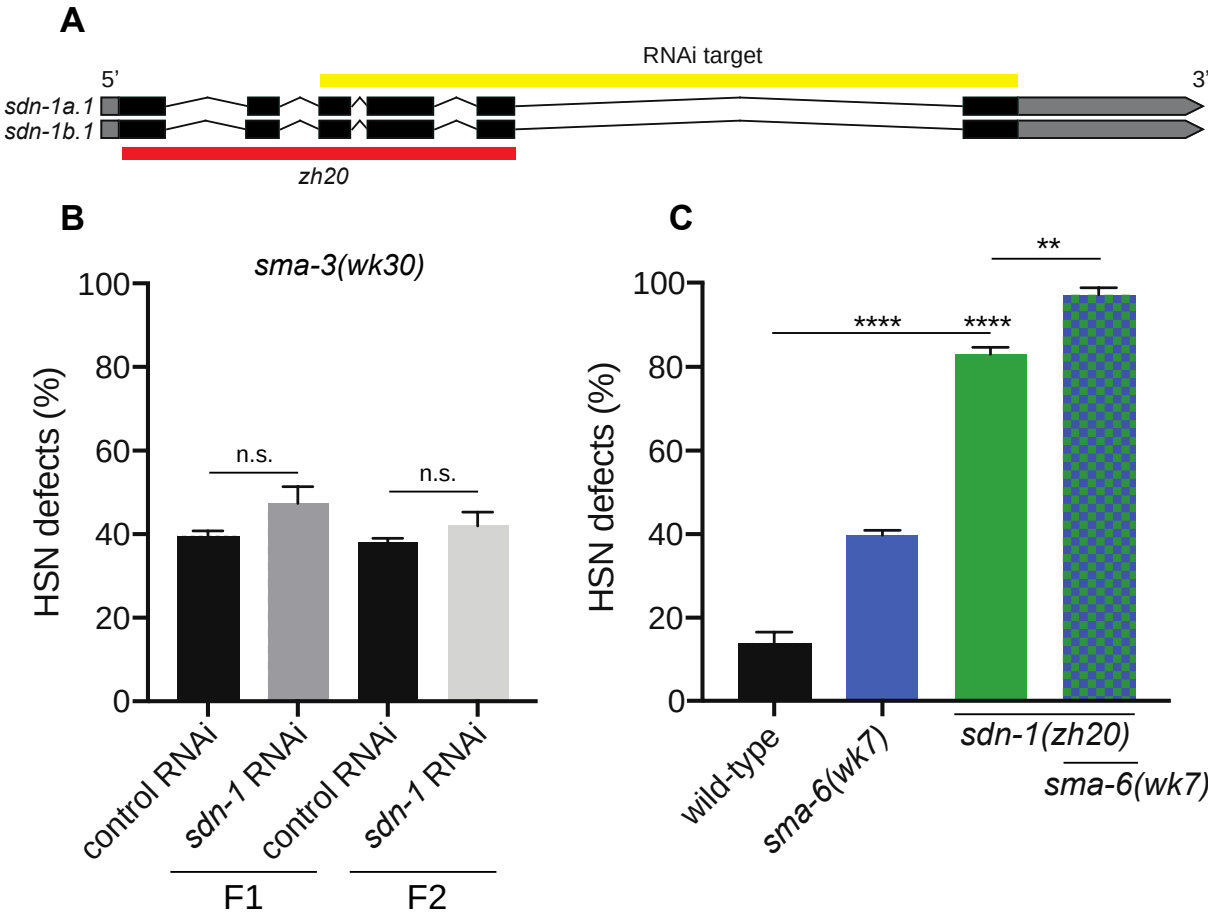

Fig. 5.14. SDN-1 and TGF-β pathway act in parallel pathways to regulate HSN development.
(A) Gene structure of *sdn-1* (adapted from WormBase). The RNAi target (yellow box) targets a common sequence between the two *sdn-1* transcripts. *zh20* (red box) is a 1258-bp deletion that causes a frameshift which results with a premature stop codon in both *sdn-1* transcripts. Black boxes represent exons, black lines represent introns and grey boxes represent UTRs. (B) Quantification of HSN defects in *sma-3(wk30)* mutants fed with *sdn*-1-specific or control vector RNAi. Statistical analysis of F1 and F2 scoring was performed separately using an unpaired *t*-test. (C) Quantification of HSN defects in *sdn-1(zh20)* and *sma-6(wk7)* mutants as well as *sdn-1; sma-6* double mutant. Statistical analysis of (C) was performed using one-way ANOVA and Tukey's multiple comparison test, comparing the mean of all the columns with every other column. At least one hundred animals were scored per condition. **p < 0.01, ****p < 0.0001, n.s., not significant. Error bars represent mean ± SEM of three biological replicates.

nlr-1

Neurexin Like Receptor-1 (NLR-1) is a cell adhesion molecule that belongs to the neurexin superfamily, specifically the Caspr subfamily. Members of the neurexin superfamily are implicated in neurodevelopmental diseases in humans [176-179]. One example is cortical dysplasia-focal epilepsy syndrome, in which *contactin associated*

protein like 2 (*CNTNAP2*), the ortholog of *nlr-1* has been reported to be mutated in patients [180]. As well as its orthologs, *nlr-1* is vital for the organism as null mutations within the gene causes lethality, however, no specific function has been reported. According to my RNA sequencing data *nlr-1* expression was upregulated in *sma-3* mutants (Log_2Fold change: 0.27). I hypothesized that the HSN defects of *sma-3* mutants could be alleviated by reducing the upregulated *nlr-1* levels if these defects are attributable to the *nlr-1* upregulation. In order to investigate this hypothesis, I conducted *nlr-1*-specific RNAi knockdown experiments in *sma-3* mutants. The RNAi clone targets the 7th, 8th and 9th exons of *nlr-1* gene (Fig. 5.15A). Strikingly, examination of HSN phenotypes of these worms revealed suppression of the HSN phenotype in the F2 generation (Fig. 5.15B). This suggests that NLR-1 acts with SMA-3 in the regulation of HSN development. As the null mutant of *nlr-1* is lethal, I was not able to examine the HSN phenotype of these worms.

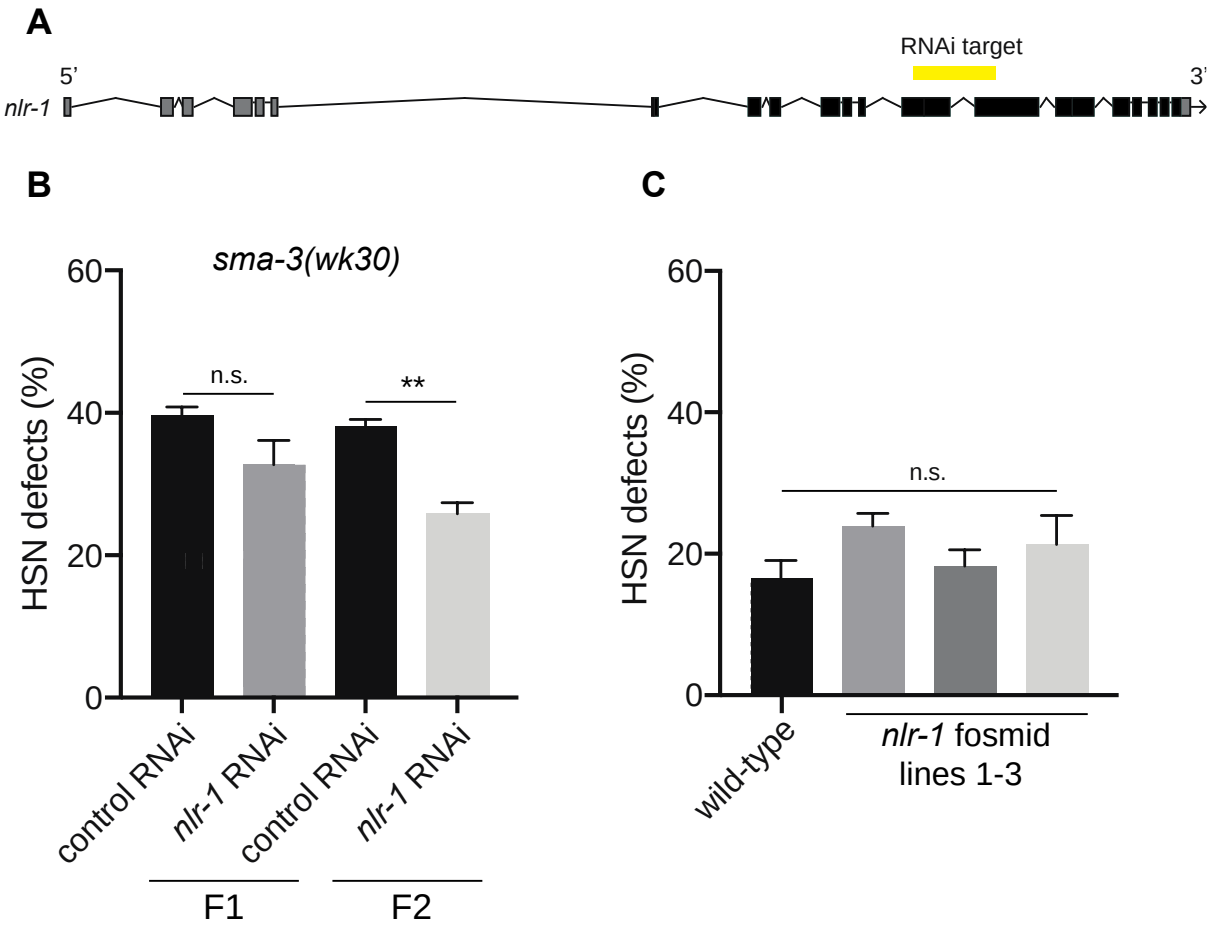

Fig. 5.15. *nlr-1* knockdown suppresses the HSN defects in *sma-3* mutants.

(A) Gene structure of *nlr-1* (adapted from WormBase). The RNAi target (yellow box) targets a sequence between the 7th and 9th exons of the *nlr-1* transcript. Black boxes represent exons, black lines represent introns and grey boxes represent UTRs. (B) Quantification of HSN defects in *sma-3(wk30)* mutants fed with *nlr-1*-specific or control vector RNAi. Statistical analysis of F1 and F2 scoring was performed separately using an unpaired *t*-test. (C) Quantification of HSN defects in *nlr-1* overexpression lines generated by the injection of wild-type worms with a fosmid clone (WRM0615aH06) that includes the *nlr-1* locus. Statistical analysis was performed using one-way ANOVA and Dunnett's multiple comparison test. At least one hundred animals were scored per condition. **p < 0.01; n.s., not significant. Error bars represent mean ± SEM of three biological replicates.

In order to further substantiate my findings on NLR-1 action in the SMA-3-mediated HSN development, I overexpressed *nlr-1* in wild-type (*HSN::GFP*) worms, hypothesizing that these worms would phenocopy the HSNs of *sma-3* mutants. For *nlr-1* overexpression, I used a fosmid clone, WRM0615aH06, which is 29885-bp long and covers the *nlr-1* locus. The fosmid was injected into wild-type (*HSN::GFP*) worms *at* 1 ng/µl final concentration and three independent transgenic lines were generated. Surprisingly, I found no significant HSN defects compared to wild-type worms after examining the HSN phenotypes of these lines (Fig. 5.15C). This could be due to insufficient overexpression of *nlr-1* to cause developmental HSN defects. Alternatively, the presence of SMA-3 which potentially repress *nlr-1* expression is strong enough to repress the *nlr-1* overexpression, therefore overcome the detrimental effect on HSN development.

5.5 Discussion

In Chapters 3 and 4, I described a non-canonical TGF-β family signaling required for the development of hermaphrodite specific motor neurons. This mechanism involves a TGF-β family receptor type I receptor, SMA-6, acting with multiple extracellular ligands, TIG-2, TIG-3 and UNC-129, independently of the type II receptor, DAF-4. In this chapter, I focused on identifying the downstream targets of this pathway which controls HSN development.

In Chapter 3, I showed that particular intracellular signaling SMADs, SMA-2, -3 and -4, are required for HSN development (Fig. 3.6). SMA-2 and SMA-3 are the receptor activated SMADs, whereas SMA-4 acts as a co-regulator. Upon activation by SMA-6, these molecules translocate into nucleus and act as a transcriptional regulator [55, 96]. In order to identify the target genes of my proposed pathway, I performed an RNA sequencing on *sma-3* mutants and wild-type (N2) animals. Considering that HSN axon outgrowth starts at larval stage 2, I decided to extract RNA from L2-stage worms. It would be also valuable to perform an RNA sequencing on embryos of these mutants as HSN migration occurs during embryogenesis [61, 67, 73].

Analysis of RNA sequencing resulted with 1922 differentially expressed genes in *sma-3* mutants compared to wild-type worms. TGF-β family signaling mediates a wide-range of biological processes, thus interference with this pathway results with dysregulation of many genes which makes the analysis of the RNA sequencing data challenging. To overcome this issue, RNA sequencing on the components of dauer pathway can be performed in the future studies. Considering that this pathway is not involved in HSN development, putative targets identified by RNA sequencing can be eliminated. Based on statistical significance and biological relevance, I focused on twelve of the dysregulated genes (Table 5.1) as potential gene target of the TGF-β pathway for the regulation of HSN development. These genes encode a wide-range of molecules such as kinases, cell adhesion molecules and guidance cues some of which have been reported to be required for HSN development [92, 95]. My hypothesis on how TGF-β pathway regulates HSN development is based on potential activation and/or inhibition of downstream molecules or pathways which can directly act as regulators of HSNs or can regulate another pathway which would potentially control HSN development. For instance, the HSN defects discovered in *sma-3* could be

attributable to the downregulation of downstream targets genes. In this scenario, restoring the expression of the downregulated target genes in these mutant backgrounds could rescue the HSN defects. Alternatively, these defects could be occurring due to the action of the upregulated genes, thus hypothetically, reduction in the expression of these upregulated genes could alleviate the HSN defects. To interrogate these hypotheses, I established two approaches. For the genes downregulated in *sma-3* mutants, I performed RNAi knockdown experiments in wild-type (*HSN::GFP*) worms, hypothesizing that knockdown of the relevant candidates genes would phenocopy the HSN defects displayed in *sma-3* mutants. For the investigation of the upregulated genes, I performed RNAi knockdown experiments in *sma-3* mutants, hypothesizing that knockdown of the relevant candidate genes would suppress the HSN defects identified in *sma-3* mutants. Depending on the availability of the strains, I also analyzed the null mutants of some of these genes as well as the double mutants generated with *sma-3* and/or *sma-6* mutants.

Among the downregulated genes, I determined *sgk-1, kpc-1* and *mboa-6* as potential targets of SMA-3 in HSN development. RNAi knockdown experiments revealed that the reduction of none of these genes caused significantly increased HSN defects in wild-type worms (*HSN::GFP*) (Fig. 5.3B, Fig. 5.4B, Fig. 5.5B). *sgk-1* encodes a kinase that plays a role in a wide range of developmental processes including body size regulation [156], therefore the reduction in the mRNA levels of this gene could be related to another process mediated by TGF-β signaling. KPC-1 is a key enzyme that cleaves the long precursors of the proteins for their maturation and has been shown to be involved in dendritic branching of sensory neurons and guidance-cue trafficking in glial development [157]. The third of the shortlisted genes was MBOA-6 which is a membrane bound acyl transferase and the loss of this protein leads to developmental defects such as slow growth [159] which was also detected in my RNAi screen. This means that the RNAi construct that I generated worked properly, however the regulatory levels potentially required for HSN development could be different than the levels required for larval development. Furthermore, the highly variable HSN profile among the independent biological replicates makes it difficult to decipher the importance of MBOA-6. Thus, the examination of the *mboa-6* null mutant in the future studies could help us understand if *mboa-6* plays a role in HSN development.

The second group of screened shortlisted genes was the candidate genes that were upregulated in *sma-3* mutants (Table 5.1). Hypothesizing that upregulation of these genes could be detrimental to HSN development, I performed RNAi experiments to knockdown their expression in *sma-3* mutant animals. These candidates are composed of genes that are implicated in neuronal development; specifically, some of which were shown to be important for HSN development. Among these genes, *smp-1*, *max-1*, and *lad-2* are associated with axon guidance, whereas *mec-1* has been reported to be involved in neuronal migration [167, 168, 173, 174]. My RNAi screen showed that individual knockdown of these genes in *sma-3* mutants did not alter the HSN phenotype of these worms (Fig. 5.10, Fig. 5.11, Fig. 5.13). This suggests that the HSN defects of *sma-3* mutants do not occur due to the upregulation of these genes. However, further studies such as null mutant analysis are required to draw final conclusions.

Four of the remaining upregulated genes, *sdn-1*, *slt-1*, *vab-8*, and *vab-19*, have been linked with HSN development. Mutations in *vab-19* alter the localization of the netrin receptor UNC-40 which leads to axon guidance defects [171]. However, knockdown of *vab-19* in *sma-3* mutants did not cause a reduction in the severity of HSN defects (Fig. 5.12B) which suggests that the upregulation of *vab-19* is not associated with SMA-3-mediated HSN development. Mutations in *slt-1* have been shown to cause weak HSN migration defects, whereas perturbing with *vab-8* have been reported to cause HSN overmigration and guidance defects [89, 95, 181]. Although these genes were upregulated in *sma-3* mutants, RNAi knockdown and null mutant analysis revealed that SLT-1 and VAB-8 do not function in the same pathway as SMA-3 (Fig. 5.7, Fig. 5.8). Next, I examined *sdn-1* knockdown, which causes severe HSN migration and guidance defects [92, 93]. Interestingly, the knockdown of *sdn-1* in *sma-3* mutants did not cause a significant change in the HSN phenotype of *sma-3* mutants (Fig. 5.14B). To further investigate the potential role of SDN-1 in TGF-β-mediated HSN development, Initially, I initially examined the HSN profile of *sdn-1(zh20)* null mutants. Although I detected slightly lower penetrance of guidance defects ranging from 60 to 65% of the *sdn-1* mutants (data not shown) compared to the previously published data, I found similar results on overall penetrance of HSN defects in *sdn-1* mutants (Fig. 5.14C). Furthermore, the examination of and *sma-6; sdn-1* double mutants revealed a

significant increase in HSN defects. This suggests that TGF-β pathway and SDN-1 act in parallel pathways to control the migration of HSNs.

NLR-1 is a cell adhesion molecule which is crucial for the survival of the worm as the null mutants do not survive, however no specific function has been reported. My RNA sequencing data showed that *nlr-1* expression was significantly increased in *sma-3* mutants (Table 5.1). Strikingly, I found that *nlr-1* knockdown in *sma-3* mutants caused a significant reduction in the percentage of animals possessing defective HSNs (Fig. 5.15B). This shows that the regulation of *nlr-1* expression by the TGF-β pathway is important for proper HSN development. As my hypothesis depends upon the *nlr-1* upregulation detected in *sma-3* mutants causing HSN defects, I overexpressed *nlr-1* in wild-type (*HSN::GFP*) worms to replicate the HSN phenotype of *sma-3* mutants using a fosmid clone that includes *nlr-1* gene. Surprisingly, the transgenic lines that carry the *nlr-1*-specific fosmid did not cause significant HSN defects (Fig. 5.15C). Another potential issue could be related to the presence of SMA-3 which could repress the *nlr-1* overexpression, therefore overcome the detrimental effect on HSN development. Furthermore, HSN development is a very complex process regulated by a wide-range of signaling pathways, thus it is likely that the potential detrimental effects of *nlr-1* overexpression could be compensated for due to the redundancy. As I have previously mentioned in Chapter 3, my proposed pathway acts from hypodermis to regulate HSN development, thus overexpression of *nlr-1* exclusively in hypodermis could allow for more specific results.

Taken together, the investigation of the downstream targets of TGF-β signaling revealed that NLR-1 is a strong candidate to be acting as one of the downstream targets of TGF-β-mediated HSN development. For future studies, it is important to validate the differential expression of *nlr-1* in *sma-3* mutants. This could be achieved by performing qPCR in *sma-3* mutants, as well as comparing the *nlr-1* expression levels of *sma-3* mutants with wild-type worms using *pnlr-1::GFP* reporter lines. Moreover, *nlr-1* knockdown in *sma-6* mutant is required to ascertain whether the HSN suppression phenotype can be repeated. The investigation of other molecules such as NRX-1, which act with NRL-1 in the potential downstream mechanisms is also required to fully understand how this process eventually leads to HSN development.

5.6 Conclusion

Strict regulation of signaling pathways is crucial during development. It has previously been shown that Wnt, ephrin and netrin signaling play important roles in HSN development. As HSNs undergo long-range neuronal migration and axon guidance events during distinct periods of development, regulation of development of these neurons is a very complex process. Consequently, my results on the screen of putative downstream targets of TGF-β family signaling will provide insight into how this process occurs (Fig. 5.16). Future studies on the correlation between these processes are required to dissect the complete mechanism driving HSN development.

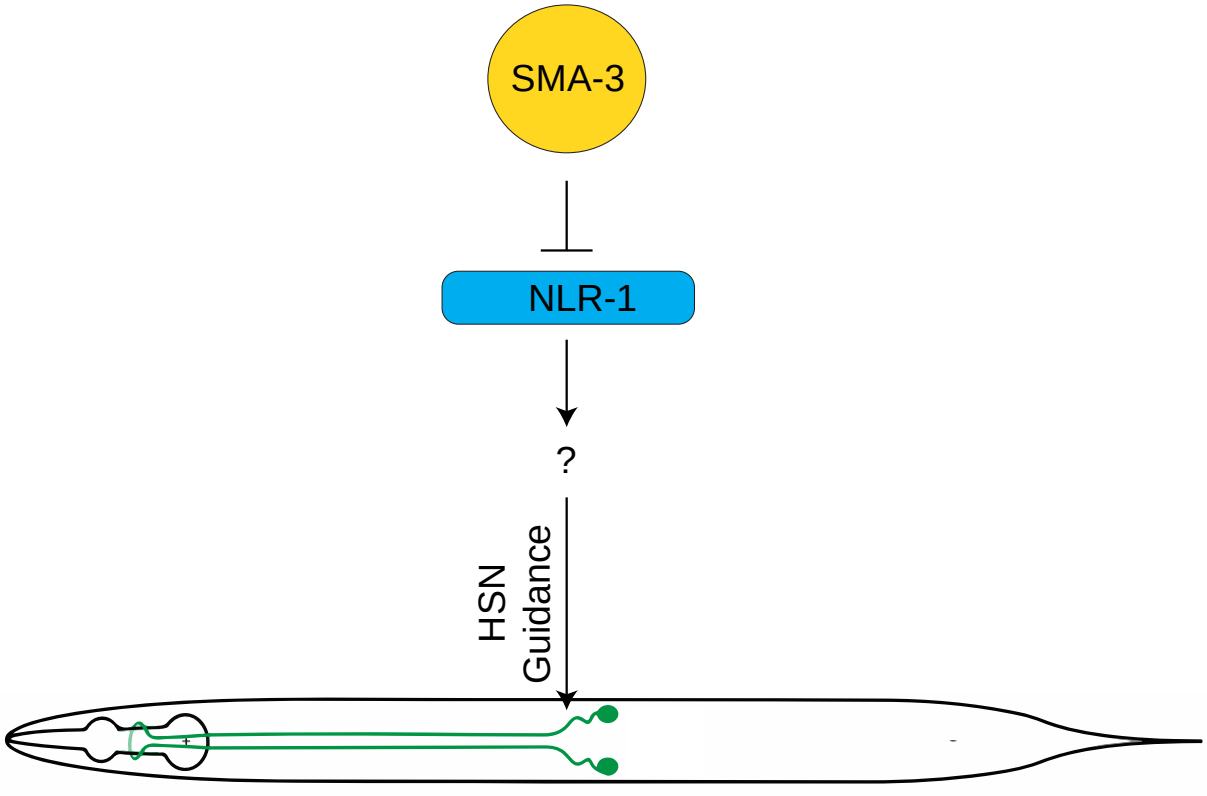

Fig. 5.16. Illustration of SMA-3 and NLR-1 action in HSN development.

6. General Discussion

6.1 Thesis summary

The aim of this thesis was to identify the role of TGF-β signaling in neuronal development. Using the hermaphrodite-specific motor neurons (HSN) of the roundworm *C. elegans*, I identified a non-canonical mechanism for TGF-β signaling in neuronal development. Due to the highly conserved nature of this pathway, we believe the outcome of this thesis will have wide range implications in neuronal development and disease.

6.2 Non-cell autonomous action of SMA-6 is essential for HSN development

TGF-β family signaling controls an array of biological processes in *C. elegans* such as body size, innate immunity and longevity [96]. In this study, we investigated the role of TGF-β family components in HSN development. Initially, we examined the mutant strains of *daf-1* and *sma-6* genes, which encode the two TGF-β family type I receptors, and found that mutations in *sma-6*, but not in *daf-1*, causes neuronal migration and axon guidance defects in the HSN neurons (Fig. 3.2). Furthermore, endogenous rescue of *sma-6* prevents these defects, which confirms the requirement for *sma-6* in HSN development. In order to identify where SMA-6 acts for this function, we conducted tissue-specific rescue experiments targeting its primary expression sites, namely the hypodermis and intestine. We found that hypodermal rescue of *sma-6* suppressed the HSN defects of *sma-6* mutants, whereas its intestinal expression was dispensable for this role (Fig. 3.3, Fig. 3.4). Furthermore, HSN-specific *sma-6* expression did not suppress the HSN defects of *sma-6* mutant animals (Fig. 3.5), therefore we concluded that SMA-6 acts non-cell autonomously from hypodermis to control HSN development. Non-cell autonomous action from the hypodermis in HSN development has previously been reported by a study that showed that the microRNA *mir-79* acts to stabilize the glycosylation state of the hypodermis [86]. In another study, hypodermal expression of *daf-16*, which encodes a transcription factor in the insulin signaling pathway, has been shown to be required for HSN development [142]. During embryogenesis, the HSN neurons migrate to the mid-body and during postembryonic

development extend their axons anteriorly through ventral nerve cord (VNC) in which the axons run along the hypodermal ridge [67]. Therefore, potential guidance cues could be secreted by hypodermis for the correct development of these neurons.

6.3 The type I receptor SMA-6 acts independently of the type II receptor DAF-4

In canonical TGF-β signaling, the type I receptor SMA-6 requires activation by the type II receptor DAF-4, therefore SMA-6 action in HSN development implies a potential role for DAF-4 in this context. Strikingly, examination of multiple independent *daf-4* mutant alleles revealed that DAF-4 is dispensable for HSN development (Fig. 3.7B). Furthermore, I generated two CRISPR-knockout strains for *daf-4*, and the HSN phenotype of these worms was not different from wild-type animals (Fig. 3.7C). Considering that DAF-4 is the sole type II receptor in *C. elegans*, these results suggest SMA-6 auto-activates to propagate downstream signaling or it could be activated by an unknown molecule. Examining the role of intracellular trafficking events of TGF-β family receptors provided corroborating results for the independent role of SMA-6 (Fig. 3.8). Gleason et al. showed that intracellular transportation of SMA-6 and DAF-4 between the cytosol and plasma membrane occur via distinct mechanisms where SMA-6 trafficking is controlled by a receptor-mediated endocytosis retromer protein (RME-1), while DAF-4 trafficking is mediated by ADP-ribosylation factor 6 (ARF-6) in a retromer-independent mechanism [117]. Intriguingly, I found that *rme-1* mutant animals displayed HSN defects, whereas *arf-6* mutants presented a wild-type HSN phenotype (Fig. 3.8). This means that perturbed transportation of DAF-4 has no effect on HSN development which further substantiate our previous findings on DAF-4-independent action of SMA-6 in this context. How can a type I receptor act independently of a type II receptor in TGF-β signaling? Zhao et al. have reported that ALK5, a TGF-β type I receptor homolog, controls mandible patterning in TGBR2-knockout mice [182]. However, TGFBR2 is not the only type II receptor, therefore ALK5 might be activated by other type II receptors. Interestingly, Gunther et al. reported that DAF-1, the type I receptor component in the dauer pathway, can signal independently of DAF-4 [112]. In this study, they showed that *daf-1* mutants displayed more severe dauer-constitutive phenotype compared to the *daf-4* mutant animals. Furthermore, *daf-1* overexpression

in *daf-4* mutant animals partially rescued the dauer-constitutive phenotype, suggesting that DAF-1 can act independently of DAF-4, however the signaling by both receptors are still required due to the partial rescue. In contrast, our results indicate a mechanism that only requires SMA-6 and DAF-4 is dispensable. To further substantiate this hypothesis, a double mutant between *daf-4* and *sma-6* mutant animals can be generated and their HSN phenotype analyzed.

6.4 Specific Smads are required for HSN development

TGF-β family receptors propagate signaling through intracellular signaling molecules called Smads. The Sma/Mab and dauer pathways – TGF-β signaling pathways in *C. elegans* – act through two groups of Smads, which are composed of SMA-2, -3, -4 and DAF-3, -8, -14, respectively [96]. My findings in Chapter 3 revealed that the Smads of Sma/Mab pathway are required for HSN development, whereas the Smads of dauer pathway are not required for this role (Fig. 3.6). These results suggest that the receptor and Smad components of Sma/Mab pathway, except the type II receptor DAF-4, act in a non-canonical manner to regulate HSN development. As mentioned in Chapter 1, the Sma/Mab pathway controls body size development and mutating the components of this pathway results with small body phenotype (Sma). This raises the possibility small body size might affect the formation of tracts in which neurons migrate and extend processes for receiving and relaying information. However, *daf-4* mutants display decreased body size, but do not exhibit HSN defects. Furthermore, in Chapter 4 I showed that *dbl-1* mutant animals do not display HSN defects, even though they are small in size, ruling out the hypothesis that HSN defects occur due to small body size.

Smads have low affinity for DNA binding, therefore require binding partners to regulate transcription [5]. In *C. elegans*, SMA-9/Schnurri has been shown function as a co-factor for Smad-mediated transcription in Sma/Mab pathway [120, 132], whereas DAF-5/Sno/Ski acts in dauer pathway by binding to the co-Smad DAF-3 for transcriptional repression [121, 122]. Considering that the role of specific Smads in HSN development, we investigated the potential role of SMA-9 as a co-factor required for transcriptional regulation in HSN development. Interestingly, *sma-9* mutant animals did not display a defective HSN phenotype (Fig. 3.9), which suggests that the SMA-2/-3/-

4 complex acts either independently of DNA binding partners or require an unknown co-factor in the context of HSN development. A suppressor screen in a Smad mutant background would help us identify potential DNA binding partner(s) in this context. Alternatively, SMA-9 might be acting antagonistically to TGF-β signaling in HSN development. The antagonistic action of SMA-9 on TGF-β signaling has been shown in the regulation of cell fate specification [101]. To investigate this hypothesis, double mutants between *sma-9* mutants and the components of TGF-β signaling can be generated and examined for their HSN phenotype.

6.5 Multiple TGF-β family ligands act with SMA-6 to regulate HSN development

Although there are over thirty TGF-β/BMP ligands in mammals, *C. elegans* possesses only five ligands. DBL-1/BMP-like and DAF-7/TGF-β-like are ligands of the canonical Sma/Mab and dauer pathway, respectively[96]. TIG-2/BMP-like and TIG-3/BMP-like ligands have not been characterized, while UNC-129/BMP-like has been shown to be involved in axon guidance events independently of the other TGF-β family components [107]. In Chapter 4, we conducted a screen of TGF-β family ligands to decipher their role in HSN development. Among these ligands, we found that loss of UNC-129, TIG-2 and TIG-3 result in HSN defects, whereas loss of DBL-1 and DAF-7 were dispensable for HSN development (Fig. 4.1). It was surprising to find that DBL-1 is not involved in this process, considering the importance of the other Sma/Mab pathway components in HSN development. Taken together with DAF-4 independency, this indicates a non-canonical action of TGF-β signaling in this process. The HSN-defective phenotype of *tig-2* and *tig-3* mutants is the first evidence on the role of these proteins. Considering these novel roles of TIG-2 and TIG-3, further studies such as expression pattern analysis, tissue-specific and endogenous rescue experiments on the mutant strains of these genes would be beneficial to illuminate how they act to regulate HSN development. UNC-129, has previously been shown to act in axon pathfinding of the D-type motor neurons [107]. My findings on the role of UNC-129 shows that it can also act in anterior-posterior axis to guide the development of motor neurons (Fig. 4.1C), however its important regulatory role on the development of multiple neurons raises the possibility of whether the disruption of HSN development in *unc-129* mutant

animals is attributable to another disrupted neuronal development. As D-type motor neurons and HSNs grow along different axes, other motor neurons growing through the anterior-posterior tract such as ventral nerve cord neurons could be examined in future studies to investigate this hypothesis.

After discovering the specific TGF-β ligands that are required for HSN development, I next investigated which of these ligands act in the same pathway as SMA-6 in this process. Examination of double mutants generated between *sma-6* and ligand mutants revealed a complex mechanism in which UNC-129, TIG-2 and TIG-3 act with SMA-6 in the same genetic pathway to regulate HSN development (Fig. 4.2). Furthermore, the triple and double mutants generated among the mutant strains of these ligands did not cause a further increase in HSN defects in comparison to the single mutant animals for the ligands (Fig. 4.3). Although the severity of the defects and the number of worms with defective HSNs were slightly lower in *tig-3* mutants, statistical analysis revealed no difference, therefore these findings suggest a complex mechanism in which multiple ligands act with a single receptor in the same genetic pathway. Another crucial point is that UNC-129, for the first time, has been shown to act with TGF-β family components in the same genetic pathway. Thus, it would be beneficial to conduct rescue experiments to elucidate the exact function of UNC-129 in HSN development.

To further investigate this complex mechanism between the ligands and the receptor, we investigated the potential interaction between SMA-6 and the ligands using co-immunoprecipitation experiments. Although SMA-6/TIG-3 and SMA-6/UNC-129 interaction experiments did not reveal a reliable result due to potential experimental problems, I found that SMA-6 and TIG-2 co-immunoprecipitate, suggesting that they form a protein complex by physically or indirectly interacting with each other (Fig. 4.5). Taken together with the scoring results, these findings suggest a potential complex formation among UNC-129, TIG-2, TIG-3 and SMA-6 as removal of any of these components perturbs the mechanism that controls HSN development. The action of multiple TGF-β ligands in the same pathway has previously been reported. The study by Fuerer et al. showed that TGF-β ligands Nodal and GDF1 form a heterodimer and act in the Nodal signaling during embryogenesis [153]. In the future studies, it would be very interesting to perform further interaction experiments between these ligands as well as investigating their potential combinatorial interaction with SMA-6.

6.6 Structural requirements of SMA-6 for ligand binding

TGF-β family type I receptors contain highly conserved phosphorylation and ligand-binding domains, which are crucial for their activation by the type II receptor and their interaction with extracellular ligands, respectively [5]. SMA-6 is no exception to this, possessing three SG repeats in the intracellular domain and the conserved cysteine box ($CCX_{4-5}CN$) in the extracellular domain. Although these domains are potentially phosphorylation and ligand-binding domains based on their homology with mammalian TGF-β receptors, no experimental evidence exists for their role in SMA-6 function. After showing complex formation between TIG-2 and SMA-6, I next investigated the requirement of the putative ligand-binding domain for this interaction. Surprisingly, substitution of the cysteine residues with alanine residues in the conserved cysteine box did not interfere with the complex formation between TIG-2 and SMA-6 (Fig. 4.9). This suggests that SMA-6 interacts with TIG-2 via another domain and/or the interaction of SMA-6 with the extracellular ligands in general require another unidentified domain. In the future studies, these hypotheses can be investigated by performing further co-immunoprecipitation experiments between SMA-6 and the other *C. elegans* TGF-β family ligands. Moreover, other potential domains in SMA-6 can be mutagenized and further interaction experiments can be performed to identify the required domain for ligand binding. In addition to ligand binding, further studies on phosphorylation domain of SMA-6 are required for determining its potential function in HSN development as well as in other contexts. For instance, the serine residues in the SG domain of SMA-6 can be mutated using CRISPR-Cas9 technique in wild-type animals and the HSN phenotype of these animals can be examined. It has been shown that the replacing the threonine residue with an aspartic acid near the GS domain causes constitutive activation of type I receptors *in vitro* [26]. Furthermore, a mutation that replaced the 253_{rd} glutamine with an aspartic acid residue in the type I receptor of *Drosophila* caused the same constitutively-active state [14]. Intriguingly, SMA-6 possesses both of these aspartic acid residues naturally which could be an indication of a more active type I receptor. These aspartic residues can be mutated in wild-type animals and HSN phenotype can be examined, which would provide insights on how SMA-6 acts independently of DAF-4.

TGF-β family ligands are expressed as long precursors which require processing before function. Upon cleavage by proteolytic enzymes into their mature forms, they bind to their target receptors to initiate signaling [10]. To date, these alternative forms of TGF-β ligands have not been shown in *C. elegans*. As detailed in Chapter 4, the TGF-β ligands that were found to be required for HSN development have been fused with protein tags and expressed in mammalian HEK293T cells. Analysis of both cell lysates and media upon SDS-PAGE and western blot revealed differently sized bands for UNC-129 and TIG-2 (Fig. 4.8, Fig. 4.5). These bands included the proteins that are very similar in size to the estimated UNC-129 and TIG-2 proteins. Furthermore, they included shorter bands that were stronger in the media compared to the cell lysates. Considering that these ligands should hypothetically be secreted to the extracellular space, these smaller bands are highly likely to be the mature forms of UNC-129 and TIG-2. In our previous work, I detected the same sized mature form of TIG-2 which validates this hypothesis [91]. Surprisingly, no TIG-3 band was detected in the cell culture media of TIG-3-transfected cells (Fig. 4.6), which could be due to the lack of secretion, low expression levels and/or possible degradation of the protein during the experimental process. Taken together with my previous work, these results provide the first evidence on the alternative forms of *C. elegans* TGF-β family ligands. Correct maturation of ligands is crucial for signal initiation, and thus for the biological response. The maturation process is controlled by proteolytic enzymes such as members of proprotein convertase (PC) family [10]. Interfering with these enzymes can lead to disrupted signaling and developmental defects [10]. For instance, mouse embryos lacking the proprotein convertase PC5/6 displayed altered anteroposterior patterning which is a process controlled by TGF-β signaling [183]. In *C. elegans*, there are four PCs which are AEX-5, BLI-4, KPC-1 and EGL-3 [184, 185], however it is unclear whether these enzymes are involved in the maturation process of TGF-β family ligands. Interestingly, mutants of *kpc-1* exhibit HSN migration defects [186], therefore analysis of the processing of TGF-β ligands by KPC-1 could be investigated. In future experiments, it would be beneficial to investigate the role of all of these enzymes in TGF-β ligand maturation and therefore, in HSN development. Using CRISPR-Cas9 technology, *unc-129*, *tig-2* and *tig-3* genes could be fused with small protein tags, therefore their endogenous secretion can be examined in wild-type and PC-mutant backgrounds by western blot using antibodies specific to these tags. In case of a

potential detrimental effect on the ligand secretion in PC-enzyme mutants, it would be also interesting to investigate how this would affect the TGF-β signaling strength, and therefore the HSN development.

6.7 NLR-1 is a downstream effector of SMA-3 in HSN development

The TGF-β pathway relays signals through intracellular Smads to regulate transcription of downstream effectors. After screening the ligands, receptors and Smads for their role in HSN development, I wanted to identify downstream effectors mediating the effect of TGF-β signaling in this process. In order to investigate these effectors, RNA sequencing was conducted in *sma-3* mutants and wild-type animals. Based on their biological relevance and statistical significance I selected twelve genes as putative targets of SMA-3 (Table 5.1) and analyzed their role in HSN development by conducting RNA interference (RNAi) knockdown experiments as well as analyzing double mutants between the null mutants of the candidate genes and *sma-3* and/or *sma-6* mutants. A very interesting putative target I identified is the neurexin-like receptor 1 (NLR-1), which is a cell adhesion molecule. According to my RNA-sequencing data, *nlr-1* expression was elevated in *sma-3* mutants compared to wild-type animals. Strikingly, *nlr-1*-specific RNAi knockdown in *sma-3* mutants resulted with the partial suppression in HSN defects of these animals (Fig. 5.15B), suggesting that *nlr-1* acts as a downstream effector of SMA-3 in HSN development. *nlr-1* has been shown to be expressed primarily in the head of the worm; pharyngeal muscle, neurons and gland cells [187]. The function of NLR-1 is unclear, however the null mutant is lethal, indicating a vital role for the survival of the organism. If NLR-1 is acting as a downstream effector of TGF-β-mediated HSN development and the HSN defects detected in the mutant components of TGF-β signaling are attributable to the *nlr-1* overexpression, I hypothesized that overexpressing *nlr-1* in wild-type animals would also result with increased HSN defects. Surprisingly, I found that *nlr-1* overexpression by a fosmid clone that covers *nlr-1* locus did not cause a change in the HSN phenotype (Fig. 5.15C). As discussed in Chapter 4, there could be many reasons for the wild-type-like HSN phenotype of *nlr-1* overexpression lines such as a potential SMA-3 inhibition of *nlr-1* overexpression or compensation of potential detrimental effects of *nlr-1*

overexpression by other pathways. Considering my hypothesis on TGF-β-mediated regulation of HSN development being from the hypodermis, overexpressing *nlr-1* specifically in the hypodermis could provide more meaningful results. Also, the RNA sequencing data that shows overexpression of *nlr-1* in *sma-3* mutant animals needs to be confirmed by independent experiments such as qRT-PCR as well as examining the expression pattern of *nlr*-1-promoter driven reporters in wild-type and *sma-3* mutant animals.

TGF-β signaling controls a broad range of biological functions, therefore interference with this pathway can lead to transcriptional changes in a high number of molecules, some of which may be downstream effectors. The RNA-sequencing conducted in *sma-3* mutant animals is a great representative example for this, as I found 1922 differentially expressed genes (DEG) in these mutants compared to wild-type. As shown in Chapter 5, it is highly unlikely that all of these genes function in HSN development. In order to apply a better filtering system for these genes, further RNA-sequencing can be conducted on the TGF-β components associated with HSN development and common DEGs may be analyzed. Alternatively, the transcriptomes of TGF-β components that were found dispensable for HSN development can be analyzed. For instance, dauer pathway regulates an array of biological processes such as dauer formation, fat metabolism and longevity, however I found that they are not required for HSN development (Fig. 3.2B, Fig. 3.6C). Thus, analyzing the transcriptomes of components of this pathway would enable the removal of potentially irrelevant genes for HSN development. Moreover, my RNA sequencing data can be compared with previous transcriptome analyses and common DEGs can be further analyzed for their role in HSN development. The downstream effectors of TGF-β signaling have previously been investigated in the context of body size regulation [120, 128]. In a recent study, Madaan et al. identified that the regulation of body size by TGF-β signaling depends on the transcriptional regulation of cuticle collagen genes such as *col-41*, *col-141*, *col-142* and *rol-6* [128]. By a microarray analysis, *col-141* and *col-142* have been shown to be elevated in *dbl-1* mutants, while *col-41* and *rol-6* were downregulated [120] which were also confirmed in *sma-3* and *dbl-1* mutants by Madaan et al. using quantitative RT-PCR [128]. Interestingly, none of these genes were significantly changed in *sma-3* mutant animals according to our RNA-sequencing data,

which could be due to the dynamic nature of *sma-3* expression throughout development.

TGF-β signaling can act in a temporal and stage-specific manner, therefore the same signaling mechanism can have positive or negative regulatory effects on its target genes. For instance, Madaan et al. showed that the expression of *col-141*, a downstream target of TGF-β signaling, was upregulated in the Sma/Mab pathway mutants at L2 stage, whereas it was downregulated at adulthood [128]. Similar opposite patterns in expression levels were detected for *col-41* and *rol-6*, which are also targets of Sma/Mab pathway [128]. These results show that Sma/Mab signaling can differentially regulate target genes in a stage-specific manner. As explained in Chapter 5, I conducted the RNAi knockdown experiments by placing parental worms on RNAi plates at the L4 stage and examined the HSN phenotypes of F1 and F2 generations. Considering the stage-specific action of TGF-β signaling on downstream effectors, further RNA sequencing can be performed analyzing the transcriptome of the Sma/Mab pathway mutants at various developmental stages. For instance, embryogenesis is a critical stage for HSN migration, therefore embryonic stage RNA sequencing would be beneficial to identify the effector molecules regulated by TGF-β signaling in HSN development. Moreover, further RNAi knockdown experiments can be conducted using the target genes identified from transcriptome analyses of worms at distinct developmental stages. Worms can be exposed to the gene-specific RNAi bacteria at various developmental stages and their HSN phenotypes can be examined.

6.8 Alternative TGF-β mediators/interactors for driving HSN development

It is well-established that there is a cross-talk between the TGF-β and BMP signaling pathways, which could act together or antagonistically in a context-dependent manner. For instance, BMP-9 and BMP-10 have been shown to activate endothelial cell proliferation by activating the type I receptor ALK-1, whereas TGF-β inhibits the proliferation of endothelial cells by binding to another type I receptor ALK5 and inducing Smad2/3 signaling [188]. Cross-talk between the Sma/Mab pathway and dauer pathway have previously been reported. For example, Liu et al. showed that *dbl-1* is

downregulated when dauer pathway function is lost [189]. Moreover, dauer-constitutive phenotype of *daf-1* mutant animals is enhanced when *sma-6*, a component of Sma/Mab pathway, is mutated [57]. Furthermore, the type II receptor DAF-4 acts in both pathways, although this is due to DAF-4 being the sole type II receptor in *C. elegans*. Perhaps, by removing SMA-6 enables more DAF-4 to be available to regulate the dauer pathway, leading to the increased activity and interference of HSN development. To interrogate this hypothesis, double mutants can be generated using the mutant strains of the components of Sma/Mab and the dauer pathways. If the double mutants do not cause a change in the HSN phenotype of the single mutants of Sma/Mab components, this possibility can be ruled out as a potential cause of HSN defects.

As described in detail in Chapter 1, the developmental process of HSNs start during embryogenesis and continue throughout larval development which requires the control of long-range migration and axon guidance events [67]. In concurrence with the complexity of this process, many HSN regulators have been identified such as Wnt, ephrin, netrin and syndecan pathways. This raises the possibility of redundancy among these pathways with TGF-β pathway in the regulation of HSN development. To investigate this hypothesis, double mutant strains between the components of TGF-β pathway and other known regulators of HSN development can be generated and analyzed for their HSN phenotypes. An example for this can be found in Chapter 5, where I found that SDN-1 and TGF-β signaling mediates HSN development in parallel pathways (Fig. 5.14).

TGF-β signaling pathways have been shown to act in a dose-sensitive manner in many biological processes across different species [5]. In *C. elegans*, EGL-20/Wnt signaling has been shown to regulate HSN migration in a dose-sensitive manner as the EGL-20/Wnt gradient generated along the antero-posterior axis is crucial for determining the correct position of HSN cell bodies during embryogenesis [73, 88]. I showed that null mutations in specific components of Sma/Mab pathway cause development of defective HSNs, however it is unclear whether these components act in a dose-dependent manner, thus further experiments are required to investigate this hypothesis. Another important component of TGF-β signaling is inhibitory Smads (I-Smad) which act as inhibitors of signaling by restricting the activities of Smads [46]. In

C. elegans, TAG-68 is hypothesized to be an I-Smad homolog, however its precise function has not yet been identified. It could be interesting to examine the HSN phenotype of *tag-68* mutant animals as well as observing the double mutants generated between *tag-68* and Sma/Mab pathway components to explore its potential function in TGF-β-mediated HSN development.

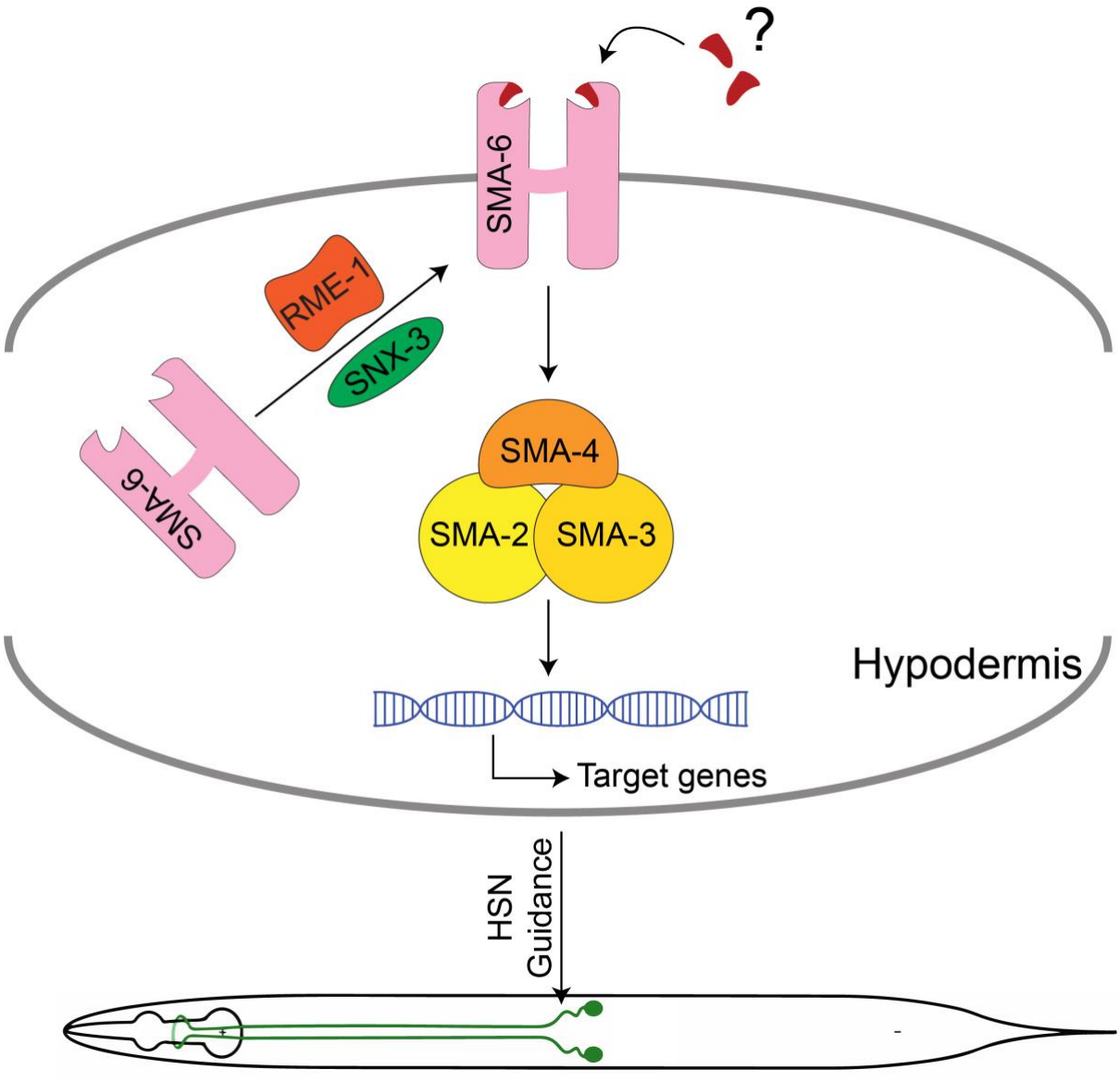

Fig. 6.1. The proposed mechanism of non-canonical TGFB signaling in HSN development.

6.9 Conclusion

TGF-β signaling controls an enormous range of biological processes in a highly context-dependent nature. Thanks to the genetic amenability, transparency and small nervous system of *C. elegans*, I was able to investigate the role of TGF-β signaling in the development of neurons at single cell resolution. I believe that my results on the development of the HSN neurons which involves long-range cell migration and axon guidance events provide important insight on how cell signaling events control neuronal development (Fig. 6.1).

7. References

1. Wrighton, K.H. and X.H. Feng, *To (TGF)beta or not to (TGF)beta: fine-tuning of Smad signaling via post-translational modifications.* Cell Signal, 2008. **20**(9): p. 1579-91.
2. de Larco, J.E. and G.J. Todaro, *Growth factors from murine sarcoma virus-transformed cells.* Proc Natl Acad Sci U S A, 1978. **75**(8): p. 4001-5.
3. Roberts, A.B., et al., *New class of transforming growth factors potentiated by epidermal growth factor: isolation from non-neoplastic tissues.* Proc Natl Acad Sci U S A, 1981. **78**(9): p. 5339-43.
4. Moses, H.L., et al., *Transforming growth factor production by chemically transformed cells.* Cancer Res, 1981. **41**(7): p. 2842-8.
5. Massague, J., *TGFbeta signalling in context.* Nat Rev Mol Cell Biol, 2012. **13**(10): p. 616-30.
6. Huang, F. and Y.G. Chen, *Regulation of TGF-beta receptor activity.* Cell Biosci, 2012. **2**: p. 9.
7. Liu, F., et al., *Human type II receptor for bone morphogenic proteins (BMPs): extension of the two-kinase receptor model to the BMPs.* Mol Cell Biol, 1995. **15**(7): p. 3479-86.
8. Rosenzweig, B.L., et al., *Cloning and characterization of a human type II receptor for bone morphogenetic proteins.* Proc Natl Acad Sci U S A, 1995. **92**(17): p. 7632-6.
9. Weiss, A. and L. Attisano, *The TGFbeta superfamily signaling pathway.* Wiley Interdiscip Rev Dev Biol, 2013. **2**(1): p. 47-63.
10. Harrison, C.A., S.L. Al-Musawi, and K.L. Walton, *Prodomains regulate the synthesis, extracellular localisation and activity of TGF-beta superfamily ligands.* Growth Factors, 2011. **29**(5): p. 174-86.
11. Gregory, K.E., et al., *The prodomain of BMP-7 targets the BMP-7 complex to the extracellular matrix.* J Biol Chem, 2005. **280**(30): p. 27970-80.
12. Sengle, G., et al., *Targeting of bone morphogenetic protein growth factor complexes to fibrillin.* J Biol Chem, 2008. **283**(20): p. 13874-88.
13. Sengle, G., et al., *Prodomains of transforming growth factor beta (TGFbeta) superfamily members specify different functions: extracellular matrix interactions and growth factor bioavailability.* J Biol Chem, 2011. **286**(7): p. 5087-99.
14. Nellen, D., et al., *Direct and long-range action of a DPP morphogen gradient.* Cell, 1996. **85**(3): p. 357-68.
15. Teleman, A.A. and S.M. Cohen, *Dpp gradient formation in the Drosophila wing imaginal disc.* Cell, 2000. **103**(6): p. 971-80.
16. Zilberberg, L., et al., *Specificity of latent TGF-beta binding protein (LTBP) incorporation into matrix: role of fibrillins and fibronectin.* J Cell Physiol, 2012. **227**(12): p. 3828-36.
17. Chaudhry, S.S., et al., *Fibrillin-1 regulates the bioavailability of TGFbeta1.* J Cell Biol, 2007. **176**(3): p. 355-67.
18. Chen, R.H. and R. Derynck, *Homomeric interactions between type II transforming growth factor-beta receptors.* J Biol Chem, 1994. **269**(36): p. 22868-74.
19. Gilboa, L., et al., *Oligomeric structure of type I and type II transforming growth factor beta receptors: homodimers form in the ER and persist at the plasma membrane.* J Cell Biol, 1998. **140**(4): p. 767-77.
20. Zhang, W., et al., *Monomeric type I and type III transforming growth factor-beta receptors and their dimerization revealed by single-molecule imaging.* Cell Res, 2010. **20**(11): p. 1216-23.
21. Kingsley, D.M., *The TGF-beta superfamily: new members, new receptors, and new genetic tests of function in different organisms.* Genes Dev, 1994. **8**(2): p. 133-46.
22. Luo, K. and H.F. Lodish, *Positive and negative regulation of type II TGF-beta receptor signal transduction by autophosphorylation on multiple serine residues.* EMBO J, 1997. **16**(8): p. 1970-81.
23. Wrana, J.L., et al., *Mechanism of activation of the TGF-beta receptor.* Nature, 1994. **370**(6488): p. 341-7.
24. Wieser, R., J.L. Wrana, and J. Massague, *GS domain mutations that constitutively activate T beta R-I, the downstream signaling component in the TGF-beta receptor complex.* EMBO J, 1995. **14**(10): p. 2199-208.
25. Huse, M., et al., *Crystal structure of the cytoplasmic domain of the type I TGF beta receptor in complex with FKBP12.* Cell, 1999. **96**(3): p. 425-36.
26. Weis-Garcia, F. and J. Massague, *Complementation between kinase-defective and activation-defective TGF-beta receptors reveals a novel form of receptor cooperativity essential for signaling.* EMBO J, 1996. **15**(2): p. 276-89.
27. Kang, J.S., C. Liu, and R. Derynck, *New regulatory mechanisms of TGF-beta receptor function.* Trends Cell Biol, 2009. **19**(8): p. 385-94.

28. Xu, P., J. Liu, and R. Derynck, *Post-translational regulation of TGF-beta receptor and Smad signaling.* FEBS Lett, 2012. **586**(14): p. 1871-84.
29. Kang, J.S., et al., *The type I TGF-beta receptor is covalently modified and regulated by sumoylation.* Nat Cell Biol, 2008. **10**(6): p. 654-64.
30. Zuo, W., et al., *c-Cbl-mediated neddylation antagonizes ubiquitination and degradation of the TGF-beta type II receptor.* Mol Cell, 2013. **49**(3): p. 499-510.
31. Park, G.T. and M.I. Morasso, *Bone morphogenetic protein-2 (BMP-2) transactivates Dlx3 through Smad1 and Smad4: alternative mode for Dlx3 induction in mouse keratinocytes.* Nucleic Acids Res, 2002. **30**(2): p. 515-22.
32. Xu, L., et al., *Distinct domain utilization by Smad3 and Smad4 for nucleoporin interaction and nuclear import.* J Biol Chem, 2003. **278**(43): p. 42569-77.
33. Lo, R.S., et al., *The L3 loop: a structural motif determining specific interactions between SMAD proteins and TGF-beta receptors.* EMBO J, 1998. **17**(4): p. 996-1005.
34. Inman, G.J. and C.S. Hill, *Stoichiometry of active smad-transcription factor complexes on DNA.* J Biol Chem, 2002. **277**(52): p. 51008-16.
35. Hill, C.S., *Transcriptional Control by the SMADs.* Cold Spring Harb Perspect Biol, 2016. **8**(10).
36. Mullen, A.C., et al., *Master transcription factors determine cell-type-specific responses to TGF-beta signaling.* Cell, 2011. **147**(3): p. 565-76.
37. Chen, X., M.J. Rubock, and M. Whitman, *A transcriptional partner for MAD proteins in TGF-beta signalling.* Nature, 1996. **383**(6602): p. 691-6.
38. Chen, X., et al., *Smad4 and FAST-1 in the assembly of activin-responsive factor.* Nature, 1997. **389**(6646): p. 85-9.
39. Kunwar, P.S., et al., *Mixer/Bon and FoxH1/Sur have overlapping and divergent roles in Nodal signaling and mesendoderm induction.* Development, 2003. **130**(23): p. 5589-99.
40. Ross, S., et al., *Smads orchestrate specific histone modifications and chromatin remodeling to activate transcription.* EMBO J, 2006. **25**(19): p. 4490-502.
41. Kang, Y., et al., *Breast cancer bone metastasis mediated by the Smad tumor suppressor pathway.* Proc Natl Acad Sci U S A, 2005. **102**(39): p. 13909-14.
42. Kang, Y., C.R. Chen, and J. Massague, *A self-enabling TGFbeta response coupled to stress signaling: Smad engages stress response factor ATF3 for Id1 repression in epithelial cells.* Mol Cell, 2003. **11**(4): p. 915-26.
43. Blahna, M.T. and A. Hata, *Smad-mediated regulation of microRNA biosynthesis.* FEBS Lett, 2012. **586**(14): p. 1906-12.
44. Davis, B.N., et al., *Smad proteins bind a conserved RNA sequence to promote microRNA maturation by Drosha.* Mol Cell, 2010. **39**(3): p. 373-84.
45. Gumienny, T.L., et al., *Glypican LON-2 is a conserved negative regulator of BMP-like signaling in Caenorhabditis elegans.* Curr Biol, 2007. **17**(2): p. 159-64.
46. Miyazawa, K. and K. Miyazono, *Regulation of TGF-beta Family Signaling by Inhibitory Smads.* Cold Spring Harb Perspect Biol, 2017. **9**(3).
47. Varelas, X., et al., *TAZ controls Smad nucleocytoplasmic shuttling and regulates human embryonic stem-cell self-renewal.* Nat Cell Biol, 2008. **10**(7): p. 837-48.
48. Cordenonsi, M., et al., *Integration of TGF-beta and Ras/MAPK signaling through p53 phosphorylation.* Science, 2007. **315**(5813): p. 840-3.
49. Hoppler, S. and R.T. Moon, *BMP-2/-4 and Wnt-8 cooperatively pattern the Xenopus mesoderm.* Mech Dev, 1998. **71**(1-2): p. 119-29.
50. Plata-Salaman, C.R., et al., *Kindling modulates the IL-1beta system, TNF-alpha, TGF-beta1, and neuropeptide mRNAs in specific brain regions.* Brain Res Mol Brain Res, 2000. **75**(2): p. 248-58.
51. Bar-Klein, G., et al., *Losartan prevents acquired epilepsy via TGF-beta signaling suppression.* Ann Neurol, 2014. **75**(6): p. 864-75.
52. Hughes, P.E., et al., *Administration of recombinant human Activin-A has powerful neurotrophic effects on select striatal phenotypes in the quinolinic acid lesion model of Huntington's disease.* Neuroscience, 1999. **92**(1): p. 197-209.
53. Stayte, S., et al., *Activin A Inhibits MPTP and LPS-Induced Increases in Inflammatory Cell Populations and Loss of Dopamine Neurons in the Mouse Midbrain In Vivo.* PLoS One, 2017. **12**(1): p. e0167211.
54. Zheng, F., et al., *Activin tunes GABAergic neurotransmission and modulates anxiety-like behavior.* Mol Psychiatry, 2009. **14**(3): p. 332-46.

55. Savage, C., et al., *Caenorhabditis elegans genes sma-2, sma-3, and sma-4 define a conserved family of transforming growth factor beta pathway components.* Proc Natl Acad Sci U S A, 1996. **93**(2): p. 790-4.
56. Suzuki, Y., et al., *A BMP homolog acts as a dose-dependent regulator of body size and male tail patterning in Caenorhabditis elegans.* Development, 1999. **126**(2): p. 241-50.
57. Krishna, S., L.L. Maduzia, and R.W. Padgett, *Specificity of TGFbeta signaling is conferred by distinct type I receptors and their associated SMAD proteins in Caenorhabditis elegans.* Development, 1999. **126**(2): p. 251-60.
58. Corsi, A.K., B. Wightman, and M. Chalfie, *A Transparent Window into Biology: A Primer on Caenorhabditis elegans.* Genetics, 2015. **200**(2): p. 387-407.
59. Felix, M.A. and C. Braendle, *The natural history of Caenorhabditis elegans.* Curr Biol, 2010. **20**(22): p. R965-9.
60. Brenner, S., *The genetics of Caenorhabditis elegans.* Genetics, 1974. **77**(1): p. 71-94.
61. Sulston, J.E., et al., *The embryonic cell lineage of the nematode Caenorhabditis elegans.* Dev Biol, 1983. **100**(1): p. 64-119.
62. Cassada, R.C. and R.L. Russell, *The dauerlarva, a post-embryonic developmental variant of the nematode Caenorhabditis elegans.* Dev Biol, 1975. **46**(2): p. 326-42.
63. Consortium, C.e.S., *Genome sequence of the nematode C. elegans: a platform for investigating biology.* Science, 1998. **282**(5396): p. 2012-8.
64. Shaye, D.D. and I. Greenwald, *OrthoList: a compendium of C. elegans genes with human orthologs.* PLoS One, 2011. **6**(5): p. e20085.
65. Cook, S.J., et al., *Whole-animal connectomes of both Caenorhabditis elegans sexes.* Nature, 2019. **571**(7763): p. 63-71.
66. Hobert, O., *Neurogenesis in the nematode Caenorhabditis elegans.* WormBook, 2010: p. 1-24.
67. White, J.G., et al., *The structure of the nervous system of the nematode Caenorhabditis elegans.* Philos Trans R Soc Lond B Biol Sci, 1986. **314**(1165): p. 1-340.
68. Altun, Z.F.a.H., D.H. *Nervous system, general description*. 2011 [cited 10/04/2017; Available from: http://www.wormatlas.org/hermaphrodite/nervous/Neuroframeset.html.
69. McColl, G., et al., *Utility of an improved model of amyloid-beta (Abeta(1)(-)(4)(2)) toxicity in Caenorhabditis elegans for drug screening for Alzheimer's disease.* Mol Neurodegener, 2012. **7**: p. 57.
70. Giraldez-Perez, R., et al., *Models of alpha-synuclein aggregation in Parkinson's disease.* Acta Neuropathol Commun, 2014. **2**: p. 176.
71. Hutter, H., *Formation of longitudinal axon pathways in Caenorhabditis elegans.* Semin Cell Dev Biol, 2019. **85**: p. 60-70.
72. Ren, X.C., et al., *Role of netrin UNC-6 in patterning the longitudinal nerves of Caenorhabditis elegans.* J Neurobiol, 1999. **39**(1): p. 107-18.
73. Desai, C., et al., *A genetic pathway for the development of the Caenorhabditis elegans HSN motor neurons.* Nature, 1988. **336**(6200): p. 638-46.
74. Seeger, M., et al., *Mutations affecting growth cone guidance in Drosophila: genes necessary for guidance toward or away from the midline.* Neuron, 1993. **10**(3): p. 409-26.
75. Zallen, J.A., B.A. Yi, and C.I. Bargmann, *The conserved immunoglobulin superfamily member SAX-3/Robo directs multiple aspects of axon guidance in C. elegans.* Cell, 1998. **92**(2): p. 217-27.
76. Chan, S.S., et al., *UNC-40, a C. elegans homolog of DCC (Deleted in Colorectal Cancer), is required in motile cells responding to UNC-6 netrin cues.* Cell, 1996. **87**(2): p. 187-95.
77. Hao, J.C., et al., *C. elegans slit acts in midline, dorsal-ventral, and anterior-posterior guidance via the SAX-3/Robo receptor.* Neuron, 2001. **32**(1): p. 25-38.
78. Zallen, J.A., S.A. Kirch, and C.I. Bargmann, *Genes required for axon pathfinding and extension in the C. elegans nerve ring.* Development, 1999. **126**(16): p. 3679-92.
79. Wang, X., et al., *Multiple ephrins control cell organization in C. elegans using kinase-dependent and -independent functions of the VAB-1 Eph receptor.* Mol Cell, 1999. **4**(6): p. 903-13.
80. Yang, Y.S. and S.M. Strittmatter, *The reticulons: a family of proteins with diverse functions.* Genome Biol, 2007. **8**(12): p. 234.
81. O'Sullivan, N.C., et al., *Reticulon-like-1, the Drosophila orthologue of the hereditary spastic paraplegia gene reticulon 2, is required for organization of endoplasmic reticulum and of distal motor axons.* Hum Mol Genet, 2012. **21**(15): p. 3356-65.

82. Torpe, N., et al., *Developmental Wiring of Specific Neurons Is Regulated by RET-1/Nogo-A in Caenorhabditis elegans.* Genetics, 2017. **205**(1): p. 295-302.
83. Pan, C.L., et al., *Multiple Wnts and frizzled receptors regulate anteriorly directed cell and growth cone migrations in Caenorhabditis elegans.* Dev Cell, 2006. **10**(3): p. 367-77.
84. McMahon, A.P. and A. Bradley, *The Wnt-1 (int-1) proto-oncogene is required for development of a large region of the mouse brain.* Cell, 1990. **62**(6): p. 1073-85.
85. Shen, Y., *Traffic lights for axon growth: proteoglycans and their neuronal receptors.* Neural Regen Res, 2014. **9**(4): p. 356-61.
86. Pedersen, M.E., et al., *An epidermal microRNA regulates neuronal migration through control of the cellular glycosylation state.* Science, 2013. **341**(6152): p. 1404-8.
87. Trent, C., N. Tsuing, and H.R. Horvitz, *Egg-laying defective mutants of the nematode Caenorhabditis elegans.* Genetics, 1983. **104**(4): p. 619-47.
88. Modzelewska, K., et al., *Neurons refine the Caenorhabditis elegans body plan by directing axial patterning by Wnts.* PLoS Biol, 2013. **11**(1): p. e1001465.
89. Wightman, B., et al., *The C. elegans gene vab-8 guides posteriorly directed axon outgrowth and cell migration.* Development, 1996. **122**(2): p. 671-82.
90. Pan, C.L., et al., *C. elegans AP-2 and retromer control Wnt signaling by regulating mig-14/Wntless.* Dev Cell, 2008. **14**(1): p. 132-9.
91. Torpe, N., et al., *A Protein Disulfide Isomerase Controls Neuronal Migration through Regulation of Wnt Secretion.* Cell Rep, 2019. **26**(12): p. 3183-3190 e5.
92. Rhiner, C., et al., *Syndecan regulates cell migration and axon guidance in C. elegans.* Development, 2005. **132**(20): p. 4621-33.
93. Saied-Santiago, K., et al., *Coordination of Heparan Sulfate Proteoglycans with Wnt Signaling To Control Cellular Migrations and Positioning in Caenorhabditis elegans.* Genetics, 2017. **206**(4): p. 1951-1967.
94. Gopal, S., J. Couchman, and R. Pocock, *Redefining the role of syndecans in C. elegans biology.* Worm, 2016. **5**(1): p. e1142042.
95. Wolf, F.W., et al., *vab-8 is a key regulator of posteriorly directed migrations in C. elegans and encodes a novel protein with kinesin motor similarity.* Neuron, 1998. **20**(4): p. 655-66.
96. Savage-Dunn, C. and R.W. Padgett, *The TGF-beta Family in Caenorhabditis elegans.* Cold Spring Harb Perspect Biol, 2017.
97. Ren, P., et al., *Control of C. elegans larval development by neuronal expression of a TGF-beta homolog.* Science, 1996. **274**(5291): p. 1389-91.
98. Schackwitz, W.S., T. Inoue, and J.H. Thomas, *Chemosensory neurons function in parallel to mediate a pheromone response in C. elegans.* Neuron, 1996. **17**(4): p. 719-28.
99. Narbonne, P. and R. Roy, *Caenorhabditis elegans dauers need LKB1/AMPK to ration lipid reserves and ensure long-term survival.* Nature, 2009. **457**(7226): p. 210-4.
100. Shaw, W.M., et al., *The C. elegans TGF-beta Dauer pathway regulates longevity via insulin signaling.* Curr Biol, 2007. **17**(19): p. 1635-45.
101. Foehr, M.L., et al., *An antagonistic role for the C. elegans Schnurri homolog SMA-9 in modulating TGFbeta signaling during mesodermal patterning.* Development, 2006. **133**(15): p. 2887-96.
102. Zhang, X. and Y. Zhang, *DBL-1, a TGF-beta, is essential for Caenorhabditis elegans aversive olfactory learning.* Proc Natl Acad Sci U S A, 2012. **109**(42): p. 17081-6.
103. Savage-Dunn, C., et al., *Non-stringent tissue-source requirements for BMP ligand expression in regulation of body size in Caenorhabditis elegans.* Genet Res (Camb), 2011. **93**(6): p. 427-32.
104. Fox, R.M., et al., *A gene expression fingerprint of C. elegans embryonic motor neurons.* BMC Genomics, 2005. **6**: p. 42.
105. Von Stetina, S.E., et al., *Cell-specific microarray profiling experiments reveal a comprehensive picture of gene expression in the C. elegans nervous system.* Genome Biol, 2007. **8**(7): p. R135.
106. Cao, J., et al., *Comprehensive single-cell transcriptional profiling of a multicellular organism.* Science, 2017. **357**(6352): p. 661-667.
107. Colavita, A., et al., *Pioneer axon guidance by UNC-129, a C. elegans TGF-beta.* Science, 1998. **281**(5377): p. 706-9.
108. MacNeil, L.T., et al., *UNC-129 regulates the balance between UNC-40 dependent and independent UNC-5 signaling pathways.* Nat Neurosci, 2009. **12**(2): p. 150-5.

109. Nash, B., et al., *The forkhead transcription factor UNC-130 is required for the graded spatial expression of the UNC-129 TGF-beta guidance factor in C. elegans.* Genes Dev, 2000. **14**(19): p. 2486-500.
110. Estevez, M., et al., *The daf-4 gene encodes a bone morphogenetic protein receptor controlling C. elegans dauer larva development.* Nature, 1993. **365**(6447): p. 644-9.
111. Patterson, G.I., et al., *The DAF-3 Smad protein antagonizes TGF-beta-related receptor signaling in the Caenorhabditis elegans dauer pathway.* Genes Dev, 1997. **11**(20): p. 2679-90.
112. Gunther, C.V., L.L. Georgi, and D.L. Riddle, *A Caenorhabditis elegans type I TGF beta receptor can function in the absence of type II kinase to promote larval development.* Development, 2000. **127**(15): p. 3337-47.
113. Georgi, L.L., P.S. Albert, and D.L. Riddle, *daf-1, a C. elegans gene controlling dauer larva development, encodes a novel receptor protein kinase.* Cell, 1990. **61**(4): p. 635-45.
114. Greer, E.R., et al., *Neural and molecular dissection of a C. elegans sensory circuit that regulates fat and feeding.* Cell Metab, 2008. **8**(2): p. 118-31.
115. Yoshida, S., et al., *Hypodermal expression of Caenorhabditis elegans TGF-beta type I receptor SMA-6 is essential for the growth and maintenance of body length.* Dev Biol, 2001. **240**(1): p. 32-45.
116. Harterink, M., et al., *A SNX3-dependent retromer pathway mediates retrograde transport of the Wnt sorting receptor Wntless and is required for Wnt secretion.* Nat Cell Biol, 2011. **13**(8): p. 914-923.
117. Gleason, R.J., et al., *BMP signaling requires retromer-dependent recycling of the type I receptor.* Proc Natl Acad Sci U S A, 2014. **111**(7): p. 2578-83.
118. Dong, C., et al., *ADP-ribosylation factors modulate the cell surface transport of G protein-coupled receptors.* J Pharmacol Exp Ther, 2010. **333**(1): p. 174-83.
119. Reece-Hoyes, J.S., et al., *Insight into transcription factor gene duplication from Caenorhabditis elegans Promoterome-driven expression patterns.* BMC Genomics, 2007. **8**: p. 27.
120. Liang, J., et al., *Transcriptional repressor and activator activities of SMA-9 contribute differentially to BMP-related signaling outputs.* Dev Biol, 2007. **305**(2): p. 714-25.
121. Thomas, J.H., D.A. Birnby, and J.J. Vowels, *Evidence for parallel processing of sensory information controlling dauer formation in Caenorhabditis elegans.* Genetics, 1993. **134**(4): p. 1105-17.
122. da Graca, L.S., et al., *DAF-5 is a Ski oncoprotein homolog that functions in a neuronal TGF beta pathway to regulate C. elegans dauer development.* Development, 2004. **131**(2): p. 435-46.
123. Gumienny, T.L., et al., *Caenorhabditis elegans SMA-10/LRIG is a conserved transmembrane protein that enhances bone morphogenetic protein signaling.* PLoS Genet, 2010. **6**(5): p. e1000963.
124. Gleason, R.J., et al., *C. elegans SMA-10 regulates BMP receptor trafficking.* PLoS One, 2017. **12**(7): p. e0180681.
125. Fernando, T., et al., *C. elegans ADAMTS ADT-2 regulates body size by modulating TGFbeta signaling and cuticle collagen organization.* Dev Biol, 2011. **352**(1): p. 92-103.
126. Nagamatsu, Y. and Y. Ohshima, *Mechanisms for the control of body size by a G-kinase and a downstream TGFbeta signal pathway in Caenorhabditis elegans.* Genes Cells, 2004. **9**(1): p. 39-47.
127. Wang, J., R. Tokarz, and C. Savage-Dunn, *The expression of TGFbeta signal transducers in the hypodermis regulates body size in C. elegans.* Development, 2002. **129**(21): p. 4989-98.
128. Madaan, U., et al., *BMP Signaling Determines Body Size via Transcriptional Regulation of Collagen Genes in Caenorhabditis elegans.* Genetics, 2018. **210**(4): p. 1355-1367.
129. Nicholas, H.R. and J. Hodgkin, *Responses to infection and possible recognition strategies in the innate immune system of Caenorhabditis elegans.* Mol Immunol, 2004. **41**(5): p. 479-93.
130. Mallo, G.V., et al., *Inducible antibacterial defense system in C. elegans.* Curr Biol, 2002. **12**(14): p. 1209-14.
131. Roberts, A.F., et al., *Regulation of genes affecting body size and innate immunity by the DBL-1/BMP-like pathway in Caenorhabditis elegans.* BMC Dev Biol, 2010. **10**: p. 61.
132. Liang, J., et al., *The Caenorhabditis elegans schnurri homolog sma-9 mediates stage- and cell type-specific responses to DBL-1 BMP-related signaling.* Development, 2003. **130**(26): p. 6453-64.
133. Qi, W., et al., *C. elegans DAF-16/FOXO interacts with TGF-ss/BMP signaling to induce germline tumor formation via mTORC1 activation.* PLoS Genet, 2017. **13**(5): p. e1006801.

134. Clark, J.F., et al., *Caenorhabditis elegans DBL-1/BMP Regulates Lipid Accumulation via Interaction with Insulin Signaling.* G3 (Bethesda), 2018. **8**(1): p. 343-351.
135. Kenyon, C., et al., *A C. elegans mutant that lives twice as long as wild type.* Nature, 1993. **366**(6454): p. 461-4.
136. Mello, C.C., et al., *Efficient gene transfer in C.elegans: extrachromosomal maintenance and integration of transforming sequences.* EMBO J, 1991. **10**(12): p. 3959-70.
137. Hsu, P.D., et al., *DNA targeting specificity of RNA-guided Cas9 nucleases.* Nat Biotechnol, 2013. **31**(9): p. 827-32.
138. Kamath, R.S., et al., *Effectiveness of specific RNA-mediated interference through ingested double-stranded RNA in Caenorhabditis elegans.* Genome Biol, 2001. **2**(1): p. RESEARCH0002.
139. Massague, J., *TGFbeta in Cancer.* Cell, 2008. **134**(2): p. 215-30.
140. Savage-Dunn, C., et al., *Genetic screen for small body size mutants in C. elegans reveals many TGFbeta pathway components.* Genesis, 2003. **35**(4): p. 239-47.
141. Consortium, C.e.D.M., *large-scale screening for targeted knockouts in the Caenorhabditis elegans genome.* G3 (Bethesda), 2012. **2**(11): p. 1415-25.
142. Kennedy, L.M., S.C. Pham, and A. Grishok, *Nonautonomous regulation of neuronal migration by insulin signaling, DAF-16/FOXO, and PAK-1.* Cell Rep, 2013. **4**(5): p. 996-1009.
143. Soukas, A.A., et al., *Rictor/TORC2 regulates fat metabolism, feeding, growth, and life span in Caenorhabditis elegans.* Genes Dev, 2009. **23**(4): p. 496-511.
144. Weir, H.J., et al., *Dietary Restriction and AMPK Increase Lifespan via Mitochondrial Network and Peroxisome Remodeling.* Cell Metab, 2017. **26**(6): p. 884-896 e5.
145. Savage-Dunn, C., et al., *SMA-3 smad has specific and critical functions in DBL-1/SMA-6 TGFbeta-related signaling.* Dev Biol, 2000. **223**(1): p. 70-6.
146. Grant, B.D. and J.G. Donaldson, *Pathways and mechanisms of endocytic recycling.* Nat Rev Mol Cell Biol, 2009. **10**(9): p. 597-608.
147. McKay, S.J., et al., *Gene expression profiling of cells, tissues, and developmental stages of the nematode C. elegans.* Cold Spring Harb Symp Quant Biol, 2003. **68**: p. 159-69.
148. Ogata, S., et al., *TGF-beta signaling-mediated morphogenesis: modulation of cell adhesion via cadherin endocytosis.* Genes Dev, 2007. **21**(14): p. 1817-31.
149. Di-Gregorio, A., et al., *BMP signalling inhibits premature neural differentiation in the mouse embryo.* Development, 2007. **134**(18): p. 3359-69.
150. Ozdamar, B., et al., *Regulation of the polarity protein Par6 by TGFbeta receptors controls epithelial cell plasticity.* Science, 2005. **307**(5715): p. 1603-9.
151. Chu, G.C., et al., *Differential requirements for Smad4 in TGFbeta-dependent patterning of the early mouse embryo.* Development, 2004. **131**(15): p. 3501-12.
152. Pierce, S.B., et al., *Regulation of DAF-2 receptor signaling by human insulin and ins-1, a member of the unusually large and diverse C. elegans insulin gene family.* Genes Dev, 2001. **15**(6): p. 672-86.
153. Fuerer, C., M.C. Nostro, and D.B. Constam, *Nodal.Gdf1 heterodimers with bound prodomains enable serum-independent nodal signaling and endoderm differentiation.* J Biol Chem, 2014. **289**(25): p. 17854-71.
154. Zhu, M., et al., *Serum- and Glucocorticoid-Inducible Kinase-1 (SGK-1) Plays a Role in Membrane Trafficking in Caenorhabditis elegans.* PLoS One, 2015. **10**(6): p. e0130778.
155. Gatsi, R., et al., *Prohibitin-mediated lifespan and mitochondrial stress implicate SGK-1, insulin/IGF and mTORC2 in C. elegans.* PLoS One, 2014. **9**(9): p. e107671.
156. Jones, K.T., et al., *Rictor/TORC2 regulates Caenorhabditis elegans fat storage, body size, and development through sgk-1.* PLoS Biol, 2009. **7**(3): p. e60.
157. Dong, X., et al., *Precise regulation of the guidance receptor DMA-1 by KPC-1/Furin instructs dendritic branching decisions.* Elife, 2016. **5**.
158. Rapti, G., et al., *Glia initiate brain assembly through noncanonical Chimaerin-Furin axon guidance in C. elegans.* Nat Neurosci, 2017. **20**(10): p. 1350-1360.
159. Matsuda, S., et al., *Member of the membrane-bound O-acyltransferase (MBOAT) family encodes a lysophospholipid acyltransferase with broad substrate specificity.* Genes Cells, 2008. **13**(8): p. 879-88.
160. Xu, Y., et al., *Axon response to guidance cues is stimulated by acetylcholine in Caenorhabditis elegans.* Genetics, 2011. **189**(3): p. 899-906.
161. Hao, J.C., et al., *The tripartite motif protein MADD-2 functions with the receptor UNC-40 (DCC) in Netrin-mediated axon attraction and branching.* Dev Cell, 2010. **18**(6): p. 950-60.

162. Kulkarni, G., H. Li, and W.G. Wadsworth, *CLEC-38, a transmembrane protein with C-type lectin-like domains, negatively regulates UNC-40-mediated axon outgrowth and promotes presynaptic development in Caenorhabditis elegans.* J Neurosci, 2008. **28**(17): p. 4541-50.
163. Song, S., et al., *TRIM-9 functions in the UNC-6/UNC-40 pathway to regulate ventral guidance.* J Genet Genomics, 2011. **38**(1): p. 1-11.
164. Liu, Z., et al., *C. elegans PlexinA PLX-1 mediates a cell contact-dependent stop signal in vulval precursor cells.* Dev Biol, 2005. **282**(1): p. 138-51.
165. Nakao, F., et al., *The PLEXIN PLX-2 and the ephrin EFN-4 have distinct roles in MAB-20/Semaphorin 2A signaling in Caenorhabditis elegans morphogenesis.* Genetics, 2007. **176**(3): p. 1591-607.
166. Mizumoto, K. and K. Shen, *Interaxonal interaction defines tiled presynaptic innervation in C. elegans.* Neuron, 2013. **77**(4): p. 655-66.
167. Huang, X., et al., *MAX-1, a novel PH/MyTH4/FERM domain cytoplasmic protein implicated in netrin-mediated axon repulsion.* Neuron, 2002. **34**(4): p. 563-76.
168. Wang, X., et al., *The C. elegans L1CAM homologue LAD-2 functions as a coreceptor in MAB-20/Sema2 mediated axon guidance.* J Cell Biol, 2008. **180**(1): p. 233-46.
169. Dong, B., et al., *EFN-4 functions in LAD-2-mediated axon guidance in Caenorhabditis elegans.* Development, 2016. **143**(7): p. 1182-91.
170. Ihara, S., et al., *Basement membrane sliding and targeted adhesion remodels tissue boundaries during uterine-vulval attachment in Caenorhabditis elegans.* Nat Cell Biol, 2011. **13**(6): p. 641-51.
171. Ding, M., et al., *C. elegans ankyrin repeat protein VAB-19 is a component of epidermal attachment structures and is essential for epidermal morphogenesis.* Development, 2003. **130**(23): p. 5791-801.
172. Yang, Y., et al., *Extracellular matrix regulates UNC-6 (netrin) axon guidance by controlling the direction of intracellular UNC-40 (DCC) outgrowth activity.* PLoS One, 2014. **9**(5): p. e97258.
173. Emtage, L., et al., *Extracellular proteins organize the mechanosensory channel complex in C. elegans touch receptor neurons.* Neuron, 2004. **44**(5): p. 795-807.
174. Gu, G., G.A. Caldwell, and M. Chalfie, *Genetic interactions affecting touch sensitivity in Caenorhabditis elegans.* Proc Natl Acad Sci U S A, 1996. **93**(13): p. 6577-82.
175. Axang, C., et al., *Developmental genetics of the C. elegans pharyngeal neurons NSML and NSMR.* BMC Dev Biol, 2008. **8**: p. 38.
176. Smogavec, M., et al., *Eight further individuals with intellectual disability and epilepsy carrying bi-allelic CNTNAP2 aberrations allow delineation of the mutational and phenotypic spectrum.* J Med Genet, 2016. **53**(12): p. 820-827.
177. Belloso, J.M., et al., *Disruption of the CNTNAP2 gene in a t(7;15) translocation family without symptoms of Gilles de la Tourette syndrome.* Eur J Hum Genet, 2007. **15**(6): p. 711-3.
178. Krumbiegel, M., et al., *Genome-wide association study with DNA pooling identifies variants at CNTNAP2 associated with pseudoexfoliation syndrome.* Eur J Hum Genet, 2011. **19**(2): p. 186-93.
179. Alarcon, M., et al., *Linkage, association, and gene-expression analyses identify CNTNAP2 as an autism-susceptibility gene.* Am J Hum Genet, 2008. **82**(1): p. 150-9.
180. Strauss, K.A., et al., *Recessive symptomatic focal epilepsy and mutant contactin-associated protein-like 2.* N Engl J Med, 2006. **354**(13): p. 1370-7.
181. Quinn, C.C., et al., *UNC-6/netrin and SLT-1/slit guidance cues orient axon outgrowth mediated by MIG-10/RIAM/lamellipodin.* Curr Biol, 2006. **16**(9): p. 845-53.
182. Zhao, H., et al., *TGF-beta type I receptor Alk5 regulates tooth initiation and mandible patterning in a type II receptor-independent manner.* Dev Biol, 2008. **320**(1): p. 19-29.
183. Essalmani, R., et al., *In vivo functions of the proprotein convertase PC5/6 during mouse development: Gdf11 is a likely substrate.* Proc Natl Acad Sci U S A, 2008. **105**(15): p. 5750-5.
184. Thacker, C. and A.M. Rose, *A look at the Caenorhabditis elegans Kex2/Subtilisin-like proprotein convertase family.* Bioessays, 2000. **22**(6): p. 545-53.
185. Kass, J., et al., *The EGL-3 proprotein convertase regulates mechanosensory responses of Caenorhabditis elegans.* J Neurosci, 2001. **21**(23): p. 9265-72.
186. Salzberg, Y., N.J. Ramirez-Suarez, and H.E. Bulow, *The proprotein convertase KPC-1/furin controls branching and self-avoidance of sensory dendrites in Caenorhabditis elegans.* PLoS Genet, 2014. **10**(9): p. e1004657.
187. Haklai-Topper, L., et al., *The neurexin superfamily of Caenorhabditis elegans.* Gene Expr Patterns, 2011. **11**(1-2): p. 144-50.

188. Ning, J., et al., *Opposing roles and potential antagonistic mechanism between TGF-beta and BMP pathways: Implications for cancer progression.* EBioMedicine, 2019. **41**: p. 702-710.
189. Liu, T., K.K. Zimmerman, and G.I. Patterson, *Regulation of signaling genes by TGFbeta during entry into dauer diapause in C. elegans.* BMC Dev Biol, 2004. **4**: p. 11.

8. Appendices

8.1 Oligonucleotides

Appendix Table 8.1. Oligonucleotides for genotyping and cloning

Name	Sequence (5’ to 3’)
GSN9	GCATCCCTTATTATTGATCCAAA
GSN10	GTCATTATGGCCAAAAAAATGGC
GSN18	GCGGCAAATTTATTTGTCAGC
GSN19	GCGAGCTCTTCAACATCGA
OFB58	AGCACCATGGATGAACATCACCTTTATATTTATTC
OFB62	AAGTATTGGTGCTGCCTATGAAGGTAACTATTGC
OFB63	TTAGGAGAATGGTGAGCTG
OFB64	TTTTCCATGGTTAAGATTGATTGGTGGCTGAC
OFB66	TGGATCGAATTTCCACGATGC
OFB77	CAATGGCACTTGTTATGTGGG
OFB79	CACGAACGTACAGGTCTGG
OFB81	TAGGAGATTACAGGCCCATAG
OFB84	GCGATATGCACACAACTGCC
OFB86	GCAGTGCAAATGGCATCCG
OFB123	GCCCATTTCCTATAAGGTGCGTTTTAGAGCTAGAAATAGCAAGT
OFB124	CTACAAGAACCTTACAAGAGGTTTTAGAGCTAGAAATAGCAAGT
OFB131	AGGTAACTATGCCAATAAGAATTTGATTCCG
OFB132	TCATAGGCAGCACCAATAC
OFB135	AGGACCCTTGGCTAGCATGAACATCACCTTTATATTTATTC

Name	Sequence (5’ to 3’)
OFB136	TACCGTCGACGCTAGCTTAAGATTGATTGGTGGCTG
OFB139	AAAAGCTAGCATGTCGACTTCAAGAAAGCATG
OFB140	TTTTGGTACCTTAATGGTGGTGGTGATGATGAGTACAACTGCAAGAAAGAGC
OFB141	GGTAAGCCTATCCCTAACCCTCTCC
OFB142	GGTGAAGGGGGCGGCCGC
OFB143	GCCGCCCCCTTCACCATGAGGCGACTTCCGATTGTC
OFB144	AGGGATAGGCTTACCAAGACAAGAGCATGAGCCAATG
OFB150	GATGTCTACGACGGAGCAC
OFB151	CTCCGCAGTGTTTGCGTAC
OFB152	AAAAAAGCTTCAGTATCCCGTGCTCTATCC
OFB153	TTTTAAGCTTGGAGCAGTAGAATCCGCATC
OFB156	CCTCAAATGCAAGATTCCGAC
OFB158	GAATTGAGATCGACGGTAGAG
pDD162R	GGTGTGAAATACCGCACAGA